Master Thesis

Landau Gauge Quark Propagator with External Magnetic Fields

Niklas Müller

September 2013

Institut für Theoretische Physik
Justus-Liebig-Universität Giessen

Supervisor: Prof. Dr. C. S. Fischer

Contents

1 Introduction

Quantum Chromodynamics (QCD) is a remarkable theory as it has founded the success of quantum field theory already long time ago, consolidating and deepening the significant insights into quantum physics that Quantum Electrodynamics (QED) had just given a few years before.
The feature of asymptotic freedom [1] makes QCD behave like a free theory at small distances, making it easily treatable with very intuitive (perturbative) methods one learns already in basic quantum field theory classes. However once one goes to larger distances, things become very different. QCD is a prime example of a strongly correlated system in this range, thereby stripping us from almost all tools that we are familiar with and which made us capable of obtaining deeper insight. Of course this is not unique to QCD, one could name a variety of systems whose microscopic behaviour is well understood but turn into a mess with all sorts of new effects when going to large scales. Conventional superconductors or quantum Hall systems are such examples.
In QCD large distance effects are the most important reason why the world around us looks the way it is. Chiral symmetry breaking and confinement are the certainly most puzzling features of strong Quantum Chromodynamics. Our limited understanding concerning these two is related to two things: First, we are far from having a rigorous mathematical understanding of the structure of (strong) non-Abelian gauge theories. Second, it is incredibly hard to extract any numbers from those theories. The latter is caused by the fact that QCD by itself does not have any small intrinsic parameter that one could expand in. Instead it has an intrinsic scale of $\Lambda_{\mathrm{QCD}} \approx 1$ GeV whose origin is dynamical.
So far lattice gauge theory seems to be the only *ab initio* ansatz that is able to numerically derive properties of long distance QCD. The many successes of lattice gauge theory however overshadow a very important point, namely that lattice gauge theory might be a consistent and nice theory by itself, but it is not really a continuum quantum theory in the original sense. Lattice gauge theory relies on the assumptation that a probabilistic interpretation of the path integral with Euclidian action is possible, so that sampling a finite set of field configurations to approximate a system with infinitely many degrees of freedom is sufficient. Once there is a finite ($U(1)$) chemical potential, the famous sign problem arises and such an interpretation is difficult.

There exist approaches to solve quantum field theories, whose reliability does not depend on any small parameters and that are truly continuum methods. The Dyson-Schwinger [2–4] and the Functional Renormalization Group [5, 6] ansätze are probably the two most important ones. This thesis will make use of the powerful Dyson-Schwinger formalism. Its basic idea is to derive relations between n-point correlation functions from general considerations, thus making it applicable to any quantum field theory.
As always there is a hook. Being able to write down the exact relations between all correlation functions still does not buy you much, for there is an infinite number of such correlation functions and an infinite tower of equations relating those. A good part of the effort necessary, when putting the Dyson Schwinger method to use, is therefore choosing a finite set of these infinitely many equations and algebraically closing them by truncating the left over relations. Having no small parameters, it is incredibly difficult to estimate the quality of such a trunctation in a systematic way. Luckily, other methods are available in certain areas of parameter space, offering plenty of comparison.

Why are magnetic fields interesting in the investigation of strongly coupled systems? Most importantly magnetic fields are a relevant ingredient for the descripition of various effects relevant in these systems. Non-central heavy ion collissions, neutron stars and the evolution of the early universe are the most striking and interesting examples. Some of them even being relatively easily testable with present (BNL, LHC) and future research facilities (FAIR).
Magnetic fields were shown to modify the behaviour of quantum systems in a non trivial way, thus being an interesting topic by themselves. It was shown that (strong) magnetic fields lead to magnetic catalysis (the dynamical generation of mass) in fermionic systems in a somewhat similar fashion as it happens in Quantum Chromodynamics with chiral symmetry breaking [21,22]. Furthermore magnetic

fields alter the thermodynamics of QCD, thereby adding an additional dimension to the phase diagram and changing the phases of matter found in the latter. Thus being able to tune a magnetic field from the theoretical point of view, one might get insights in the structure of the QCD phase diagram even in the absence of external fields.
An additional aspect is appealing. Owing to its Abelian nature, Quantum Electrodynamics in four dimensions is not confining, no matter how strong one turns its interaction. This means that electric charges are never screened, unlike color charges. Then, although the fundamental degrees of freedom (quarks and gluons) are never found isolated but always confined in hadrons, their electric charge is "visible" to the outside world. In fact, the first experimental proof of QCD in terms of Deep Inelastic Scattering probed the electric charge of quarks [7].
Magnetic fields are a nice tool to test color charged objects at arbitrary scales, its Abelian nature making it quite straightforward to put it atop a non-Abelian quantum theory. By doing that, one is equipped with the possibility to turn the field and observe the quantum system react. We thus have a systematic tool to modify the quantum vacuum of QCD, the latter being the key to a lot of the mysteries described above.
This thesis aims to establish the techniques needed for an analysis of the influence of magnetic fields on QCD in the continuum Dyson-Schwinger ansatz. Quite some work has been done in QED already and I will make use of ideas approached there.

This thesis is organized as follows: Chapter 2 aims to give a short introduction into the Dyson-Schwinger method and the theory of Quantum Chromodynamics. A review of the important issues and shortcomings of the current knowledge of this theory can be found here. In Chapter 3 an introduction is given of how to treat quantum field theories involving charged (fermionic) and gauge boson fields. The (quenched) Dyson-Schwinger equation for the quark in the presence of a magnetic field will be derived there. Chapter 4 will show results found when solving the quark DSE in the quenched approximation. The structure of the quak propagator will be discussed and important properties of the QCD vacuum, such as chiral symmetry and spin polarization will be investigated. After having all necessary tools established, Chapter 5 will include the effect of the magnetic field onto the gauge sector as well. As systematic discussion of the structure of the gluon polarization in magentic fields can be found here. Finally exemplary approximate solutions to the coupled system of quark and gluon DSE are performed for illustration. The last Chapter 6 will give a conclusion of the results obtained in this work. Furthermore it will suggest an outlook on how the established methods can be used to gain deeper insight into Quantum Chromodynamics.

2 Basics

The following section gives an overview over the most important points of the theories and concepts that will be used in the following sections. We follow the traces of [10–12]. Before proceeding to the theory of Quantum Chromodynamics, I will focus first on the concepts of the Dyson-Schwinger framework. The principles and methods found here are generic properties of quantum field theories. For simplicity a simple scalar field theory is used without losing any generality. Subsequently I will give a short introduction to Quantum Chromodynamics (QCD) and discuss the relevance of investigations done here for a better understanding of the very same. The experienced reader might skip those sections.

2.1 Dyson-Schwinger Equations

2.1.1 Path Integrals and Functional Integral Formalism

Quantum field theories are a serious challenge to solve, compared to classical theories. The reason for that is that a quantum theory might possess completely different dynamics as could be anticipated from its classical equivalent. Quantum fluctuations modify basic properties of a theory in an important way, possibly leading even to the breaking of (classical) symmetries.
In order to actually solve a quantum field theory, we are interested in expectation values of operators that we can relate to physical observables. The most important operators for us are, of course, the field operators themselves and we will call the (vacuum-) expectation value of a product of field operators $\varphi_i \equiv \varphi(x_i)$ at different space time points a correlation function or n-point Green's function

$$G^{(n)}(\varphi_1 \dots \varphi_n) = \langle \varphi_1 \dots \varphi_n \rangle \,. \tag{2.1}$$

Such a correlation function, as for example a 2-point function, gives the quantum mechanical amplitude of a field created at point x_1 propagating to point x_2 (or the other way around if we include proper time ordering). The (full) propagator is then given by

$$S(x,y) \equiv i \, \langle T(\varphi(x)\varphi(y)) \rangle \,. \tag{2.2}$$

In the path integral formalism such a Green's function can be obtained from the partition function

$$Z[J] = \langle 0|0 \rangle_J = \int D\varphi \; e^{iS[\varphi] + \int J\varphi} \tag{2.3}$$

which is a functional of the source J. Further

$$D\varphi \equiv \prod_x \mathrm{d}\varphi_i$$

denotes the Haar measure on the field manifold for every space-time point x. Let us proceed with a generic scalar field φ for simplicity. The generalization to other types of fields (also fermionic) is straightforward. An n-point function now can be obtained from

$$\langle T(\varphi_1 \dots \varphi_n) \rangle = \int D\varphi \; \varphi_1 \dots \varphi_n \; e^{iS[\varphi] + \int J\varphi} \Big|_{J=0} \tag{2.4}$$

In case of a non-interacting theory this is a rather trivial expression since the exponential is at most quadratic in the field variable φ, leaving a simple Gaussian integral[1]. Hence for an even number of φ fields we simply get a sum over all possible pairings of propagators between the space-time positions x_i. The method of choice to obtain such a result is by functional variation, where

$$\langle T(\varphi_1 \dots \varphi_n) \rangle = \frac{1}{i^n} \frac{\delta^{(n)} Z[J]}{\delta J_i \dots \delta J_n} \Big|_{J=0} \tag{2.5}$$

[1] Provided you believe that this converges. However inserting a small damping in the exponential should do the job.

yields the previous equation. This is a general property, whether the theory is interacting or not. Variation of the path integral with respect to n sources produces the corresponding full n-point function which also contains disconnected pieces. As we will see later, there is a deep relation between sources J and fields φ.
$Z[J]$ can be interpreted as something like a zero-point function allowing us to obtain higher Green's functons by functional variation. An expansion wrt. to the sources could be pictorially represented by

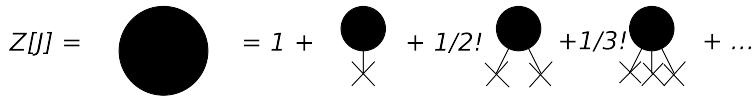

such that for example the single field vacuum expectation value can be written

$$\phi(x) \equiv \langle \varphi(x) \rangle = \frac{1}{i} \frac{\delta}{\delta J(x)} Z[J] \Big|_{J=0} \tag{2.6}$$

where the following abbreviations where used:

The question now arises of how to calculate such a Green's function? As we have seen above this is trivial in the non-interacting case. Our (classical) action S however will contain terms of powers in φ beyond quadratic order. In this case, we cannot obtain simple Gaussian integrals and need to find another ansatz.
The simplest solution would be to use pertubation theory (PT) which was the basis of the early success of quantum field theory when theories were in focus that contained a small parameter (such as QED). The idea behind PT is simple, let us assume a simple lagrangian for illustration

$$\mathcal{L} = -\frac{1}{2}\partial^\mu \varphi \partial_\mu \varphi - \frac{1}{2} m^2 \varphi^2 - \frac{\lambda}{4!}\varphi^4 = \mathcal{L}_0 + \mathcal{L}_{\text{int}}. \tag{2.7}$$

Provided the coupling λ is sufficiently small, we can expand the interacting part of the partition function in powers of λ.

$$Z[J] = \int D\varphi \; e^{i(S_0 + S_{\text{int}}) + \int J\varphi} = e^{i \int \mathcal{L}_{\text{int}}\left[\frac{1}{i}\frac{\delta}{\delta J}\right]} Z_0[J] \tag{2.8}$$

where Z_0 is the path integral in the absence of interactions. For the Lagrangian given above we can expand

$$e^{i \int \mathcal{L}_{\text{int}}\left[\frac{1}{i}\frac{\delta}{\delta J}\right]} = e^{-\frac{\lambda}{4!} i \int \left(\frac{1}{i}\frac{\delta}{\delta J}\right)^4} \approx 1 - \frac{i\lambda}{4!} \int \left(\frac{1}{i}\frac{\delta}{\delta J}\right)^4 + \dots \tag{2.9}$$

This can be depicted in the very intuitive Feynman diagrams that are nothing more than representations of a certain expansion of n-point functions. Provided we started from a proper theory, this

expansion has the nice feature to be renormalizble to every order in the coupling constant, a property that we will later have to really work hard for in the Dyson-Schwinger framework.
However, once the theory is sufficiently strong the expansion such as in Eq.(2.9) breaks down. Here one might be tempted to evaluate the path integral $Z[J]$ by using only a finite number of field configurations (i.e. discretizing space-time and putting the system in a box) in order to calculate Green's functions explicitly by averaging over all possible field configurations weighted by the Euclidean phase factor e^{-S}. This is then called lattice field theory, which can be very powerful, but comes with some major drawbacks. First it lives in Euclidean rather than Minkowskian space-time in order to define a probability measure. When introducing a finite U(1) chemical potential this fails. Secondly it lives on a finite lattice with finitely many degrees of freedom which causes it to have some rather different topological properties.
Dyson-Schwinger equations are a truly continuum method, making them very powerful and somewhat complimentary to lattice theories. Most important there is no sign problem in the DSE ansatz, allowing for finite density. In the following section I will discuss the main ideas behind the Dyson-Schwinger ansatz by introducing some basic concepts.

2.1.2 1PI, Legendre Transforms, Effective Action and all that

Although the expansion in the coupling constant does not make sense in a strong field theory, the complete resummation of the interactions to every order in the path integral $Z[J]$ is still a well defined quantity.
A functional related to the path integral is the sum of all connected diagrams $W[J]$, that generates the *connected* Green's functions $G_c^{(n)}$. Normalizing $Z[0] = 1$ defines $W[J]$ via

$$Z[J] = e^{iW[J]}, \tag{2.10}$$

which is equivalent to discarding all disconnected diagrams. Similar to the preceding sections we obtain connected Green's functions from variation wrt. the source.

$$G_c^{(n)}(x_1 \dots x_n) = \frac{1}{i^n} \frac{\delta^{(n)} W[J]}{\delta J_i \dots \delta J_n}\Big|_{J=0}. \tag{2.11}$$

Next we define the *one particle irreducible* (1PI) functions. A diagram is called 1PI if it stays connected once a single internal line is cut.
So far this did not lead us to any further insight, we found three different kind of "blobs": full n-point functions, connected n-point functions and n-point functions (diagrams) that are 1PI. How do these help solving a quantum theory?
It can be easily understood that it is possible to expand every full Green's function in terms of 1PI diagrams. For the propagator this would for example look as depicted in Fig. (1).

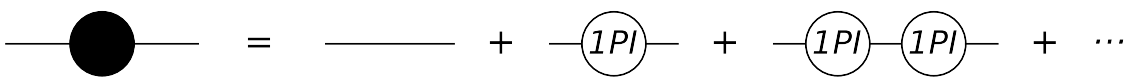

Figure 1: Expansion of the full quark propagator in 1PI diagrams.

In a similar way we can proceed with all other Greens functions by drawing the correponding tree level diagrams with n external legs and replacing all vertices by 1PI functions and all propagators by exact propagators. Due to the 1PI expansion, loops are automatically accounted for. At least formally we have an exact expression for every Green's function $G^{(n)}$. But can this be made a bit more watertight by defining a functional that can be used to generate such an expansion? The answer is yes, as we will soon see.
Let us define the so called *effective action* $\Gamma[\varphi]$ which is the quantum equivalent of the classical action

(note that similarly the classical action would correspond to all the tree level diagrams but with bare vertices and propagators). An expansion in 1PI functions can be formally written as

$$\begin{aligned}\Gamma[\varphi] \equiv -\frac{1}{2}\int \frac{\mathrm{d}^4k}{(2\pi)^4}\tilde{\varphi}(-k)(k^2+m^2-\Pi(k^2))\tilde{\varphi}(k) \\ +\sum_{n=3}^{\infty}\frac{1}{n!}\int \frac{\mathrm{d}^4k_1}{(2\pi)^4}\cdots\frac{\mathrm{d}^4k_n}{(2\pi)^4}(2\pi)^4\delta^{(4)}(k_1+\cdots+k_n)\Gamma^{(n)}(k_1\ldots k_n)\tilde{\varphi}(k_1)\ldots\tilde{\varphi}(k_n)\end{aligned} \tag{2.12}$$

where $\tilde{\varphi}$ is the field in Fourier representation and $\Gamma^{(n)}$ stands for the 1PI-function with n legs. It is convenient working in momentum space but not necessary. Why is such an expansion useful for us now [2]?

Remember that the variation principle applied to the classical action gives us the classical equations of motion. It would be nice to do the same with the effective action in order to get the quantum equations of motion, e.g. equations of motion for the Green's functions that contain all the quantum fluctuations implicitly. This sounds to good to be true since of course knowledge of all the 1PI functions $\Gamma^{(n)}$ would be required.

From the above we can define the following path integral

$$Z_\Gamma[J] = \int \mathrm{D}\varphi\ e^{i\Gamma[\varphi]+\int J\varphi} = e^{iW_\Gamma[J]} \tag{2.13}$$

Here W_Γ is the sum of all connected tree-level diagrams with 1PI vertices as in Eq.(2.12). Note that W_Γ reduces in the classical limit ($\hbar \to 0$) to the sum of bare tree level diagrams only. The path integral then gives the quantum equation of motion

$$\frac{\delta}{\delta\varphi(x)}\Gamma[\varphi] = -J[x], \tag{2.14}$$

which we obtain for the point at which the exponent is stationary (at the classical solution). Let $\phi_J(x)$ be the solution to Eq.(2.14). The approximation in the stationary case is then given by

$$Z_\Gamma = e^{i\Gamma[\phi_J]+\int J\phi_J}. \tag{2.15}$$

As we argued before, in this limit $W_\Gamma[J] \to W[J]$ and from Eq.(2.13) we get

$$W[J] = \Gamma[\phi_J] + \int \mathrm{d}^4x\ J(x)\phi_J(x). \tag{2.16}$$

We see that $W[J]$ and $\Gamma[\Phi_J]$ are related by a Legendre transform uncovering the relation between sources and fields. Now consider

$$\langle\varphi(x)\rangle_J = \frac{\delta}{\delta J(x)}W[J], \tag{2.17}$$

which leads to

$$\langle\varphi(x)\rangle_J = \phi_J(x), \tag{2.18}$$

thereby showing us that the expectation value of the field operator in the presence of the source is the solution of Eq.(2.14). In the absence of sources we will have

$$\frac{\delta}{\delta\phi}\Gamma[\phi] = 0, \tag{2.19}$$

which has the solution $\phi = const$ as it should not surprise us due to the Poincare invariance of the ground state. However, in a system with broken symmetry there might actually be position dependend

[2] Note that the expansion in 1PI functions is not unique. An expansion in general nPI functions is possible for example.

solutions to Eq.(2.19). They are called solitons[3].
With $\Gamma[\phi]$ at hand, the question arises if, similar to the classical action $S = T - V$, it is possible to define an effective potential V_{eff} from the effective action, too. This would certainly be nice, since the minima of V_{eff} would correspond to the true ground state of the theory, including all quantum fluctuations. This ground state could indeed be very different from the ground state obtained from the classical potential. It is indeed possible!

$$\Gamma[\phi] = \int \mathrm{d}^4x \left[-V_{eff}(x) - \frac{1}{2} Z[\phi] \left(\partial\phi(x)\right)^2 + (\text{terms with more derivatives}) \right] \qquad V_{eff} = V_{eff}[\phi] = V_0 + V_2\phi^2 + \dots \tag{2.20}$$

With the concept of the effective action, we are finally able to give Fig. (1) on page 7 a solid meaning. Let us go back a little to the generating functional of connected correlation functions $W[J]$. We already saw that

$$\frac{\delta^n W[J]}{i\delta J(x_1)\dots i\delta J(x_n)} = i \left\langle T(\varphi(x_1)\dots\varphi(x_n))\right\rangle_c \tag{2.21}$$

and specifically

$$\frac{\delta^2 W[J]}{i\delta J(x_1) i\delta J(x_2)} = i \left\langle T(\varphi(x_1)\varphi(x_2))\right\rangle = -iS(x_1, x_2), \tag{2.22}$$

which is the exact propagator. Taking the derivative with respect to $J(y)$ of Eq.(2.14) gives

$$\frac{\delta}{\delta J(y)} \frac{\delta\Gamma}{\delta\phi(x)} = -\delta^{(4)}(x-y). \tag{2.23}$$

The left hand side can be evaluated using the chain rule

$$\begin{aligned} \frac{\delta}{\delta J(y)} \frac{\delta\Gamma}{\delta\phi(x)} &= -\int \mathrm{d}^4x \, \frac{\delta\phi(z)}{\delta J(y)} \frac{\delta^2\Gamma}{\delta\phi(z)\delta\phi(x)} \\ = \int \mathrm{d}^4x \frac{\delta^2 W}{\delta J(y)\delta J(z)} \frac{\delta^2\Gamma}{\delta\phi(z)\delta\phi(x)} &\stackrel{!}{=} -\delta^{(4)}(x-y) \end{aligned} \tag{2.24}$$

and it follows

$$\left(\frac{\delta^2 W}{\delta J \delta J}\right)_{xy} = \left(\frac{\delta^2\Gamma}{\delta\phi\delta\phi}\right)^{-1}_{xy} \tag{2.25}$$

and we see that

$$\left(\frac{\delta^2\Gamma}{\delta\phi(x)\delta\phi(y)}\right) = S^{-1}(x,y) \tag{2.26}$$

Similar we can proceed for a higher number of fields, using the chain rule

$$\frac{\delta}{\delta J(z)} = i\int \mathrm{d}^4w \, \frac{\delta\phi(w)}{\delta J(z)} \frac{\delta}{\delta\phi(w)} = i\int \mathrm{d}^4w \, \underbrace{\frac{\delta W[J]}{\delta J(w)\delta J(z)}}_{S(z,w)} \frac{\delta}{\delta\phi(w)} \tag{2.27}$$

and

$$\frac{\partial}{\partial\alpha} M^{-1}(\alpha) = -M^{-1} \frac{\partial M}{\partial\alpha} M^{-1}$$

we find for example

$$\frac{\delta^3 W[J]}{\delta J(x)\delta J(y)\delta J(z)} = i\int \mathrm{d}^4u \, \mathrm{d}^4v \, \mathrm{d}^4w \; S(x,u)S(y,v)S(z,w) \frac{\delta^3\Gamma[\phi]}{\delta\phi(x)\delta\phi(y)\delta\phi(z)}. \tag{2.28}$$

This is nothing else but a proper derivation of the decomposition of the three-point function, as it is show in Fig. (2)
With all these tools at hand, the following section is devoted to the derivation of the Dyson-Schwinger equations. These will actually relate the Green's functions to each other.

[3]Sidney Colemans "Aspects of symmetries" is a terrific read on that [18].

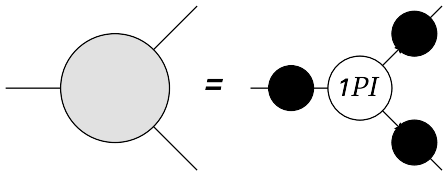

Figure 2: 1PI-expansion of the connected three point function.

2.1.3 Derivation of the Dyson-Schwinger Equations

After discussing the functional integral formalism, I am going to derive the Dyson-Schwinger equations in this section. As we have learned from the preceding sections, obtaining Green's functions of a strongly interacting field theory is hard (and we did not even make it a non-Abelian gauge theory yet).
As one remembers from freshman physics, we get the classical equations of motions for our fields from variation of the classical action (Noether's theorem). In an interacting quantum theory things are not that easy any more. The idea behind Dyson-Schwinger equations is to derive *quantum* equations of motion, that relate different Green's functions in a similar way.
Again, we consider the path integral

$$Z[J] = \int D\varphi \; e^{iS+\int J_a \varphi_a}, \tag{2.29}$$

now for a set of fields φ_a, $a = 1, \ldots, n$. In a classical theory we required the action to be stationary under the variation

$$\varphi_a(x) \to \varphi'_a(x) = \varphi_a(x) + \delta\varphi_a(x), \tag{2.30}$$

which we can perform by analogy for our quantum theory, assuming the field space measure being invariant under this variation, too ($\mathrm{D}\varphi = \mathrm{D}\varphi'$). It follows then

$$0 = \delta Z[J] = i \int \mathrm{D}\varphi \; e^{iS+\int J_b \varphi_b} \int \mathrm{d}^4x \; \left(\frac{\delta S}{\delta \varphi_a(x)} + J_a(x) \right) \delta\varphi_a(x) \tag{2.31}$$

Taking n functional derivatives wrt. $J_{a_j}(x_j)$, $j = 1, \ldots, n$, i.e.

$$\frac{1}{i} \frac{\delta}{\delta J_{a_n}(x_n)} \cdots \frac{1}{i} \frac{\delta}{\delta J_{a_1}(x_1)} \delta Z[J] \tag{2.32}$$

gives

$$\begin{aligned} 0 = i \int \mathrm{D}\varphi \; \varphi_{a_n}(x_n) \ldots \varphi_{a_1}(x_1) e^{iS+\int J_b \varphi_b} \left(\frac{\delta S}{\delta \varphi_a(x)} + J_a(x) \right) \delta\varphi_a(x) \\ + i \int D\varphi \; e^{iS+\int J_b \varphi_b} \varphi_{a_n}(x_n) \ldots \varphi_{a_2}(x_2) \delta\varphi_1(x_1) \\ + \ldots \\ + i \int D\varphi \; e^{iS+\int J_b \varphi_b} \varphi_{a_n}(x_n) \ldots \varphi_{a_{j+1}}(x_{j+1}) \varphi_{a_{j-1}}(x_{j-1}) \ldots \varphi_{a_1}(x_1) \delta\varphi_{a_j}(x_j) \\ + \ldots \\ + i \int D\varphi \; e^{iS+\int J_b \varphi_b} \varphi_{a_{n-1}}(x_{n-1}) \ldots \varphi_{a_1}(x_1) \delta\varphi_{a_n}(x_n). \end{aligned} \tag{2.33}$$

Setting $J = 0$ and using $\delta\varphi_{a_j} = \int \mathrm{d}^4x\ \delta\varphi_a(x)\delta_{a,a_j}\delta^{(4)}(x - x_j)$ we obtain

$$\begin{aligned} 0 = i \int D\varphi e^{iS} \int \mathrm{d}^4x \Bigg[& i\frac{\delta S}{\delta\varphi_a(x)}\varphi_{a_1}(x_1)\dots\varphi_{a_n}(x_n) \\ & + \sum_{j=1}^{n} \varphi_{a_1}(x\dots\delta_{a,a_j})\delta^{(4)}(x - x_j)\dots\varphi_{a_n}(x_n)\Bigg]\delta\varphi_a(x) \end{aligned} \tag{2.34}$$

Since $\varphi_a(x)$ is arbitrary, we can drop it as well as the integral over d^4x . We thus get

$$0 = i\,\langle T\frac{\delta S}{\delta\varphi_a(x)}\varphi_{a_1}(x_1)\dots\varphi_{a_n}(x_n)\rangle + \sum_{j=1}^{n}\langle\varphi_{a_1}(x\dots\delta_{a,a_j})\delta^{(4)}(x - x_j)\dots\varphi_{a_n}(x_n)\rangle \tag{2.35}$$

which are the Dyson-Schwinger equations of the theory. The dependencies generated through this equation are in terms of full n-point functions. These are easily understood in the free case. Let us assume the Lagrangian of a single free scalar field ($n = 1$). Since $\frac{\delta S}{\delta\varphi(x)} = (\partial^2 - m^2)\varphi(x)$ we get

$$\begin{aligned} i\,\langle(-\partial^2 + m^2)\varphi(x)\varphi(y)\rangle &= i(-\partial^2 + m^2)\,\langle\varphi(x)\varphi(y)\rangle \\ &= (-\partial^2 + m^2)G^{(2)}(x - y) \overset{!}{=} \delta^{(4)}(x - y) \end{aligned} \tag{2.36}$$

The Dyson-Schwinger equations in the interacting case follow easily. It will be seen in the preceeding sections how to construct the quark DSE in QCD.
The results founds so far are handy, but how to relate this to the generating functional of the connected correlation functions $W[J]$ or the effective action $\Gamma[\phi]$? We go back and start from Eq.(2.31) which can be rewritten as [12]

$$\begin{aligned} 0 &= \left(\frac{\delta S}{\delta\varphi}\left[\frac{\delta}{i\delta J_a}\right] + J_a\right)\int \mathrm{D}\varphi\ e^{iS+\int J_b\varphi_b} \\ &\Leftrightarrow e^{-iW}\frac{\delta S}{\delta\varphi}\left[\frac{\delta}{i\delta J_a}\right]e^{iW} = -J_a. \end{aligned} \tag{2.37}$$

This equation is equivalent to

$$\frac{\delta S}{\delta\varphi}\left[\frac{\delta}{i\delta J_a} + \frac{\delta W}{\delta J_a}\right]\cdot 1 = -J_a, \tag{2.38}$$

where the "1" indicates that all derivatives shall be applied to everything on the right of the operator. Similarly, we can use the chain rule from Eq.(2.27) with which Eq.(2.37) turns into (when setting $J = 0$)

$$\frac{\delta\Gamma}{\delta\phi} = \frac{\delta S}{\delta\varphi}\left[\phi(x) + i\int \mathrm{d}^4z\ \left(\frac{\delta^2\Gamma}{\delta\phi(z)\delta\phi(x)}\right)^{-1}\frac{\delta}{\delta\phi(z)}\right]\cdot 1. \tag{2.39}$$

This is the Dyson-Schwinger master equation, it generates all Dyson-Schwinger equations in terms of 1PI functions and relates variations of the classical action wrt. to the field operators to variations of the effective action.
The Dyson-Schwinger equation for the propagator is obtained by taking the derivative wrt. the field once more

$$\frac{\delta^2\Gamma}{\delta\phi(x)\delta\phi(y)}\Big|_{J=0} = \frac{\delta}{\delta\phi(x)}\frac{\delta S}{\delta\varphi}\left[\phi(y) + i\int \mathrm{d}^4z\ \left(\frac{\delta^2\Gamma}{\delta\phi(z)\delta\phi(y)}\right)^{-1}\frac{\delta}{\delta\phi(z)}\right]. \tag{2.40}$$

To conclude: We have found three equivalent formulations of the Dyson-Schwinger equations [13, 20]

$$\left(-\frac{\delta S}{\delta\varphi_a}\left[\frac{\delta}{\delta J}+J_a\right]\right)Z[J] = 0 \qquad \text{(full)} \tag{2.41}$$

$$-\frac{\delta S}{\delta\varphi_a}\left[\frac{\delta W}{\delta J}+\frac{\delta}{\delta J}\right]+J_a = 0 \qquad \text{(connected)} \tag{2.42}$$

$$\frac{\delta S}{\delta\varphi_a}\left[\phi+\frac{\delta^2 W}{\delta J_x \delta J_z}\frac{\delta}{\delta\phi_z}\right] = \frac{\delta\Gamma}{\delta\phi_a} \qquad \text{(1PI)} \tag{2.43}$$

These give all Green's functions after setting the sources to zero, $J = 0$.

2.2 Quantum Chromodynamics

This section is meant to give a short overview of the gauge theory, that is believed to describe all phenomena encountered in the strong interactions. We emphasize the aspects relevant in the following sections.
Quantum Chromodynamics (QCD) offers a variety of puzzles and its mathematical foundation is anything but settled. A few comments will be given here, however for a thorough overview the reader is refered to the literature, e.g. [10].

2.2.1 Quantum Chromodynamics as a Quantum Theory

Quantum Chromodynamics is formulated as a Yang-Mills theory with quarks as its fundamental matter degrees of freedom. It is known today that these are invariant under a local SU(3) gauge transformation, which comes with the introduction of eight non-Abelian gauge fields. The latter are called gluons. The Lagrangian of QCD (in Euclidian space time) is given by

$$\mathcal{L} = \bar{q}(x)(-\not{D}+m)q(x) - \frac{1}{4}\mathrm{Tr}\ F^a_{\mu\nu}(x)F^{a\mu\nu}(x), \tag{2.44}$$

with the covariant derivative $D_\mu = \partial_\mu + igT^a A^a_\mu(x)$. The matter fields are usually taken to be in the fundamental representation of the group which corresponds to three colors. Further the above equation can be written for a number of quark flavors, the difference being that q are then interpreted as vectors and $(-\not{D}+m)$ as a matrix in flavor space.
Eq.(2.44) comes with some complications due to its non-Abelian nature. The field strength F, which in differential geometry langauge is nothing else than the curvature (relating internal spaces at different space-time points), is given in terms of the gauge connection A as

$$F = \mathrm{d}A + A \wedge A \tag{2.45}$$

This, as one can easily see when put into the kinetic term in the Lagrangian Eq.(2.44), produces gauge boson interaction terms which would be absent in an Abelian theory.
QCD further has the peculiarity of asymptotic freedom, decoupling its degrees of freedom in the high energy limit and rendering it a free theory, whereas in the regime below 1 GeV it is strong and highly non linear. This non-linear regime shows a few features that cannot be inferred from the classical Lagrangian given above for they are of a purely quantum nature. Chiral symmetry breaking and confinement are the two important puzzles encountered here. These shall be discussed in the following sections. However before doing so we would like to define the path integral for Quantum Chromodynamics, similar to what was discussed before.
The naïve ansatz for the generating functional of full Green's function with fermionic quark fields and bosonic gluon gauge fields would be

$$Z[J,\bar{\eta},\eta] = \int D[A,\bar{q},q]e^{-S[A,\bar{\Psi},\Psi]+\int AJ+\bar{\eta}q+\bar{q}\eta} \tag{2.46}$$

with the action defined by Eq.(2.44). Note that with this action there is no covariant conjugate momentum to the A_0 component, leaving us with an ambiguity. Related to that, the Haar measure here includes integration over an infinite number of gauge equivalent configurations. The choice of a representative from the equivalence class of gauge equivalent field configurations is realized by means of a gauge condition, for example

$$\partial_\mu A^\mu = 0, \tag{2.47}$$

which reduces the independent field components and thus removes the above ambiguity. We can follow the Faddev-Popov description of eliminating gauge equivalent configurations by defining a hypersurface in the gauge field space that we hope is only intersected once by each gauge orbit. This allows for a covariant quantization then. Thus inserting the Faddev-Popov determinant together with a gauge condition $\Delta(A)\delta(f^a(A))$, which in a covariant gauge would be $f^a = \partial_\mu A^{a\mu} - \zeta^a$, we get

$$Z[J,\bar{\eta},\eta] = \int D[A,\bar{q},q]\Delta(A)\delta(f^a(A))e^{-S[A,\bar{q},q]+\int A^a J^a + \bar{\eta}q + \bar{q}\eta}. \tag{2.48}$$

A further issue here is that the gauge condition f^a might not be fulfilled uniquely owing to the nature of the gauge orbits being closed and hence intersecting the gauge condition hypersurface at least twice. This leads to the so called Gribov copies [16].
The Faddev-Popov description comes with a drawback in the case of a non-abelian gauge theory. Unfortunately the Faddev-Popov determinant is not independent of A_μ, and hence must be included in the path integral explicitly. This can be dealt with at least up to a certain rigouresness within the framework of the BRST-cohomolgy [14, 15]. We are confronted with the introduction of seemingly spurious zero-norm states, the so called ghost. The appearance of these fields, violating the spin-statistics theorem, guarantees the conservation of unitarity. Furthermore BRST symmetry ensures that they do not appear in asymptotic states. This formalism then leads to

$$Z[J,\bar{\eta},\eta] = \int D[A,\bar{q},q,\bar{\sigma},\sigma]e^{-\int \mathrm{d}^4x\ \mathcal{L}_{eff}+\int A^a J^a + \bar{\eta}q + \bar{q}\eta + \bar{\sigma}^a c^a + \bar{c}^a \sigma^a}, \tag{2.49}$$

where (in a covariant gauge)

$$\begin{aligned}\mathcal{L}_{eff} = \frac{1}{2}A^a_\mu\left(-\partial^2\delta_{\mu\nu} - (\frac{1}{\zeta}-1)\partial_\mu\partial_\nu\right)A^a_\nu + \bar{c}^a\partial^2 c^a + gf^{abc}\bar{c}^a\partial_\mu(A^c_\mu c^b)\\ -gf^{abc}(\partial_\mu A^a_\nu)A^b_\mu A_n u^c + \frac{1}{4}g^2 f^{abc}f^{cde}A^a_\mu A^b_\nu A^c_\mu A^d_\nu + \bar{q}(-\not{D}+m)q\end{aligned} \tag{2.50}$$

All these issues are not properly settled until today and a proper discussion of this subject would not fit this frame, but can be found for example in [17]. Eq.(2.50) will form the basis of the investigations done here.

QCD is multiplicative renormalizable, therefore the bare quantities in Eq.(2.50) can be replaced by their renormalized counterparts

$$\begin{aligned} q \to Z_2^{1/2}q \quad m \to Z_m m \quad A^a_\mu \to Z_3^{1/2}A^a_\mu \\ g \to Z_g g \quad c \to \tilde{Z}_3^{1/2}c \quad (\zeta \to Z_\zeta \zeta)\end{aligned} \tag{2.51}$$

and one finds the Slavonv-Taylor identities

$$\begin{aligned} Z_{1F} &= Z_2 Z_g Z_3^{1/2} \\ \tilde{Z}_1 &= \tilde{Z}_3 Z_g Z_3^{1/2} \\ Z_1 &= Z_g Z_3^{3/2}\end{aligned} \tag{2.52}$$

It can be seen from Eq.(2.52) that the renormalization constants of the QCD Green's functions are related and it is indeed difficult to find a truncation that can be renormalized consistently. In parts of this thesis renormalization will play a secondary role for reasons that soon will be apparent. This negligence is due to the fact that a quantum system inside a magnetic field shows a much easier renormalization behavior than in vacuum, since it lives effectively in three dimensions as will be seen.

2.2.2 Symmetries and Symmetry Breaking

As already mentioned before, a classical theory and its quantized version do not need to share the same symmetries. Let us look at the QCD Lagrangian Eq.(2.44) in the chiral case $m = 0$ with two quark flavors (up and down) for simplicitly. By introducing chirality projectors $P_{L/R} = (1 \pm \gamma^5)/2$ this can be decomposed into left and right handed fields[4]

$$-\bar{q}\not{D}q = -\bar{q}\not{D}(P_L + P_R)q = -\bar{q}_L\not{D}q_L - \bar{q}_R\not{D}q_R \tag{2.53}$$

This Lagrangian has obviously a $U(2)_L \otimes U(2)_R$ symmetry, which can be decomposed into $SU(2) \otimes U(1)_L \otimes SU(2)_R \otimes U(1)_R$ or alternatively as $SU(2)_V \otimes SU(2)_A \otimes U(1)_V \otimes U(1)_A$. These match the following symmetry operations (with τ^a being the $SU(2)$ generators)

$$q(x) \to q'(x) = \quad e^{i\theta^a\tau^a}q(x) \quad \textbf{(isospin)} \tag{2.54}$$

$$q(x) \to q'(x) = \quad e^{i\gamma^5\theta^a\tau^a}q(x) \quad \textbf{(isovector-axialvector)} \tag{2.55}$$

$$q(x) \to q'(x) = \quad e^{i\theta}q(x) \quad \textbf{(baryon number)} \tag{2.56}$$

$$q(x) \to q'(x) = \quad e^{i\gamma^5\theta}q(x) \quad \textbf{(isoscalar-axialvector)} \tag{2.57}$$

where the isoscalar-axialvector symmetry is actually spoiled by the axial anomaly coming from the quantum nature of the QCD vacuum and therefore does not correspond to a conserved quantity.
It is obvious that introducing a mass term would break the chiral symmetry since it would mix left and right handed fields

$$\bar{q}Mq = \bar{q}_L M q_R + \bar{q}_R M q_L, \tag{2.58}$$

where M is a 2×2 diagonal matrix in flavor space, assuming $m_u = m_d$ isospin is still a godd symmetry. Due to the smallness of the mass terms compared to the hadronic scale in QCD, we can treat those terms as a small perturbation to an approximate chiral theory.
Although the classical Lagrangian of QCD is chiral, in the full quantum theory this symmetry will be dynamically broken. This explains why the mass of a constituent quark is around 300 MeV whereas the mass of the bare (u- and d-) quarks are less than 10 MeV. Due to self interaction with the non-perturbative QCD vacuum, quarks gain a large mass dynamically. This is a distinct non-perturbative feature, since it even appears in the case of chiral bare quarks, a property perturbation theory fails to describe. This explains why an investigation of the non-perturbative quantum dynamics is necessary in order to grasp an understanding of chiral symmetry breaking. The Dyson-Schwinger equations are useful here, since they do not rely on the expansion of some small parameter but rather relate Green's function to each other in an exact way.
An important order parameter for the transition between the chirally broken and the restored phase is the chiral condensate, which is nothing more but the vacuum correlator of the scalar bilinear $\bar{q}q$ at the same space time point

$$-\langle\bar{q}q\rangle = \lim_{x\to y} S(x,y). \tag{2.59}$$

In a Poincare invariant theory this quantity is position independent and hence can be written in form of

$$-\langle\bar{q}q\rangle = \mathrm{Tr}\left(S(p)\right), \tag{2.60}$$

the trace hereby including integration over momenta and summation over all indices. This quantity will be in the center of the investigations presented in the follwowing sections.

[4]Chirality hereby meaning the spin projection onto the momentum direction, a quantity that for a massive particle certainly depends on the reference frame.

2.2.3 Confinement

A proper definition of the word confinement is not without controversy [28]. In the simplest case confinement means *color confinement* referring to the absence of color charged states in the spectrum. In terms of lattice gauge theory one can define order parameters for confinement, the most important being the so called Wilson loop related to the static quark potential.
The Wilson-Loop is defined as the expectation value of links around a plaquette[5], a quantity a continuum theory is missing.

$$W(C) = \langle \prod_{\text{plaq.}} U(C_i) \rangle \tag{2.61}$$

It can be shown that the expectation value of the static rectangular contour $R \times T$ is related to the static inter-quark potential

$$W(R,T) \propto e^{-V(R)T} \quad (\text{as } T \to \infty) \tag{2.62}$$

If the gauge theory is in the confined phase, the potential is asymptotically linear

$$V(R) = \sigma R + 2V_0 \tag{2.63}$$

with σ being the string tension. So far this quantity can only obtained from lattice calculations. The Wilson-Loop has thus an area-law falloff and correlations over large distances vanish.
There exists a quantity called the dressed Wilson-Loop [21, 23] which is the Fourier transform of the chiral condensate with respect to the magnetic field. Area and magnetic field strength are hereby taken as dual variables. This quantity should also show a falloff similar to the usual Wilson-Loop. To investigate this quantity in the continuum with the ansatz that is employed in this thesis, one needs to include the quark loop for the gluon self energy in order to have inverse magnetic catalysis. The chiral condensate as a function of the external magnetic field is then Lebesgue integrable and the Fourier transform exists.
A further order parameter for confinement is the so called dressed Polyakov-Loop, which is the Fourier transform of the quark condensate wrt. the U(1) valued boundary phase φ and therefore can only be calculated on a torus at finite temperature (otherwise it would not be a loop)

$$\Sigma = \int_0^{2\pi} \frac{\mathrm{d}\varphi}{2\pi} e^{-i\phi} \langle \bar{q}q \rangle_\varphi \tag{2.64}$$

which is an order parameter for center symmetry breaking/restoration. A non-zero value of Σ indicates a broken center symmetry phase and thus a deconfined phase of the gauge theory. Detailed discussions can be found in [24–27]
The definitions given here concerning confinement are everything but complete for this is meant to give an overview only. An emphasis was placed on topics relevant to the Dyson-Schwinger framework and magnetic fields. A very comprehensive study can be found in [28]. There are of course other order parameters such as the thin Polyakov-Loop or the 't Hooft Loop. Even more important there exists no rigorous mathematical definition of what confinement actually is and how it can be deduced from Yang-Mills theories. There are however sophisticated ansätze in the literature, such as for example in terms of the Kugo-Ojima criterium [29] and the Gribov-Zwanziger scenario [30, 31]

2.2.4 Dyson-Schwinger Equations for QCD

Section 2.1.3 gave an introduction on how to derive the Dyson-Schwinger equations in a systematic way. In this section the action derived from Eq.(2.50) shall be used to derive the quark DSE as an

[5] For a definition and introduction into lattice gauge theory see for example [19].

example [20].
From Eq.(2.35) using

$$\frac{\delta S}{\delta \bar{q}(x)} = (-\partial\!\!\!/ + m)q(x) - ig\gamma^\mu t^a A^a_\mu(x)q(x)$$

one gets

$$\begin{aligned} \delta^{(4)}(x-y) = \langle \frac{\delta S}{\delta \bar{q}(x)} \bar{q}(y) \rangle = (-\partial\!\!\!/ + m)S(x,y) \\ -ig \int \mathrm{d}^4 z \; \mathrm{d}^4 z' \; \delta^{(4)}(x-z)\delta^{(4)}(x-z') \, (\gamma^\mu t^a) \, \langle q(z)\bar{q(y)}A^a_\mu(z') \rangle \end{aligned} \tag{2.65}$$

Hereby including the $1PI$ qqg-vertex, which can be expanded similar to Eq.(2.28), giving pictorially

$< q(z)\bar{q}(y)A^a_\mu(z') >=$

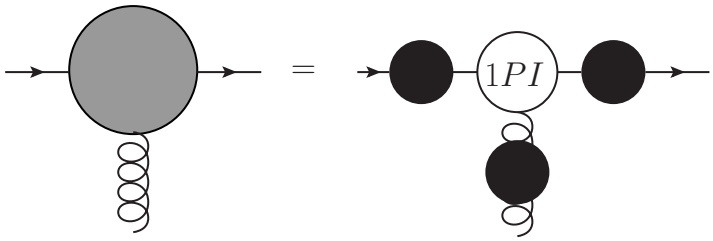

$$= -\int \mathrm{d}^4 u \; \mathrm{d}^4 v \; \mathrm{d}^4 w \; S(z,u)\Gamma^{b\nu}(u,v,w)S(v,y)D^{ba}_{\nu\mu}(z',w) \tag{2.66}$$

Inserting this into Eq.(2.65) and multiplying by $S^{-1}(x,y)$ yields

$$S^{-1}(x,y) = S_0^{-1}(x,y) + igC_F\gamma^\mu S(x,y)\Gamma^\nu(y)D_{\mu\nu}(x,y) \tag{2.67}$$

It was assumed here that the qqg-vertex is a local interaction $\Gamma^{b\nu}(u,v,w) = t^b\Gamma^\nu(v)\delta^{(4)}(u-v)\delta^{(4)}(w-v)$ furthermore the color factor $C_F\delta_{ij} = (t^a t^a)_{ij}$ was written explicitly. Eq.(2.67) can be seen pictorially in Fig. (3). In a simliar way one can continue with the other 2-point functions in QCD. The gluon

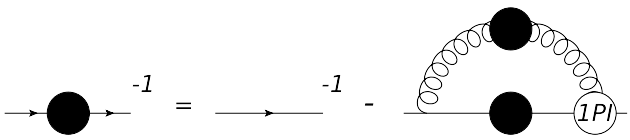

Figure 3: Pictorial representation of the quark DSE

DSE is shown in Fig. (4), an exact derivation is omitted here for brevity. Fig. (5) represents the ghost DSE. Already at this point it becomes apparent that a solution of these equations is intrinsically difficult. All these two point functions are coupled in a nontrivial way. Further they depend on higher n-point functions that I did not even derive here.
Since the effective action is a well defined quantity (although it contains an infinite number of 1PI terms), the system of all infinitely many Dyson-Schwinger equations is closed and by solving all of them the quantum theory would be known exactly.

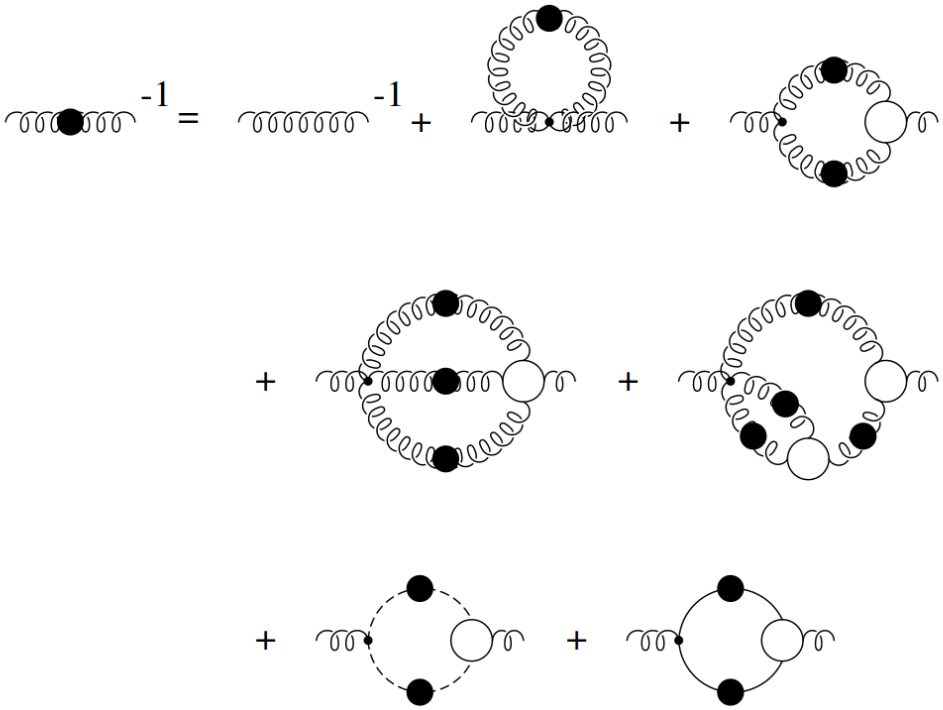

Figure 4: Diagrams contributing to the gluon DSE. All loop diagrams except that containing the quark loop would be absent in an Abelian theory.

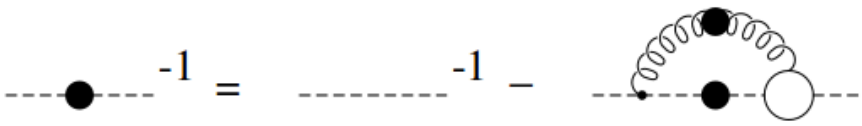

Figure 5: Ghost DSE

2.3 Magnetic Catalysis

Magnetic catalysis [32] is defined as the enhancement of dynamical chiral symmetry breaking by an external magnetic field. The mass of quarks in Quantum Chromodynamics arises largely from its self interaction or, statet otherwise, is caused by the non-trivial vacuum structure of QCD. This work will be concerned with the influence of a magnetic field on a quantum system in thermal equilibrium. The possible applications of such investigations, such as heavy ion collisions [33] or the evolution of the earliy universe [34], involve systems far from equilibrium of course. Therefore further studies are certainly interesting.

A magnetic fields modifies the quantum vacuum in an essential way. It should be noted that the dynamics in QCD are very different compared to the related effects in superconductors. In superconductors the condensate in form of cooper pairs are charged, therefore showing the well known Meissner effect in the ground state. Furthermore the magentic moments of the fermions building the Cooper pair are antiparallel, so that an external magentic field makes this configuration unfavorable. The magnetic field tends to reduce this fermion-fermion correlation (see [32] for a detailed discussion).

In contrast to that, the external field enhances the chiral condensate in QCD, since the (chiral) condensate is electrical neutral and the magnetic moments of quark and antiquark are aligned. At

zero temperature a magnetic field catalyses the generation of a non zero quark condensate, even at weakest interactions. The underlying reason was found in [35] to be the effective dimensional reduction of the charged fermionic system in the external field, which comes from the Landau quantization of fermionic "orbits" in a plane perpendicular to the direction of the magnetic field (as far as this simple picture is valid for not too complicated forms of the external field). The dynamics of this effect are rather intricate and the following sections will treat it in greater detail.
It was found that the effects of a magnetic field on the QCD vacuum are even more complicated than what was described above. According to [36] two competing mechanisms are observed, both effecting the chiral condensate. The direct coupling of the magentic field to (valence) quarks enhances chiral symmetry breaking, whereas the modification of the gluonic sector due to the QCD background (vacuum sea) reduces the effect.
Once the quantum system is at a finite temperatur the magnetic catalysis gets modified. For rather large temperatures thermical fluctuations can break up the fermion-antifermion condensate so that there is a critical temperature $T_c(eH)$ at which the transition between chirally broken and restored phases occurs, as it was in the zero field case.

3 Quantum Theories in Magnetic Fields

As we discussed in the introduction, (external) magnetic fields in quantum field theories are part of a lot of interesting physical effects from particle physics to cosmology. Moreover they are a unique theoretical tool, that can be used to modify quantum theories.
The color charge of quarks is screened, leaving us with actually no $SU(3)$ charged objects to play with. However even in the presence of (color) confinement, the electric charge is *not* screened due to its Abelian nature. This gives a nice handle to probe color charged objects directly.
However including an external field in a quantum theory is not easy. Therefore we will describe the basics of how to treat magnetic fields in a quantum theory and especially how to use them in the Dyson-Schwinger formalism in the following chapter.

3.1 Fermion Eigenfunctions in an Abelian Background Field

There are different ways of treating a quantum field theory in an external $U(1)$ field. One way would be to introduce sources to which the charged fields of the theory can couple. This however only makes sense when the Abelian field is weak enough to be treated perturbatively and additionally if the magnetic field asymptotically vanishes. More importantly a magnetic field breaks Poincaré invariance explicitly, rendering the well known expansion in Fourier modes in a perturbative atempt useless.
In reality magnetic fields are often strong, as for expample in heavy ion collisions or neutron stars, and their effect must be included to every order. Furthermore we can construct magnetically non-interacting asymptotic states only in very special cases, as for example for a field that covers only a finite volume.

The case of a strong magnetic field however is quasi classical. In this case, we can treat the interaction of the background Abelian field statistically by solving the equations of motion of, for example, a fermion in that field. By doing so, the eigenfunctions of that particle are obtained and we can start expanding the field theory that we are actually interested in (such as QCD) in those eigenfunctions.
The advantages are obvious: by transforming into the eigensystem of the particle in the background field, we achieve that, for example, the Dirac equation (see Eq.(3.1)) of a fermion including the background field now looks like the Dirac equation of a free fermion (only in a different eigensystem).

By transforming the Feynman rules into position space, using the new eigensystem, we obtain that the effect of the external field is already fully accounted for in the Green's functions. We get a set of new Feynman rules that include the interaction with the external field to every order. In some sense, this can be seen as the quantum theory implemented in a medium rather than the vacuum. We will find some similarities to the imaginary time formalism, that one can use for finite temperature field theory, therefore. Later we will see that fermions in a magnetic fields come with the discretization of one of their eigenvalues due to the compactification on Landau levels, simliar as it is with the Matsubara quantization for a compact time dimension.
In order to deduce these Feynman rules, we begin with the Dirac equation of a fermion in an arbitrary external U(1) field

$$(i\gamma \cdot \Pi + m)\Psi(x) = 0 \tag{3.1}$$

where $\Pi_\mu = \partial_\mu + ieA_\mu(x)$ is the covariant derivative, which prevents the plane wave expansion of the equation. Here e is the electric charge. Without loss of generality we took a fermion with charge one here. Of course rescaling $e \to q_f e$ is straightforward. For simplicity let us consider $A_\mu(x) = (0, 0, Hx, 0)$ which corresponds to a constant magnetic field along the z-direction. In principle, every step performed here can be done with an arbitrary A_μ. However it can get arbitrary complicated as well and we will stick to this instructive case.
It was shown by Ritus [37, 38] that the fermion two-point greens function can only depend on four independend scalar structures

$$\gamma\Pi, \quad \sigma F, \quad (F\Pi)^2, \quad \gamma^5 F F^* \tag{3.2}$$

where I omitted indices that are being summed over. Hereby $F = \mathrm{d}A$ is the field strength tensor of the magnetic field, with ${}^*F$ being its Hodge dual. Further $\sigma^{\mu\nu} = -i/2[\gamma^\mu, \gamma^\nu]$ is the anticommutator of two Dirac matrices. It can be seen that all the operators in Eq.(3.2) commute with $(\gamma\Pi)^2 = \Pi^2 - \frac{1}{2}e\sigma F$. This tells us that they possess the same eigenfunctions. Therefore we are left with solving the eigenvalue equation

$$(\gamma\Pi)^2 E_p = p^2 E_p \tag{3.3}$$

where we inserted the generic eigenvalue p^2 on the right hand side of Eq.(3.3), that remains to be determined. Furthermore, we see other operators exist, that commute with $(\gamma\Pi)$. These are $i\partial_0$, $i\partial_3$ and $i\partial_2$, corresponding to the eigenvalues $p_\parallel = (p_0, p_3)$ and p_2. The eigenfunctions in 0,2- and 3-direction are still plane waves. However the 1-direction resembles a harmonic oscillator.
There is one other operator, which is denoted by

$$\mathcal{H} = -(\gamma\Pi)^2 + \Pi_0^2 = \Pi_1^2 + \Pi_2^2 - eH\Sigma^3, \tag{3.4}$$

that has the same eigenfunctions as the operators given in Eq.(3.2). Here Σ^3 is the third Pauli spin matrix, given by $\Sigma^3 = \sigma^{12}$. We have $\mathcal{H}E_p = kE_p$. The eigenfunctions will be of the form

$$E_p = E_{p,\sigma}\Delta(\sigma) \tag{3.5}$$

where $\Delta(\sigma) = \frac{1}{2}(1 + \sigma\Sigma^3)$ is the spin projector along the z-axis with eigenvalue $\sigma = \pm 1$. With the above knowledge, the form of the eigenfunctions should be clear

$$E_{p,\sigma} = N_\sigma e^{i(p_0x_0 - p_2x_2 - p_3x_3)} F_{k,p_2,\sigma} \tag{3.6}$$

Here $F_{k,p_2,\sigma}$ is an unknown scalar function and N_σ a generic normalization. This ansatz can be plugged into Eq.(3.3) and solved. An instructive derivation can be found in [46]. After doing so, we obtain

$$\begin{aligned} E_{p,\sigma}(x) &= N(n)e^{i(p_0x_0 - p_2x_2 - p_3x_3)} D_n(\rho) \\ \rho &= \sqrt{2|eH|}\left(x_1 - \frac{p_2}{eH}\right) \\ N(n) &= \frac{(4\pi\,|eH|)^{\frac{1}{4}}}{\sqrt{n!}}, \end{aligned} \tag{3.7}$$

where $D_n(\rho)$ are the parabolic cylinder functions, which can be expressed in terms of Hermite polynomials

$$D_n(x) = 2^{-n/2}e^{-x^2/4}H_n(x/\sqrt{2}) \tag{3.8}$$

of order

$$n = k + \frac{\sigma}{2}sgn(eH) - \frac{1}{2}.$$

Furthermore between the eigenvalues one can find the relation

$$\begin{aligned} p^2 &= p_0^2 - p_3^2 - k \\ k &= |eH|(2n+1) + \sigma|eH| \end{aligned} \tag{3.9}$$

and realize that k are the eigenvalues of a harmonic oscillator with $k \in \mathbb{N}_0$. Here, we can also see an interesting feature: This harmonic oscillator is supersymmetric in the quantum mechanical sense. Except for the lowest eigenvalue (the lowest Landau level), every fermionic energy value is degenerate with respect to two spin orientations differing by ± 1. Furthermore, the transition between two adjacent energy levels (note these are fermionic eigenstates) is identical to a bosonic spin one transition of a harmonic oscillator. We can regroup those eigenvalues and denote them by a new quantum number $l \in \mathbb{N}_0$. However we need to keep in mind that all values of l, except for $l = 0$, are twice degenerate.

The reason for this is that k would be negative for $l = 0$ if not $\sigma = \mathrm{sgn}(eH)$. The quantum number k can therefore be replaced by $p_\perp = \sqrt{2|eH|l}$, which we could call an orbital "momentum" quantum number. In fact, l is the total angular momentum quantum number for each Landau level, of course realized by two spin directions.
Finally, we see that the eigenvalues corresponding to the Ritus eigenfunctions are (p_0, p_3, p_2, l) or equivalently the "momenta" $(p_0, 0, p_\perp, p_3)$. Effectively, the magnetic field reduces the problem to 2+1 dimensions, breaking an O(4) symmetry to an $O_\parallel(2) \otimes O_\perp(2)$. The $O_\perp(2)$ symmetry is not obvious from the definition of $p_\perp$. Actually $O_\perp(2)$ represents the gauge freedom, for we could have chosen a different vector potential giving the same magnetic field (but a different equivalent definition of $p_\perp$). For $l = 0$ we have $p_\perp = 0$, so that the problem is in fact 1+1 dimensional on the lowest Landau level (LLL). This removes UV- but introduces IR-divergences.
It can be shown that the Ritus basis is in fact orthonormal and complete [41–44],

$$\int \mathrm{d}^4x \quad \bar{E}_p(x) E_{p'}(x) \quad = \quad (2\pi)^4 \delta^{(4)}(p - p')\Pi(l) \tag{3.10}$$

$$\sum\!\!\!\!\!\!\int \frac{\mathrm{d}^4 p}{(2\pi)^4} E_p(x) \bar{E}_p(y) \quad = \quad (2\pi)^4 \delta^{(4)}(x - y), \tag{3.11}$$

where

$$\sum\!\!\!\!\!\!\int \frac{\mathrm{d}^4 p}{(2\pi)^4} = \sum_{l=0}^{\infty} \int \frac{\mathrm{d}^2 p_\parallel}{(2\pi)^4} \int_{-\infty}^{\infty} \mathrm{d}p_2 \tag{3.12}$$

and

$$\Pi(l) = \begin{cases} \Delta(\mathrm{sgn}(eH)) & l = 0 \\ 1 & l > 0 \end{cases} . \tag{3.13}$$

Remember, that we are not restricted to such trivial cases of a background field: it was show by Volkov [39, 40] that the fermion eigenfunctions in an arbitrary external abelian field of the form $A_\mu = A_\mu(k \cdot x)$ (any plane wave potential) are

$$\Psi_{pr}(x) \quad = \quad E_p(x) u_{pr} \tag{3.14}$$

$$E_p(x) \quad = \quad \left(1 + e\frac{\gamma \cdot k\gamma \cdot A}{2k \cdot p}\right) \exp\left\{ i \int_0^{k\cdot x} \left[\frac{ep \cdot A(\phi)}{k \cdot p} - \frac{e^2 A^2(\phi)}{2k \cdot p} \right] \mathrm{d}\phi + ip \cdot x \right\}. \tag{3.15}$$

What is now the advantage of the expansion in such eigenfunctions? By construction, the equations of motion for a fermion in the Ritus basis are formally identical with that of a free particle and hence can be used to add a quantum theory, such as QCD, on top. The Dirac propagator and fermion self energy are diagonal in this basis, thus also the self energy $\Sigma(x, x')$ fulfils an eigenvalue equation with eigenvalue $\Sigma(p)$

$$\int \mathrm{d}^4x' \; \Sigma(x, x') E_p(x') = E_p(x)\Sigma(p). \tag{3.16}$$

There is however a drawback that comes with this method. Since neutral particles still have plane waves as their eigenfunctions, an example being the gluon or the photon, complications arise whenever neutral and charged particles couple to each other. Different to the familiar delta-functions guaranteeing momentum conservation, that one encounters in the usual fourier expansion of a field theory, vertices in general do not conserve "momentum" any more.
As indicated by the quotation marks, it might be a bit misleading to use the word momentum here. For a particle having plane waves as its eigenfunctions, momentum is nothing more but the eigenvalues of the Dirac operator. A particle expanded in Ritus functions will have other eigenvalues (see Eq.(3.9)), that one might call quasi-momentum. Coupling two particles that live in different eigenspaces, renders the form of the vertex in (quasi)momentum space very complicated, as shall be seen. However it is

only natural that (physical) momentum is not conserved due to the loss of translational invariance caused by the external field. Still the Ritus eigenvalues (p_0, p_3, p_2, l) are conserved along every fermion line.
In the following section we will derive the Dyson-Schwinger equation for the quark propagator in Ritus functions. We will not be concerned too much with the distinction between momentum and quasi-momentum, for particles will always be expanded in their eigenbasis and it should be clear from the context, what eigenvalue is refered to.

3.2 Quark Dyson-Schwinger Equation in a Background Magnetic field

Wanting to solve the quark Dyson-Schwinger equation derived in section 2.1.3, we need to expand the fermion fields in terms of Ritus-eigenfunctions instead of the usual plane wave Fourier representation [41–43]. Applying this to the Dyson-Schwinger equation for the quark two-point function involves some difficulties, since the quark couples to gluons, which, since they do not carry electric charge, do not couple to the background field. They are to be expanded in plane waves therefore.
Still the gluon is not independent of the Ritus expansion. In fact, the gluon self energy involves fermion loops, which provide back-coupling to the external field (see chapter 5). Nevertheless the fully dressed gluon is diagonal in plane wave space (Fourier space), because the fermions appear in a closed loop only.
Because of these two eigensystems involved, the DS equation in a background magnetic field needs a systematic investigation. I will therefore start from the DS equation in position space and derive the equation in "momentum" space from first principles. Later we will see that we can use the results obtained here to make up some sort of Feynman rules describing a quantum theory in a background magnetic field, with the background field treated statistically and to every order implicitly already in the propagators and vertices of the theory.

The magnetic field here will be taken as constant and being along the z-axis with $A_\mu = (0, 0, Hx, 0)$ as before. Other cases of a magnetic fields are related and also non-constant arbitrary fields can be treated within this method, provided one is able to solve for the eigenfunctions, as was done in the previous chapter. An exponentially decaying field is an example of such a case where the Ritus eigenfunctions can be found analytically [46].
The Dyson Schwinger equation in position space is given by

$$S^{-1}(x, y) = S_0^{-1}(x, y) + M(x, y), \tag{3.17}$$

where the quark self energy is given by

$$M(x, y) = ig^2 C_F \int \mathrm{d}^4x' \mathrm{d}^4y' \; \gamma^\mu S(x, x')\Gamma^\nu(x', y, y')D_{\mu\nu}(x, y'), \tag{3.18}$$

with $C_F\delta_{ij} = (T^aT^a)_{ij}$, T being the $SU(3)$ generators in the fundamental representation. Color indices are omitted in the following calculations. The vertex Γ will be a local interaction, with $\Gamma^\nu(x', y, y') = \Gamma^\nu(y)\delta^{(4)}(x' - y')\delta^{(4)}(y - y')$, so that we obtain the familiar equation

$$G^{-1}(x, y) = G_0^{-1}(x, y) + ig^2 C_F \; \gamma^\mu G(x, y)\Gamma^\nu(y)D_{\mu\nu}(x, y) \tag{3.19}$$

We will now expand this in terms of Ritus eigenfunctions. By multiplying with $\bar{E}_p(x)$ from the left and $E_{p'}(y)$ from the right (where p and p' denote the incoming and outgoing "momenta") the integration over x and y yields

$$\begin{aligned} \int \mathrm{d}^4x\mathrm{d}^4y \; \bar{E}_p(x)S^{-1}(x, y)E_{p'}(y) = &\int \mathrm{d}^4x\mathrm{d}^4y \; \bar{E}_p(x)S_0^{-1}(x, y)E_{p'}(y) \\ &+ \int \mathrm{d}^4x\mathrm{d}^4y \; \bar{E}_p(x)M(x, y)E_{p'}(y). \end{aligned} \tag{3.20}$$

By using the completeness relation Eq.(C.3) we get

$$\begin{aligned}(2\pi)^4\delta^{(4)}(p-p')\Pi(l)(A(p)_\parallel i\gamma p_\parallel + A(p)_\perp i\gamma p_\perp + B(p)) \\ = (2\pi)^4\delta^{(4)}(p-p')\Pi(l)(\gamma p + m) + M(p,p')\end{aligned} \tag{3.21}$$

where $M(p,p')$ is an abreviation for the second term on the right of Eq.(3.20) (the self energy term). This term should better be proportional to $\delta^{(4)}(p-p')\Pi(l)$, a property we will only see later when calculating this term explicitly. We have

$$M(p,p') = g^2 C_F \int \mathrm{d}^4x\ \mathrm{d}^4y\ \bar{E}_p(x)\ \gamma^\mu S(x,y)\Gamma^\nu(y)D_{\mu\nu}(x,y)E_{p'}(y) \tag{3.22}$$

To evaluate this expression we have to use the representation of the fermion propagator in Ritus eigenfunctions. The eigenvalues of the fermion in an external magnetic field in the configuration given above are (p_0, p_3, p_2, l) where l labels the Landau level.
The quantum number p_2 is still a "good" (in terms of corresponding to a Fourier eigenfunction) quantum number, however as seen from the previous chapter, the energy of the fermion is degenerate with respect to this eigenvalue. p_2 merely fixes the origin of the x_1 component of our quantum harmonic oscillator system. The "momenta" the fermion is carrying are $p_\parallel$ and $p_\perp$ or $(p_0, \sqrt{2|eH|l}, 0, p_3)$. The fermion propagator in Ritus representation is given by

$$S(x,y) = \sum\!\!\!\!\!\!\int \frac{\mathrm{d}^4q}{(2\pi)^4}\ E_q(x)\frac{1}{A(q)_\parallel i\gamma q_\parallel + A(q)_\perp i\gamma q_\perp + B(q)}\bar{E}_q(y) \tag{3.23}$$

where the sum/integral is over the eigenvalues (p_0, p_3, p_2, l). Here the integration over p_2 accounts for the degeneracy of states on one Landau level (the spin degeneracy is not meant by that),

$$\sum\!\!\!\!\!\!\int \frac{\mathrm{d}^4q}{(2\pi)^4} = \sum_{l_q=0}^{\infty}\int\frac{\mathrm{d}^2q_\parallel}{(2\pi)^4}\int_{-\infty}^{\infty}\mathrm{d}q_2. \tag{3.24}$$

Before proceeding, one should notice that the form of Eq.(3.23) is used here in analogy to the vacuum case, accounting for the anisotropy by introducing separate dressing functions for the transverse and longitudinal components. In principle one could include all tensor structures for the quark propagator that are allowed by symmetries. The fact that there is an additional structure $F_{\mu\nu}$ gives the possibility for additional terms to appear. I will investigate them in the next section. For now we shall proceed with the simplified quark propagator structure.
The isotropic Fourier representation of the gluon, as it is used in the quenched approximation, is given by

$$D_{\mu\nu}(x,y) = \int\frac{\mathrm{d}^4k}{(2\pi)^4}Z(k^2)\frac{e^{ik(x-y)}}{k^2-i\epsilon}\left(g_{\mu\nu} - (1-\xi)\frac{k_\mu k_\nu}{k^2}\right), \tag{3.25}$$

where the integration is a momentum integration in the conventional sense since the gluon is still diagonal in Fourier space. Quenched means here that the appearance of the quark in the gluon self energy is neglected. Effectively this causes that the gluonic sector is not modified by the magnetic field, although one would need to take such a modification into account in the unquenched case. In the latter case the gluon the does in fact feel the magnetic field due to the modification of the vacuum full of charged fermion anti-fermion pairs, that it is propagating through. Therefore a proper treatment of the structure of the gluon polarization is necessary. A systematic study will befound in chapter 5.
By plugging Eq.(3.23) and Eq.(3.25) into Eq.(3.22) we obtain

$$\begin{aligned}M(p,p') = g^2C_F\sum\!\!\!\!\!\!\int\frac{\mathrm{d}^4q}{(2\pi)^4}\int\frac{\mathrm{d}^4k}{(2\pi)^4}\int\mathrm{d}^4x\mathrm{d}^4y\ \Bigg\{\bar{E}_p(x)\gamma^\mu E_q(x)\tfrac{1}{A(q)_\parallel i\gamma q_\parallel + A(q)_\perp i\gamma q_\perp + B(q)}\bar{E}_q(y)\Gamma^\nu E_{p'}(y) \\ \times\tfrac{e^{ik(x-y)}}{k^2-i\epsilon}Z(k^2)\left(g_{\mu\nu} - \tfrac{k_\mu k_\nu}{k^2}\right)\Bigg\}\end{aligned} \tag{3.26}$$

where we utilized Landau gauge ($\xi = 0$), which we will use from now on. Furthermore this quark self-energy term couples the quark to the Dyson-Schwinger equation for the 1PI antiquark-quark-gluon-vertex Γ^ν and the gluon dressing function Z. Hidden in these dressing functions are the couplings of the quark DSE to all equations for higher n-point functions (there is an infinite number of them!). This asks for finding a resonable truncation, i.e. we need to resum this infinite number of subdiagrams into phenomenological functions that resemble the behaviour of the vertex and gluon. We employ the dressing functions from [49] where they were obtained from fits to lattice studies.
A word of caution is in order here. The above lattice study was done without a background magnetic field, which should not bother us too much for the quenched gluon, since it does not know about the background field anyway.
We will take $\Gamma^\nu \to \gamma^\nu \Gamma(k^2)$, where k is the gluon momentum. A definition $\Gamma(k^2)$ and $Z(k^2)$ and a discussion of this truncation can be found in the appendix (B). Certainly a thorough investigation of the quality of this ansatz in the presence of an external field is in order. The following sections however will mainly be focussed on the necessary techniques and qualitative behavior of the Dyson-Schwinger equations in a magnetic background. Other truncations might complicate some calculations done here, but the general features are of course the same.
The integral over x involving a product of Ritus- and Fourier eigenfunctions

$$\int \mathrm{d}^4x \; \bar{E}_p(x)\gamma^\mu E_q(x) e^{ikx} \tag{3.27}$$

and a similar integral for y remain to be done. If we had only particles in Ritus or in Fourier eigenfunctions at this vertex, this integral would be trivial due to the fact of those two systems being complete orthonormal vector spaces. We would simply obtain delta functions ensuring eigenvalue/momentum conservation.
In our case we have interacting particles, that are diagonal in different bases. Nevertheless the integral in Eq.(3.27) can be done analytically. Performing the integral, which essentially involves the Fourier transform of a product of parabolic cylinder functions yields

$$\begin{aligned} \int \mathrm{d}^4x \quad \bar{E}_p(x)\gamma^\mu E_q(x) e^{ikx} &= (2\pi)^4 \delta^{(3)}(q+k-p) e^{-k_\perp^2/4|eH|} e^{ik_1(q_2+p_2)/2eH} \\ &\times \sum_{\sigma_1,\sigma_2=\pm} \frac{e^{i\mathrm{sgn}(eH)(n(\sigma_1,l)-n(\sigma_2,l_q))\phi}}{\sqrt{n(\sigma_1,l)!n(\sigma_2,l_q)!}} J_{n(\sigma_1,l)n(\sigma_2,l_q)}(k_\perp) \quad \Delta(\sigma_1)\gamma^\mu\Delta(\sigma_2) \end{aligned} \tag{3.28}$$

with the abbreviations

$$\begin{aligned} k_\perp^2 &= k_1^2 + k_2^2 \\ n(\sigma,l) &= l + \frac{\sigma}{2}\mathrm{sgn}(eH) + \frac{1}{2} \\ \phi &= \arctan(k_2/k_1) \end{aligned} \tag{3.29}$$

Furthermore

$$J_{n_1 n_2} \equiv \sum_{m=0}^{\min(n_1,n_2)} \frac{n_1! n_2!}{m!(n_1-m)!(n_2-m)!} \left(i\mathrm{sgn}(eH) k_\perp \frac{\sqrt{2|eH|}}{2eH} \right)^{n_1+n_2-2m} \tag{3.30}$$

Composing all the bits and pieces, the quark self energy now reads

$$
\begin{aligned}
M(p,p') = (2\pi)^4\delta^{(3)}(p-p')g^2C_F\sum_{l_q}\int\frac{\mathrm{d}^2q_\parallel}{(2\pi)^4}\int_{-\infty}^{\infty}\mathrm{d}q_2\int_{-\infty}^{\infty}\mathrm{d}k_1 e^{-k_\perp^2/2|eH|} \\
\times\sum_{\sigma_1,\sigma_2,\sigma_3,\sigma_4}\frac{e^{i\mathrm{sgn}(eH)(n_1-n_2+n_3-n_4)\phi}}{\sqrt{n_1!n_2!n_3!n_4!}}J_{n_1n_2}(k_\perp)J_{n_3n_4}(k_\perp) \\
\times\Delta(\sigma_1)\gamma^\mu\Delta(\sigma_2)\frac{1}{A(q)_\parallel i\gamma q_\parallel + A(q)_\perp i\gamma q_\perp + B(q)}\Delta(\sigma_3)\gamma^\nu\Delta(\sigma_4) \\
\times P^{\mu\nu}(k)\Gamma(k^2)D(k^2),
\end{aligned}
\tag{3.31}
$$

where $D(k^2)\equiv Z(k^2)/k^2$ and $P_{\mu\nu}(k)=g_{\mu\nu}-\frac{k_\mu k_\nu}{k^2}$ as in Eq.(3.26). This expression is exact with respect to the treatment of the magnetic field. Unfortunately, it is almost impossible to solve numerically as well. The reason for that lies in the form of the functions J_{nm}, as can be seen when using an alternative derivation. Starting from Eq.(3.26) it can be shown that Eq.(3.31) is identical to

$$
\begin{aligned}
M(p,p') = (2\pi)^4\delta^{(3)}(p-p')g^2C_F\sum_{l_q}\int\frac{\mathrm{d}^2q_\parallel}{(2\pi)^4}\int_{-\infty}^{\infty}\mathrm{d}q_2\int_{-\infty}^{\infty}\mathrm{d}k_1 e^{-k_\perp^2/2|eH|} \\
\times\sum_{\sigma_1,\sigma_2,\sigma_3,\sigma_4}e^{i\mathrm{sgn}(eH)(n_1-n_2+n_3-n_4)\phi}n_1!n_3!\left(i\frac{k_\perp}{\sqrt{2\,|eH|}}\right)^{n_2-n_1+n_4-n_3} \\
\times L_{n_1}^{n_2-n_1}\left(\frac{k_\perp^2}{2\,|eH|}\right)L_{n_3}^{n_4-n_3}\left(\frac{k_\perp^2}{2\,|eH|}\right) \\
\times\Delta(\sigma_1)\gamma^\mu\Delta(\sigma_2)\frac{1}{A(q)_\parallel i\gamma q_\parallel + A(q)_\perp i\gamma q_\perp + B(q)}\Delta(\sigma_3)\gamma^\nu\Delta(\sigma_4) \\
\times P^{\mu\nu}(k)\Gamma(k^2)D(k^2)
\end{aligned}
\tag{3.32}
$$

where $L_n^m(x)$ are the generalized Laguerre polynomials. Therefore solving Eq.(3.32) numerically involves an integration routine that is precise for an integrand that behaves like a polynomial of order n. Since from Eq.(3.30) n is proportional to the Landau levels l, which are arbitrary close to each other for small eH, and hence a numerical treatment of the above expression is quite impossible. This is unfortunate for QCD, where in general the gluon dressing function or the quark gluon vertex might not be known analytically and numerical approaches are the only available tool.

However there is a way out, once magnetic fields are large enough (what "large enough" means will be discussed in chapter 4). Note that the integrand in the quark self-energy is given as a function of $k_\perp/2\,|eH|$, where large values of $k_\perp$ are essentially suppressed. If the magnetic field is large, only terms up to the smallest order in $k_\perp/2\,|eH|$ need to be kept. Unfortunately, this necessary approximation renders the Ritus method unreliable at small magnetic fields, since $k_\perp/2\,|eH|$ would by no chance be small then. Section 3.5 discusses possible ansätze to solve the quark DSE at small magnetic field. In the approximation, the vertex is simplified drastically as given by

$$
J_{nm}(k_\perp)\to\frac{[\max(n,m)]!}{|n-m|!}(ik_\perp/\sqrt{2\,|eH|})^{|n-m|}\to n!\delta_{nm}. \tag{3.33}
$$

Details can be found in [41, 42]. In this case, we have

$$
\begin{aligned}
\int\mathrm{d}^4x\quad\bar{E}_p(x)\gamma^\mu E_q(x)e^{ikx} = (2\pi)^4\delta^{(3)}(q+k-p)\quad e^{-k_\perp^2/4|eH|}e^{ik_1(q_2+p_2)/2eH} \\
\times\sum_{\sigma_1,\sigma_2}\delta_{n(\sigma_1,l)n(\sigma_2,l_q)}\quad\Delta(\sigma_1)\gamma^\mu\Delta(\sigma_2)
\end{aligned}
\tag{3.34}
$$

and thus

$$M(p,p') = (2\pi)^4\delta^{(3)}(p-p')ig^2C_F\sum_{l_q=0}^{\infty}\int\frac{\mathrm{d}^2q_\parallel}{(2\pi)^4}\int_{-\infty}^{\infty}\mathrm{d}q_2\int_{-\infty}^{\infty}\mathrm{d}k_1\ e^{-k_\perp^2/2|eH|}$$
$$\times\sum_{\sigma_1\sigma_2\sigma_3\sigma_4}\delta_{n(\sigma_1,l)n(\sigma_2,l_q)}\delta_{n(\sigma_3,l_q)n(\sigma_4,l')} \tag{3.35}$$
$$\times\Delta(\sigma_1)\gamma^\mu\Delta(\sigma_2)\frac{1}{A(q)_\parallel\gamma q_\parallel + A(q)_\perp\gamma q_\perp + B(q)}\Delta(\sigma_3)\gamma^\nu\Delta(\sigma_4)D(k^2)\Gamma(k^2)P^{\mu\nu}(k)$$

From this expression we can already see the qualitative behaviour of the qqg-vertex in a background Abelian field. Remember that we would obtain $(2\pi)^4\delta^{(4)}(q+k-p)\gamma^\mu$ in the zero field case.
Obviously, momentum conservation is only fulfilled for (see previous section)

$$\delta^{(3)}(q+k-p) \equiv \delta(q_0+k_0-p_0)\delta(q_3+k_3-p_3)\delta(q_2+k_2-p_2).$$

We will find later (see section 4) that the factor $\delta_{n(\sigma_1,l)n(\sigma_2,l_q)}$ allows for transitions between adjacent Landau levels. This does not come as a suprise, since as was shown before the eigensystem of the quark in an Abelian background field is supersymmetric in the sense that transitions between two neighbouring Landau levels constitute spin one transitions (i.e. from $\pm 1/2$ to $\mp 1/2$). Perpendicular gluons will therefore induce such transitions, whereas longitudinal (perpendicular and longitudinal wrt. to the magnetic field) gluons do not change the Landau level of incoming and outgoing quark at the vertex.
The $U(1)$ field breaks the initial $O(4)$ symmetry to a $O(2)$ symmetry in the t-z-plane. This explains the modification of the vertex

$$\gamma^\mu \to \Delta(\sigma_1)\gamma^\mu\Delta(\sigma_2)$$

This calculation can be easily generalized to the unquenched case. The only difference is the appearance of an anisotropy in the gluon dressing functions accounting for the modified behaviour of the gluon polarization. Aside from this, the methods obtained here can be equally well applied to the unquenched case.
Furthermore, we will see in the following section that, due to the appearance of further Lorenz structures ($F_{\mu\nu}$), the fermion propagator could in principle possess a richer tensor structure.
By looking at Eq.(3.35), one can see that the desired diagonality of the self energy term is still hidden, only after tracing over the single tensor structures we obtain the desired form

$$M(p,p') \propto M(p)\delta^{(4)}(p-p').$$

The following relations are very usefull and can be easily checked:

$$\begin{aligned}\Delta(\sigma)\gamma_\parallel^\mu &= \gamma_\parallel^\mu\Delta(\sigma)\\ \Delta(\sigma)\gamma_\perp^\mu &= \gamma_\perp^\mu\Delta(-\sigma)\\ \Delta(\sigma_a)\Delta(\sigma_b) &= \Delta(\sigma_a)\delta_{ab}\end{aligned} \tag{3.36}$$

so that the vertex can be decomposed into two contributions

$$\Delta(\sigma_1)\gamma^\mu\Delta(\sigma_2) = \Delta(\sigma_1)\left(\gamma_\parallel^\mu+\gamma_\perp^\mu\right)\Delta(\sigma_2) = \delta_{\sigma_1,\sigma_2}\Delta(\sigma_1)\gamma_\parallel^\mu + \delta_{\sigma_1,-\sigma_2}\Delta(\sigma_1)\gamma_\perp^\mu \tag{3.37}$$

Furthermore tracing over the spin projector gives

$$\sum_\sigma \mathrm{Tr}\left[\Delta(\sigma)\right] \to \chi(l) = \begin{cases} 4, & l>0\\ 2, & l=0\end{cases} \tag{3.38}$$

since for $l=0$ the fermion can only have $\sigma = \mathrm{sgn}(eH)$.

3.3 Full Tensor Structure of the Quark Propagator in a Background Magnetic Field

As was already mentioned before, the tensor structure that was used in section 3.2 is not the most general one. Instead, a simplified form was used in analogy to the case without a magnetic field. In [41] it is argued that any other spin dependent tensor structors, other than those used before, must be absent since they would violate the remaining Z_2 symmetry by rendering the position of the particle pole dependent on the direction of the external field.
Naïvely the introduction of spin dependent tensor structures might a priori not introduce such an asymmetry, for separating the spin up and down components gives still a symmetric quark propagator. The asymmetry will however occur due to the special role of the lowest Landau level. In section 4.2 it will be seen that this will prevent a sensible solution for the quark Dyson-Schwinger equation.
When constructing the complete tensor structure for the quark propagator, we need only to write down the most general form allowed by symmetries, such as charge conjugation, parity etc. We can start constructing linear independent tensor structures from the basis

$$\left\{\mathbb{I}, \gamma^5, \gamma^\mu, \gamma^5\gamma^\mu, \sigma^{\mu\nu}\right\} \otimes \left\{\mathbb{I}, p^\mu, F_{\mu\nu}, {}^*F^{\mu\nu}\right\} \tag{3.39}$$

The general structure for the inverse quark propagator is therefore (see [37,38])

$$S^{-1} = B + i\gamma^\mu V_\mu + \sigma^{\mu\nu} T_{\mu\nu} + i\gamma^5\gamma^\mu \tilde{A}_\mu \tag{3.40}$$

where

$$V_\mu = p_\mu A + e^2 F_{\mu\nu} F_{\nu\lambda} A' \tag{3.41}$$

$$T_{\mu\nu} = eF_{\mu\nu} C + e(p_\mu F_{\nu\rho} - p_\nu F_{\mu\rho}) p_\rho C' \tag{3.42}$$

$$\tilde{A}_\mu = eF^*_{\mu\nu} p_\nu D \tag{3.43}$$

are the decompositions into vector, tensor and pseudo-vector structures. With that we obtain

$$S^{-1}(p) = B(p) + iA(p)\gamma \cdot p + i(eH)^2 A'(p)\gamma_\perp \cdot p_\perp + 2eHC(p)\Sigma^3 + 2ieHD(p)\Sigma^3\gamma_\parallel \cdot p_\parallel. \tag{3.44}$$

All dressing functions are meant to be functions of $p = (p_\parallel, p_\perp)$ and eH. By introducing

$$A_\parallel = A \tag{3.45}$$

$$A_\perp = A_\parallel + (eH)^2 A' \tag{3.46}$$

Eq.(3.44) looks more familiar, as the naïve tensor structures are now accompanied by spin dependent structures $\propto eH$

$$S^{-1}(p) = B(p) + iA_\parallel(p)\gamma_\parallel \cdot p_\parallel + iA_\perp(p)\gamma_\perp \cdot p_\perp + 2eHC(p)\Sigma^3 + 2ieHD(p)\Sigma^3\gamma_\parallel \cdot p_\parallel \tag{3.47}$$

By comparing Eq.(3.44) and Eq.(3.47) to the case of $H = 0$

$$i\gamma p A(p) + B(p),$$

we immediately see what we would obtain when switching off the field. Obtaining $S(p)$ from Eq.(3.47) however is not that trivial any more. Finding it is equivalent to solving

$$S^{-1}(x,z)S(z,y) = \delta^{(4)}(x-y). \tag{3.48}$$

The pole structure of the Green's function can be obtained by realizing that the determinant of the wave operator S^{-1} must vanish. This is equivalent to

$$\det(S^{-1}(p)) = S_+^{-1} S_-^{-1} = 0 \tag{3.49}$$

where

$$
\begin{aligned}
S_{\pm}^{-1} &= B^2(p) + V^2(p) + \tilde{A}^2(p) \pm 2\sqrt{(B(p)\tilde{A}_\mu(p) - 2T^{\mu\nu *}(p)V_\nu(p))^2} \\
&= B^2(p) + A_\parallel^2(p)p_\parallel^2 + A_\perp^2(p)p_\perp^2 + 4(eH)^2 p_\parallel^2 D^2(p) \pm 4|eH||p_\parallel| \left|B(p)D(p) - A_\parallel(p)C(p)\right|
\end{aligned} \tag{3.50}
$$

We see that there are now two different solutions corresponding to the two different spin orientations along the z-axis. We can seperate these two poles by using the spin projection operators $\Delta(\sigma) = \frac{1}{2}(1 + \sigma\Sigma^3)$. This leads us to

$$
S(p) = \sum_\sigma \frac{B(p) - iA_\parallel(p)\gamma_\parallel \cdot p_\parallel - iA_\perp(p)\gamma_\perp \cdot p_\perp - 2eHC(p)\Sigma^3 + 2ieHD(p)\Sigma^3\gamma_\parallel \cdot p_\parallel}{B^2(p) + A_\parallel^2(p)p_\parallel^2 + A_\perp^2(p)p_\perp^2 + 4(eH)^2 p_\parallel^2 D^2(p) + \sigma 4|eH||p_\parallel| \left|B(p)D(p) - A_\parallel(p)C(p)\right|}\Delta(\sigma) \tag{3.51}
$$

We can now rescale $2C(p) \to C(p)$ and $2D(p) \to D(p)$ to get rid of some factors of two. The complete quark Dyson Schwinger equation is now given by

$$
\begin{aligned}
(2\pi)^4\delta^{(4)}(p-p')\Pi(l)\left(B(p) + iA_\parallel(p)\gamma_\parallel \cdot p_\parallel + iA_\perp(p)\gamma_\perp \cdot p_\perp + 2eHC(p)\Sigma^3 + 2ieHD(p)\Sigma^3\gamma_\parallel \cdot p_\parallel\right) \\
= (2\pi)^4\delta^{(4)}(p-p')(m + i\gamma_\parallel \cdot p_\parallel + i\gamma_\perp \cdot p_\perp) + M(p,p'),
\end{aligned} \tag{3.52}
$$

where

$$
\begin{aligned}
M(p,p') &= (2\pi)^4\delta^{(3)}(p-p')g^2 C_F \int \frac{\mathrm{d}^2 q_\parallel}{(2\pi)^4} \int_{-\infty}^{\infty} \mathrm{d}q_2 \int_{-\infty}^{\infty} \mathrm{d}k_1 \Bigg\{ \\
&\times \sum_{\sigma_1\sigma_2\sigma_3\sigma_4} \delta_{n(\sigma_1,l)n(\sigma_2,l_q)}\delta_{n(\sigma_3,l_q)n(\sigma_4,l')}\Delta(\sigma_1)\gamma^\mu\Delta(\sigma_2) \\
&\times \sum_\sigma \frac{B(p) - iA_\parallel(p)\gamma_\parallel \cdot p_\parallel - iA_\perp(p)\gamma_\perp \cdot p_\perp - 2eHC(p)\Sigma^3 + 2ieHD(p)\Sigma^3\gamma_\parallel \cdot p_\parallel}{B^2(p) + A_\parallel^2(p)p_\parallel^2 + A_\perp^2(p)p_\perp^2 + 4(eH)^2 p_\parallel^2 D^2(p) + \sigma 4|eH||p_\parallel| \left|B(p)D(p) - A_\parallel(p)C(p)\right|} \\
&\times \Delta(\sigma)\Delta(\sigma_3)\gamma^\nu\Delta(\sigma_4)D(k^2)\Gamma(k^2)P^{\mu\nu}(k)e^{-k_\perp^2/2|eH|}\Bigg\}
\end{aligned} \tag{3.53}
$$

Again we can proceed in analogy to the previous chapter. The relations

$$
\begin{aligned}
\left[\Delta(\sigma), \Sigma^3\right] &= 0 \\
\left[\gamma_\parallel^\mu, \Sigma^3\right] &= 0
\end{aligned} \tag{3.54}
$$

are helpful here. We will see the the desired diagonality after tracing out the different tensor structures. It comes as no surprise to see the relation between $C(p)$ and $B(p)$, as well as $D(p)$ and $A_{||}(p)$. The new dressing functions $C(p)$ and $D(p)$ can be interpreted as the spin dependent equivalent of the old ones. $A_\perp(p)$ takes a special role here since it is the dressing function along the $p_\perp$ direction.
One notices that a single degenerate pole for both spin directions in the vacuum is now split into two spin dependent poles. As mentioned before, it was argued in [41], that the additional tensor structures $C(p)$ and $D(p)$ are not allowed to appear here since they would make the position of the poles dependent on the direction of the magnetic field. The latter is indeed true since for the lowest Landau level we have $\sigma = \mathrm{sgn}(eH)$ and thus there is an asymmetry between the states parallel and antiparallel to $\vec{B}$. In sections 4.2 we discuss results supporting this statement.

3.4 Chiral Symmetry Breaking and Dimensional Reduction

According to the Mermin-Wagner-Coleman theorem (MWC) [47], continous symmetries in less than three dimensions cannot be broken in a system with sufficiently short-ranged interactions. If such symmetry breaking would occur, the corrseponding Nambu-Goldstone bosons would have an infrared divergent correlation function

$$G(0,x) \propto \log x, \tag{3.55}$$

rendering them ill defined. In other words: The scalar bosons could not be centered around a mean, a property that is quite essential in a quantum field theory. Since the dynamical mass generation is dominated by the 1+1 dimensional lowest landau level, one might become concerned here.
Luckily, a good explanation why the MWC theorem does not apply is given in [9]. The authors argue that, since the chiral condensate and the Nambu-Goldstone bosons are electrically neutral, the dimensional reduction does not affect the center (of mass) of neutral excitations. Dimensional reduction and dynamical chiral symmetry breaking are therefore compatible with each other.
Stated otherwise the dimensional reduction is a dynamical effect, reflecting the fact that charged particles are restricted to a plane when they are exposed to an external magentic field. The external field causes the motion in that plane to be bound (which is nothing else but the Landau quantization in an oscillator like potential), leaving the direction parallel to the magentic field lines free.

3.5 The Failure of Perturbation Theory

In the previous sections we discussed the difficulties in solving a quantum theory in the presence of a weak magnetic field.
In the case of a weak coupling to the external field one might be tempted to treat the problem perturbatively. To include all the dynamics from QCD, the Yang-Mills sector must still be treated explicitly, but one might aim to realize the coupling to the magnetic field by using a weak external source, corresponding to a vector potential generating a constant magnetic field.
This thought has some major flaws. First of all, perturbation theory is based on the assumption that it is possible to define a free asymptotic state, which certainly is impossible in the case of a constant, infinitely extended magnetic field. Secondly, perturbation theory is based on an expansion around the unperturbed free theory. Being free, the theory is then certainly Poincare invariant, a property explicitly destroyed by a magnetic field. Momentum is nothing more but the eigenvalues of the Dirac operators which are in a Poincaré invariant theory conserved along every particle line. In the presence of an external field momentum is explicitly not conserved, the conserved eigenvalues along particle lines are the Ritus eigenvalues discussed in the previous sections.
Indeed one could restrict the magnetic field to a finite volume, which is actually the physical case since constant magnetic fields do not exist in reality. Then however one still would need to solve the issue with momentum conservation. In this case one would not solve for the quark propagtor but rather for the quark-magnetic-field vertex (a three-point function) that is dressed with QCD effects. Diagonalizing this system so that one gets a two-point function (the quark propagtor) and including the momentum-non-conservation explicitly is then exactly equivalent to the Ritus method. There is no way around expanding in the Ritus basis once there is a constant magnetic field in the theory, in order to perform the investigations we are interested in.
The impossibilty of this specific ansatz can be made even more explicit. With a vector potential of the form $A(x) = (0, 0, Hx, 0)$, the Feynman rule for the interaction with the background gauge field would be

$$-ie\gamma^\mu \tilde{A}_\mu(p' - p) = -ie\gamma^2 \int \mathrm{d}^4x \; Hx = -(2\pi)^4 eH \frac{\partial}{\partial p_2} \delta^4(p - p') \tag{3.56}$$

where $\tilde{A}_\mu(p' - p)$ is the Fourier transform of $A(x)$. This expression is ill-defined in a translation invariant background. Furthermore, let us assume that we are considering a bare fermion, for which

an asymptotic state is defined. Then we can use the Gordon identities

$$ie\bar{u}(p')\gamma^\mu u(p)\tilde{A}_\mu(p'-p) = ie\bar{u}(p')\left[\frac{p'^\mu + p^\mu}{2m} + \frac{i\sigma^{\mu\nu}q_\nu}{2m}\right]u(p)\tilde{A}_\mu(p'-p) \tag{3.57}$$

to get

$$ie\bar{u}(p')\gamma^\mu u(p)\tilde{A}_\mu(p'-p) = i(2\pi)^4\delta^{(4)}(p-p')eH\bar{u}(p')\left[p_2\frac{\partial}{\partial p_1} + \frac{\Sigma^3}{2}\right]u(p) \tag{3.58}$$

where $\partial/\partial p_1 = -ix_1$. It can be clearly seen that the interaction can be divided into the Lorentz force and the spin interaction, the first term being explicitly position dependent and will thus look different depending on the frame.
An ansatz on how to solve the Ritus problem for small magnetic fields in QED is given in [48], where an expansion in eH was done.

So far we discussed the influence of a magnetic field on the fermionic sector of QCD. The following chapter is devoted to a systematic investigation of the properties found here. The possible structures of the quark propagator will be contrasted and the influence of a magnetic field onto dynamical mass generation and the spin structure of the QCD vacuum will be quantified in the quenched approximation.

4 Quark DSE in the Quenched Approximation

The following section is devoted to a systematic investigation of the Dyson Schwinger system for the quark within the quenched approximation and using the truncation and approximations discussed in the previous chapter. It is found in sections 4.1.3 that an external magnetic field catalyses dynamical mass generation. Further the spin structure of the QCD vacuum will be investigated in section 4.1.4 where it can be seen that the QCD vacuum possesses a non-vanishing spin expectation value when a magnetic field is switched on, even in the absence of spin dependent tensor structures in the quark propagator (see Eq.(3.23)).

4.1 Simple Tensor Structure

4.1.1 Properties of the Dressing Functions

Starting from the quark Dyson Schwinger equation Eq.(**??**), using Eq.(3.35) derived in section 3.2, the properties of the quenched quark equation can be investigated in a systematic way. After performing the traces, one obtains

$$\begin{aligned} B(p) = m \quad &+ \quad g^2 C_F \int \frac{\mathrm{d}^2 q_\parallel}{(2\pi)^4} \Bigg\{ \frac{B(q)}{B^2(q) + A_\parallel^2(q) q_\parallel^2 + A_\perp^2(q) q_\perp^2 \Big|_{l_q = l}} \\ &\qquad \times \int\limits_{-\infty}^{\infty} \mathrm{d}q_2 \int\limits_{-\infty}^{\infty} \mathrm{d}k_1 \; e^{-k_\perp^2/2|eH|} \left(2 - \frac{k_\parallel^2}{k^2}\right) D(k^2)\Gamma(k^2) \Bigg\} \\ &+ \quad \frac{g^2 C_F}{p_\parallel^2} \frac{2}{\chi(l)} \sum_{\substack{l_q = l - \mathrm{sgn}(eH), \\ l_q \geq 0,\; l_q + = 2}}^{l_q = l + \mathrm{sgn}(eH)} \int \frac{\mathrm{d}^2 q_\parallel}{(2\pi)^4} \Bigg\{ \frac{B(q)}{B(q)^2(q) + A_\parallel^2(q) q_\parallel^2 + A_\perp^2(q) q_\perp^2} \\ &\qquad \times \int\limits_{-\infty}^{\infty} \mathrm{d}q_2 \int\limits_{-\infty}^{\infty} \mathrm{d}k_1 \; e^{-k_\perp^2/2|eH|} \left(2 - \frac{k_\perp^2}{k^2}\right) D(k^2)\Gamma(k^2) \Bigg\} \end{aligned} \tag{4.1}$$

where $k_2 = q_2 - p_2$. Although p_2 appears explicitly here, it can be seen from the form of the integrand that the final result does not depend on it, as expected. Without loss of generality, we will set $p_2 = 0$ therefore. Furthermore

$$\begin{aligned} A_\parallel(p) = 1 \quad &- \quad \frac{g^2 C_F}{p_\parallel^2} \int \frac{\mathrm{d}^2 q_\parallel}{(2\pi)^4} \Bigg\{ \frac{A_\parallel(q)}{B(q)^2(q) + A_\parallel^2(q) q_\parallel^2 + A_\perp^2(q) q_\perp^2 \Big|_{l_q = l}} \int\limits_{-\infty}^{\infty} \mathrm{d}q_2 \int\limits_{-\infty}^{\infty} \mathrm{d}k_1 \; e^{-k_\perp^2/2|eH|} \\ &\qquad \times \left(p_\parallel q_\parallel \cos(\phi) \frac{k_\parallel^2}{k^2} - 2 \frac{(q_\parallel p_\parallel \cos(\phi) - p_\parallel^2)(q_\parallel^2 - q_\parallel p_\parallel \cos(\phi))}{k^2} \right) D(k^2)\Gamma(k^2) \Bigg\} \\ &+ \quad \frac{g^2 C_F}{p_\parallel^2} \frac{2}{\chi(l)} \sum_{\substack{l_q = l - \mathrm{sgn}(eH), \\ l_q \geq 0,\; l_q + = 2}}^{l_q = l + \mathrm{sgn}(eH)} \int \frac{\mathrm{d}^2 q_\parallel}{(2\pi)^4} \Bigg\{ \frac{A_\parallel(q)}{B(q)^2(q) + A_\parallel^2(q) q_\parallel^2 + A_\perp^2(q) q_\perp^2} \\ &\qquad \times \int\limits_{-\infty}^{\infty} \mathrm{d}q_2 \int\limits_{-\infty}^{\infty} \mathrm{d}k_1 \; e^{-k_\perp^2/2|eH|} \left(2 - \frac{k_\perp^2}{k^2}\right) p_\parallel q_\parallel \cos(\phi) D(k^2)\Gamma(k^2) \Bigg\} \end{aligned} \tag{4.2}$$

and

$$
\begin{aligned}
A_\perp(p) = 1 \quad + \quad & \frac{g^2 C_F}{p_\parallel^2} \int \frac{\mathrm{d}^2 q_\parallel}{(2\pi)^4} \left\{ \frac{A_\perp(q)}{B(q)^2(q) + A_\parallel^2(q) q_\parallel^2 + A_\perp^2(q) q_\perp^2 \Big|_{l_q = l}} \right. \\
& \left. \times \int\limits_{-\infty}^{\infty} \mathrm{d}q_2 \int\limits_{-\infty}^{\infty} \mathrm{d}k_1 \; e^{-k_\perp^2/2|eH|} \left(2 - \frac{k_\parallel^2}{k^2} \right) p_\perp q_\perp D(k^2) \Gamma(k^2) \right\} \\
- \quad & \frac{g^2 C_F}{p_\parallel^2} \frac{2}{\chi(l)} \sum_{\substack{l_q = l - \mathrm{sgn}(eH), \\ l_q \geq 0, \; l_q + = 2}}^{l_q = l + \mathrm{sgn}(eH)} \int \frac{\mathrm{d}^2 q_\parallel}{(2\pi)^4} \left\{ \frac{A_\perp(q)}{B(q)^2(q) + A_\parallel^2(q) q_\parallel^2 + A_\perp^2(q) q_\perp^2} \right. \\
& \left. \times \int\limits_{-\infty}^{\infty} \mathrm{d}q_2 \int\limits_{-\infty}^{\infty} \mathrm{d}k_1 \; e^{-k_\perp^2/2|eH|} \frac{k_1^2 - k_2^2}{k^2} p_\perp q_\perp D(k^2) \Gamma(k^2) \right\}, \qquad (4.3)
\end{aligned}
$$

where $\chi(l)$ is given by Eq.(3.38) and $\phi = \arctan(k_2/k_1)$. The appearance of the last three equations is as expected. Note that the contributions to the self-energy consist of two terms. The first one describes the radiation and emission of a "longitudinal" gluon which is polarized in the z-t-plane, as indicated by $= g_\parallel^{\mu\nu} - k_\parallel^\mu k_\parallel^\nu / k^2$. Such a gluon does not induce transitions bewteen Landau levels. However, the second term corresponds to Landau level transitions, it is accompanied by a gluon $\propto g_\perp^{\mu\nu} - k_\perp^\mu k_\perp^\nu / k^2$. In the latter case the gluon emission can either increase or decrease the Landau level of the internal quark, except for the case of the lowest Landau level, where only a transition up to the second Landau level can happen (for there are no negative Landau levels). This decomposition is a direct result of Eq.(3.37). Mixed terms, such as $\Delta(\sigma_1)\gamma_\parallel \Delta(\sigma_2) \ldots \Delta(\sigma_3)\gamma_\perp \Delta(\sigma_4)$, do not appear, as they would violate conservation of the Ritus eigenvalues.

Since the exact tensor structure of the gluon in an external magnetic field will be discussed later (see sec. 5.1), we have to be careful with our interpretations. In fact neither $\delta_\parallel^{\mu\nu} - k_\parallel^\mu k_\parallel^\nu / k^2$ nor $\delta_\perp^{\mu\nu} - k_\perp^\mu k_\perp^\nu / k^2$ are eigenvectors of the gluon polarization $\Pi^{\mu\nu}$, but linear combinations thereof. Thus one should not think that by calling them "longitudinal" and "perpendicular" they represent the longitudinal and perpendicular subspace of $\Pi^{\mu\nu}$. It is easy here to confuse "perpendicular" with "transverse" here. However, note that the gluon is certainly transverse in the sense of being contained in the subspace projected onto by $\delta_\perp^{\mu\nu} - k_\perp^\mu k_\perp^\nu / k^2$. Nevertheless in this subspace there needs to be a distinction between polarization components parallel and perpendicular to the magnetic field. The projectors used here are nothing more than the isotropic polarization tensor restricted to $\mu, \nu = 1, 2$ or $\mu, \nu = 0, 3$. A thorough discussion will follow in section 5.1, for now we shall proceed with the simplifications gained from the quenched approximation.
Eqs.(4.1)-(4.3) can be solved numerically, with the dressing functions being functions of $p_\parallel$ and $p_\perp$. Fig. (6) shows exemplary the dressing functions for magnetic fields between 1 GeV^2 and 50 GeV^2 for a bare mass of $m = 3.7$ MeV at $\mu = 100$ GeV. Solid lines represent the single Landau levels. For numerical reasons, the sum over Landau levels was transformed into an integral after summing over a sufficiently large number of discrete Landau levels. Due to the dependence $p_\perp \propto \sqrt{2\,|eH|\,l}$, the density of Landau levels per energy interval grows and the error due to this approximation can be neglected. Usually 30 landau levels will be included explicitly here. The difference between two adjacent Landau levels in this range is very small even for larger magnetic fields. The numerical error was found to be negligible.
Once the magnetic field is large enough, this numerical simplification cannot be followed any longer, for the energy gap between Landau levels rises significantly. The sum over the landau levels must be performed explicit. The integrals over $p_\parallel, p_2$ and k_1 are evaluated on a logarithmic grid.

The influence of the magnetic field can be clearly seen from Fig. (6). An important effect is that

with stronger magnetic field, the dynamical mass generation is dominated by the lowest Landau level, as predicted in the literature [41–43]. The perpendicular dressing function $A_\perp$ is not defined on the Lowest landau level.

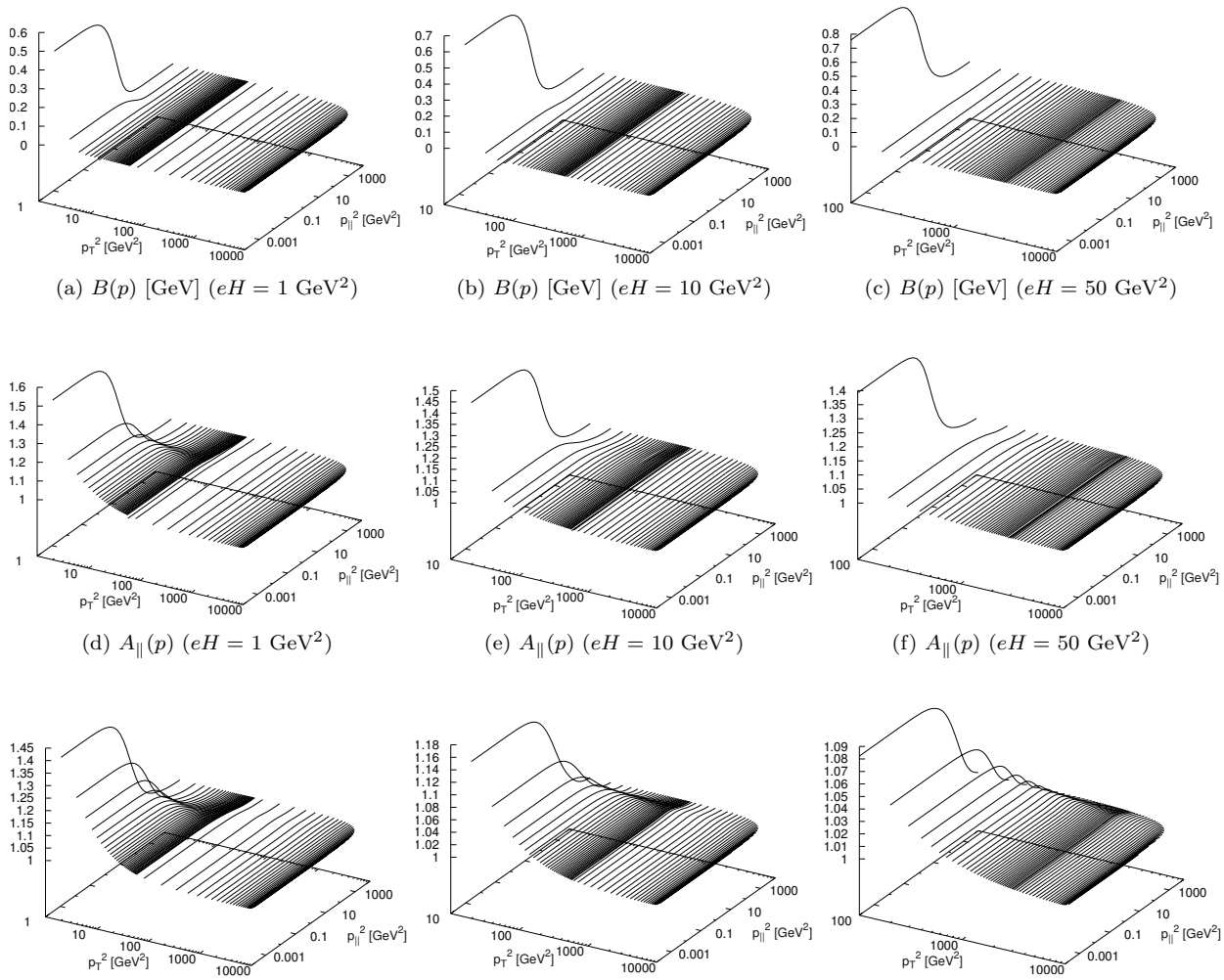

(a) $B(p)$ [GeV] ($eH = 1$ GeV^2) (b) $B(p)$ [GeV] ($eH = 10$ GeV^2) (c) $B(p)$ [GeV] ($eH = 50$ GeV^2)

(d) $A_\parallel(p)$ ($eH = 1$ GeV^2) (e) $A_\parallel(p)$ ($eH = 10$ GeV^2) (f) $A_\parallel(p)$ ($eH = 50$ GeV^2)

(g) $A_\perp(p)$ ($eH = 1$ GeV^2) (h) $A_\perp(p)$ ($eH = 10$ GeV^2) (i) $A_\perp(p)$ ($eH = 50$ GeV^2)

Figure 6: Quark dressing functions for $eH = 1$ GeV^2 (left column), $eH = 10$ GeV^2 (middle column) and $eH = 50$ GeV^2 (right column)

A better understanding of how a magnetic field modifies dynamical mass generation can be seen when looking at the lowest landau level only. In Fig. (7) $B(p)$ is shown for several values of the magnetic field. The increase of the scalar dressing function with growing magnetic field is apparent. However, the dynamics are more complex. The effect of magnetic catalysis is, in addition to the raise of the functions, also caused by the shift of the falling flank of the dressing function towards the UV. The fall-off behaviour of this function and its growing determines the behaviour of the chiral condensate which therefore increases as will be seen in the following section.
The shift of the falling flank has indeed a physical interpretation. QCD in the vacuum contains by itself only one scale, $\Lambda_{QCD} \approx 1$ GeV. An external field introduces another scale, eH, which now determines the transition between strongly coupled and perturbative regime.

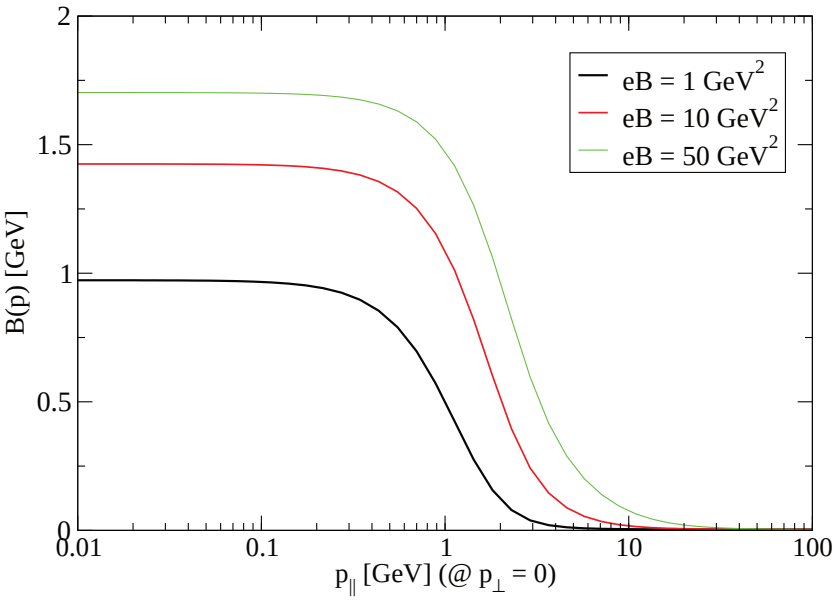

Figure 7: Scalar dressing function for the quark propagator for different magnetic fields at a bare quark mass of m = 3.7 MeV at μ = 100 GeV

4.1.2 Renormalization

In the previous section, calculations where done without special emphasis of renormalization. For simplictly all renormalization constants were set to one. However, it should be clear that the quark Dyson-Schwinger equation can be easily modified using field strength and mass renormalization constants Z_2 and Z_m. A striking feature appears once a magnetic field is turned on. Due to the presence of the magnetic field, the dimensionality of the system effectively reduces, turning a 3+1 dimensional quantum system into a 2+1 dimensional system and even a 1+1 dimensional system for the lowest Landau level. This means that the quark self-energy diagram is actually convergent rather than logarithmically divergent, as it is in the vacuum.
A word of caution is in order here. Actually the renormalization of the quark sector is coupled to the renormalization of all other possible operators through the dependence of the Dyson-Schwinger equations. Truncating these equations also means being ignorant to a certain degree about this dependence. Unfortunately there is no way to treat this perfectly consistent, as it is impossible to solve the full infinite set of Dyson-Schwinger equations. However, one should note that this is actually not a bad approximation since, as we have just learned, magnetic fields reduce the divergences that appear, thereby lessen the dependence on renormalization of the other sectors.
The validity of the given arguments is ultimately related to the quality of the truncation that is employed. For a detailed discussion of this issue, the reader is refered to the literature (see for example [49] and references therein).
Unfortunately, so far there exists no lattice study that could be used to contrast truncations at finite magnetic fields. Since this work is primarily meant to establish the techniques needed for QCD in magnetic fields, this should not bother us too much. Other truncations can be easily employed using the methods established in the previous chapters.

Next, the properties of the quark dressing functions will be investigated. Their renormalization behaviour will be treated exemplary. Due to the favourable UV convergence found here, in the following sections there will be no specific focus on renormalization. Instead, as a default, the cutoff will be set to $\Lambda = 100$ GeV with renormalization scale at the very same point $\mu = \Lambda$.

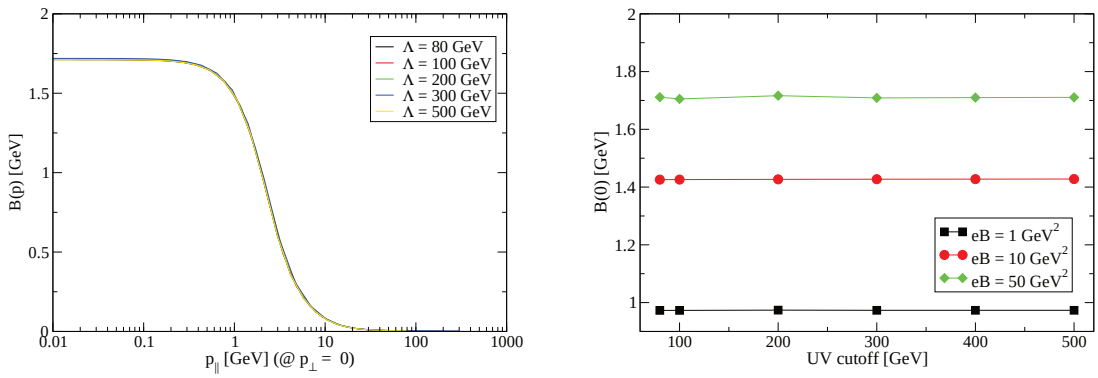

(a) Cutoff dependence of $B(p)$ [GeV]

(b) B(0) as a function of the UV cutoff Λ

Figure 8: Regularization in a magnetic field. As can be seen, the dimensional reduction causes the quark self energy to be convergent, removing any scale dependence from the dressing functions (here $Z_2 = Z_m = 1$ or $\mu = \Lambda$).

From Fig. (8) (a) and (b), one can see that indeed the quark dressing functions are not cutoff dependent due to the effective dimensional reduction. In the plot the quark propagator was only regularized by means of a cutoff, but not renormalized ($Z_2 = Z_m = 1$ or $\mu = \Lambda$). This means that for all calculations shown in Fig. (8) the renormalization point μ was at a different position. We see that the results are not dependent on the renormalization scale at all. The important point to realize is that regularized quantities in the system with reduced dimensionality do not run. The chiral dressing function tends to a constant for sufficiently high momentum and similar for the vector dressing functions $A_\parallel$ and $A_\perp$.
Further note that the introduction of a magnetic field introduces a difficulty here. Since the flank of quark mass function is shifted towards the UV, as can be seen from Fig. (7), the renormalization scale μ must be chosen large enough to be in the perturbative regime.

4.1.3 Chiral Condensate and Dynamical Mass Generation

As was described in section 2.2.2, the chiral condensate is an order parameter for the transition between the chirally broken and restored phases. However, due to the explicit loss of translational invariance, Eq.(2.60) is useless and instead Eq.(2.59) needs to be expanded in Ritus eigenfunctions. The diagrammatic representation of the chiral condensate in terms of a vacuum loop is still the same. However, the loop integration is over the eigenvalues of the Ritus functions instead of the usual four momenta.
The chiral condensate for the quark propagator, parameterized by the quark dressing functions $A_\perp$, $A_\parallel$ and B, is

$$-\langle\bar{q}q\rangle = \lim_{x\to 0} S(x,0) = N_c \frac{eH}{2\pi^2} \sum_{l_q=0}^{\infty} \int_0^{\infty} \mathrm{d}q_\parallel q_\parallel \sum_{\sigma=\pm} \frac{B(q)}{B^2(q) + A_\parallel^2(q) q_\parallel^2 + A_\perp^2(q) q_\perp^2} \tag{4.4}$$

At finite bare mass, the chiral condensate diverges linearly with the cutoff.

$$\langle \bar{q}q \rangle_{m\neq 0} \to \textbf{(finite terms)} + m\Lambda. \tag{4.5}$$

However, the divergence is the same for all bare masses, thus making it easily regularizable. The regularized condensate $\langle \bar{q}q \rangle_r$ can be defined subtracting the chiral condensate of a heavy quark,

$$\langle \bar{q}q \rangle_r = \langle \bar{q}q \rangle_m - \frac{m}{m_{\text{heavy}}} \langle \bar{q}q \rangle_{\text{heavy}}\,, \tag{4.6}$$

which leaves also an unwanted term of order m/m_{heavy} in addition to the finite part of the quark condensate. This can be neglected when the mass of the regulator quark gets sufficiently heavy. We will use the strange quark as a regulator, with $m_s = 85$ MeV, $m_{ud}/m_s \approx 5\%$, in analogy to standard lattice QCD computations.

The unregularized quark condensate, for various values of the bare quark mass, is shown in Fig. (9).

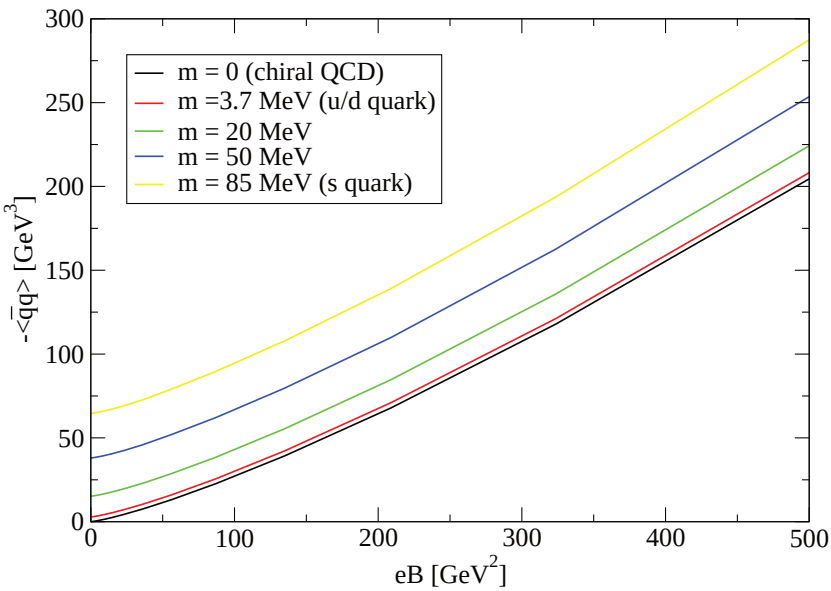

Figure 9: Unregularized Chiral Condensate for various physical and unphysical bare masses.

It can be seen that the condensate grows for an increasing magnetic field. For large eH, the growth is approximately linear, in agreement with several model calculations (see below). The slope of the curves is identical for all bare masses in the large field limit. For comparison, all electrical charges were set to $q_f = 1$. Of course in reality the dependence of bare masses is obscured by the different charges of up and down quarks. For the quenched calculations, this is however easily accounted for. By scaling $eH \to (2/3)eH$ or respectively $eH \to (-1/3)eH$ one obtains the "physical" results. Since we are interested in the general aspects of the Ritus method only, this flavour dependence is ignored for all quenched calculations. It can be seen in section 5 that for unquenched QCD the individual quark charges are important, since different flavours are coupled there.

In contrast to QCD without external fields, where dynamical chiral symmetry breaking is suppressed for heavy quarks, the bare mass dependence found here is an important difference. The dynamical

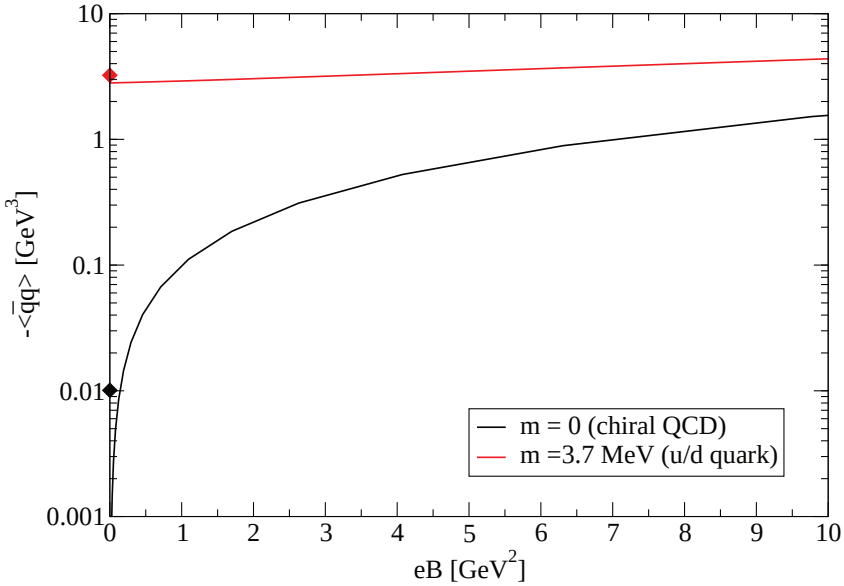

Figure 10: Unregularized Chiral Condensate for small eH. Shown are the zero field limits (dots).

mass generation in a magnetic field is an external effect, that adds to the non-perturbative dynamics of QCD.

Fig. (10) shows the unregularized chiral condensate for rather small magnetic fields, where (as it was discussed in section 3.2) our approach of the Ritus method becomes unreliable. For comparison the chiral condensate for zero magnetic field is indicated. The discrepancy can be seen clearly. From the magnitude of the difference one can infer that the approximation is probably good as long $eH > \Lambda_{QCD}^2 \approx 1$ GeV^2 [6]. Not shown here are the zero field limits for higher bare masses. In these cases, the agreement of the Ritus method with its zero field limit gets worse for small eH. Fig. (11) shows the regularized up/down quark condensate as well as the unregularized condensate the same bare mass.

The general behaviour of the chiral condensate is similar as was found in the literature. In [9], a linear behaviour of $\langle \bar{q}q \rangle$ in eH for a free fermion in (3+1) dimensions is found, comparable to the results for large magnetic fields in this work (see Fig. (9)). A comparison with lattice results would be nice to have, however this can be done to a certain extent only. By looking at [21, 22] one sees that the qualiative behaviour found for the chiral condensate matches the results of this work. Unfortunately, the calculations of [21, 22] were only done for $eH < 1$, where our present ansatz is unreliable. Further note our results for finite bare mass are regularization dependent. Therefore, in order to compare them, one would need to establish an equivalence between regularization on the lattice (essentially depending on the lattice spacing) and the continuum methods used here. The authors of [21, 22] regularize the chiral condensate wrt. to its values at zero magentic field, which unfortunately is impossible here.

The authors of [51, 52] find similar results for small magnetic fields $eH < 1$ GeV^2 using QM (quark-meson) and NJL (Nambu-Jona-Lasinio) models. References, that the results in this work (for large eH) could be compared to, are scarce. Qualitatively however, the general behaviour predicted in the literature is reproduced.

[6] Remember that this approximation follows from an expansion in $k_\perp^2/2\,|eH|$, where the largest contributions to the quark self energy come from $k_\perp < \Lambda_{QCD}$

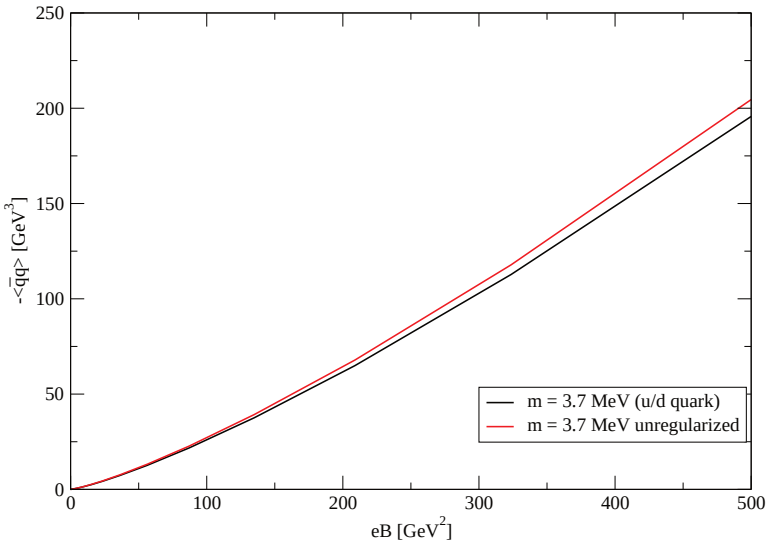

Figure 11: Regularized vs. unregularized u/d quark condensate

4.1.4 Spin Structure of QCD

It was shown in [54] that external fields can give a handle on observables, that could not be obtained otherwise. The presence of a magnetic field induces a nonzero expectation value for the tensor polarization operator $\sigma^{\mu\nu}$ as described in [21,22]. In the case of a field along the z-axis $\langle\sigma^{12}\rangle$ will correspond to the average spin alignment along this quantization axis.
In this section, it will be shown that $\langle\sigma^{12}\rangle$ obtains a non zero value even in the absence of spin dependent tensor structures in the quark propagator. In such a case, the polarization of the QCD vacuum will be caused by the special role of the lowest Landau level. The expectation value of the operator can be pictorially represented as

$< \sigma^{12} >=$

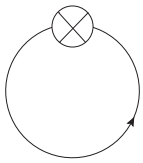

where the cross represents an insertion of σ_{12}.
All Landau levels, except the lowest, are degenerate with respect to the two spin directions $\uparrow\downarrow$, which means that for a non explicit spin dependent propagator the contributions to $\langle\sigma^{12}\rangle$ from higher Landau levels cancel on average, as can be seen from the form of the expectation value

$$\langle\sigma^{12}\rangle = N_c\frac{eH}{2\pi^2}\sum_{l_q=0}^{\infty}\int_0^{\infty}\mathrm{d}q_\parallel q_\parallel \sum_{\sigma=\pm}\frac{\sigma B(q)}{B^2(q)+A_\parallel^2(q)q_\parallel^2+A_\perp^2(q)q_\perp^2} = N_c\frac{eH}{2\pi^2}\int_0^{\infty}\mathrm{d}q_\parallel q_\parallel\frac{\Delta\mathrm{sgn}(eH)B(q)}{B^2(q)+A_\parallel^2(q)q_\parallel^2} \tag{4.7}$$

This quantity behaves in analogy to the chiral condensate in terms of regularization, simply because the inserted operator σ^{12} is dimensionless. Therefore the regularized quantity can be defined as

$$\langle\sigma^{12}\rangle_r = \langle\sigma^{12}\rangle_m - \frac{m}{m_{\text{heavy}}}\langle\sigma^{12}\rangle_{\text{heavy}}\,, \tag{4.8}$$

where $m_{\text{heavy}} = 85$ MeV, as before.
Effectively $\langle\sigma^{12}\rangle$ extracts the contribution of the lowest Landau level to the chiral condensate. From Fig. (12b), it can be seen that this actually supports the lowest Landau level dominance encountered before, as the ration $\langle\bar{q}\sigma^{12}q\rangle / \langle\bar{q}q\rangle$ tends to one for large eH. This ratio can be denoted as the polarization of the QCD vacuum

$$\mu_{\text{QCD}} = \frac{\langle\bar{q}\sigma^{12}q\rangle}{\langle\bar{q}q\rangle} \tag{4.9}$$

which saturates, $\mu_{\text{QCD}} \to 1$, for large external fields. Indeed, the lowest landau level domination is driven by this saturation.
Further the spin tensor expectation value can be expanded into operators

$$\langle\sigma^{12}\rangle = \chi\,\langle\bar{q}q\rangle\,eH + O(eH^2) \tag{4.10}$$

where terms $\propto O(eH^0)$ need to vanish, since the QCD vacuum in the zero field case is isotropic and therefore unpolarized. The coefficient in front of the $\langle\bar{q}q\rangle$-term is called the magnetic susceptibilty of QCD, which for small eH is

$$\chi \approx \frac{\langle\sigma^{12}\rangle}{\langle\bar{q}q\rangle}\frac{1}{eH} = \frac{\mu_{\text{QCD}}}{eH}. \tag{4.11}$$

The magnetic polarization of the QCD vacuum will be dominated by nonlinear effects in eH once the magnetic field is large. In that case, the polarization will tend to its saturation and the approximation, Eq.(4.11), will be modified.
Plotting μ_{QCD} as a function of eH should show a linear behaviour around vanishing eH with a slope given by χ. As was discussed before, the approximation used here unfortunately breaks down in this limit. Therefore the quantity μ_{QCD} gives us a way to further test the applicability of the approximation.

Fig. (13b) shows the regularized magnetic polarization for rather small eH. It can be seen easily that roughly for $eH < 0.06$ GeV^2 an unexpected behaviour appears, when using a regulator mass of $m_{\text{heavy}} = 85$ MeV. Between 0.06 and 0.005 GeV^2 the magnetic polarization slopes upwards when going to smaller eH instead of falling down to zero. We attribute this behaviour to the finite regulator mass. In the region of small eH both chiral condensate and the tensor polarization are quite small. Therefore errors in both these quantities effect the final result drastically, when taking the ratio. In the small eH range, a larger regulator mass should be taken.
With a regulator mass of $m_{\text{heavy}} = 500$ MeV, we find the dependence of the regularized condensates on this unphysical mass scale vanishes and we indeed find the expected behaviour. Although the magnetic field is very small here, it is remarkable that the results are as anticipated. Certainly, this tells us that the approximations at least reproduce the qualitative features.
When determining the slope of the magnetic polarization one gets a value of

$$\chi = -8.6\ \text{GeV}^{-2},$$

which, when compared to the literature, is compatible to several other calculations (an overview can be found in [51]). For example [53] give a value of $\chi = (8.6\pm0.24)$ GeV^{-2} at a renormalization point of 1 GeV, whereas [54] gives $\chi = (5.7)$ GeV^{-2} at a renormalization point of 0.5 GeV. Both values where obtained from sum rules. Perhaps there is a rather large quantitative uncertainty in the observable obtained in the present work (although the dependence on the regulator mass is negligible as higher

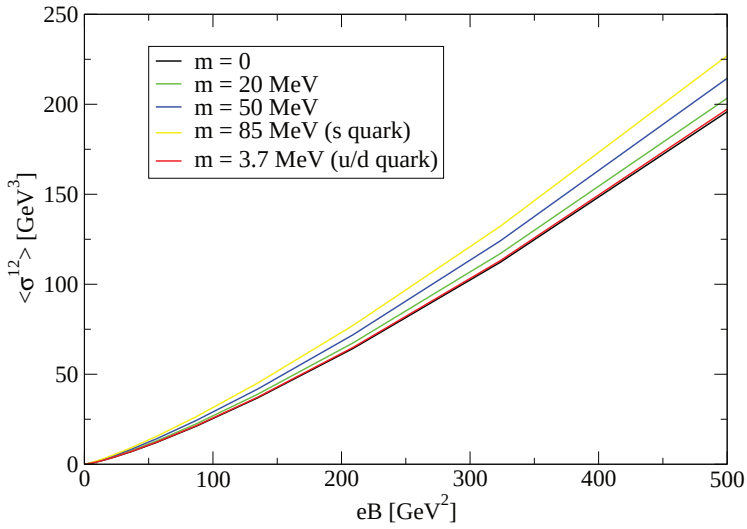

(a) Unregularized expectation value of the spin polarization tensor $\langle \sigma^{12} \rangle$ for different bare masses.

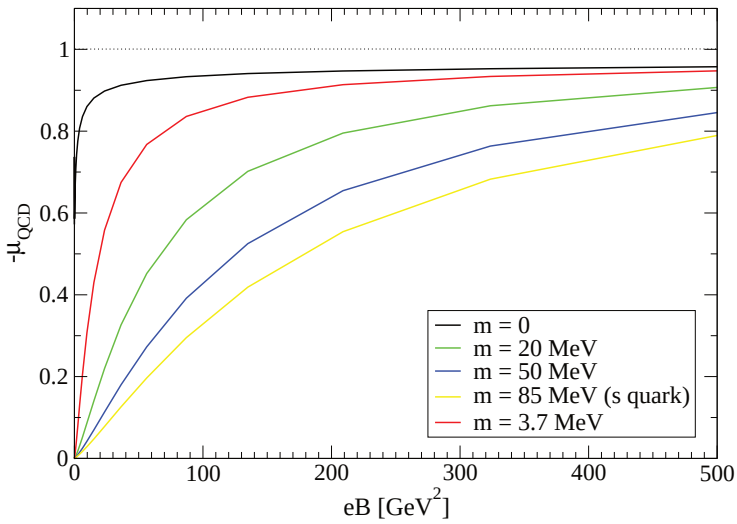

(b) Unregularized magnetic polarization of the QCD vacuum.

Figure 12

regulator masses were found not to change this result), which is very hard to estimate. A quantitative exact result could be obtained once a method is found to carry out the Ritus method correctly for small eH, too.

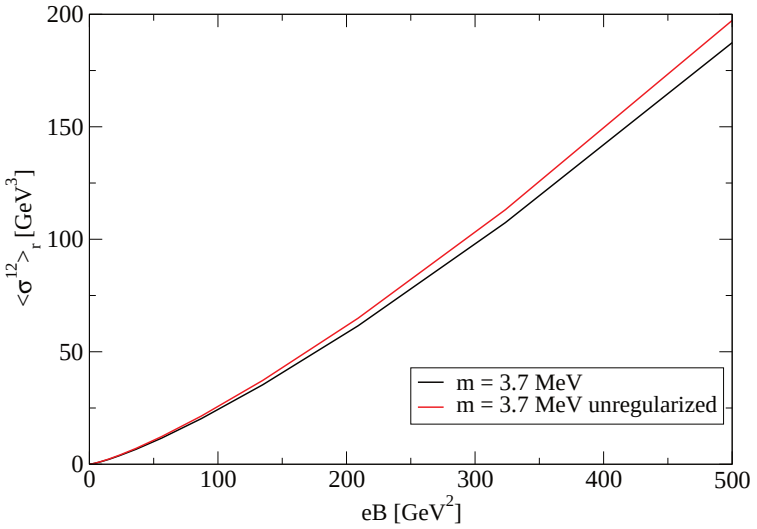

(a) Regularized expectation value of the spin polarization tensor $\langle \sigma^{12} \rangle$ for different bare masses.

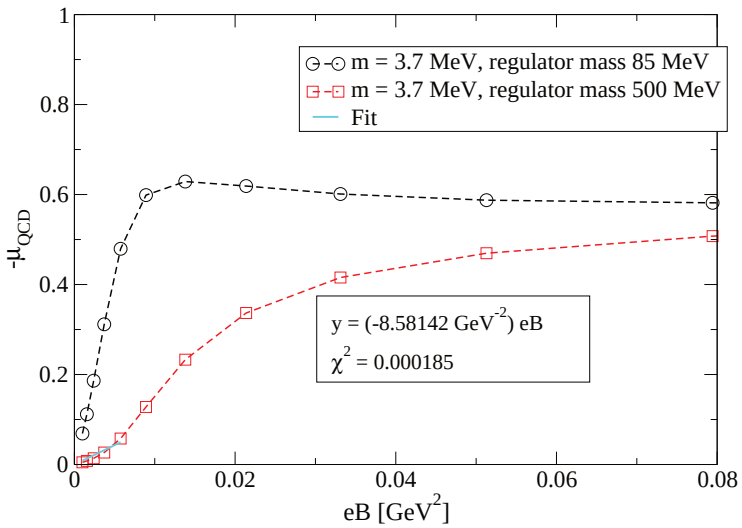

(b) Regularized magnetic polarization of the QCD vacuum.

Figure 13

4.2 Full Tensor Structure

As was argued in section 3.3, the additional tensor structures $C(p)eH\Sigma^3$ and $D(p)eH\Sigma^3\gamma p$ should not be included in the full quark propagator because of symmetry considerations. In this section we find that including those structures actually suppresses a non-trivial solution of the quark DSE.

4.2.1 Influence of the Additional Tensor Structures

The appearance of a magnetic field offers possibilities to construct spin-dependent tensor structures for the quark propagator. These were determined by general symmetry considerations. The additional structures are something like a spin dependent version of some of the existing tensor structures. This explains the similarities between $A_\parallel$ and D, as well as B and C.
The different dressing functions can be obtained by multiplying the DSE with the corresponding tensors and taking the trace afterwards. We define

$$\mathcal{D}(q,\sigma) = B^2(q) + A_\parallel^2(q)q_\parallel^2 + A_\perp^2(q)q_\perp^2 + (eH)^2 q_\parallel^2 D^2(q) + 2\sigma|eH||q_\parallel|\left|B(q)D(q) - 2A_\parallel(q)C(q)\right| \quad (4.12)$$

and obtain the coupled equations for the quark dressing functions

$$\begin{aligned} B(p) = m \quad &+ \quad \frac{2}{\chi(l)} g^2 C_F \int \frac{\mathrm{d}^2 q_\parallel}{(2\pi)^4} \Bigg\{ \sum_{\sigma=\pm} \frac{B(q) - \sigma C(q) eH}{\mathcal{D}(q,\sigma)}\Big|_{l_q=l} \\ &\qquad \times \int_{-\infty}^{\infty} \mathrm{d}q_2 \int_{-\infty}^{\infty} \mathrm{d}k_1 \; e^{-k_\perp^2/2|eH|} \left(2 - \frac{k_\parallel^2}{k^2}\right) D(k^2)\Gamma(k^2) \Bigg\}_{l_q=l} \\ &+ \quad \frac{2}{\chi(l)} g^2 C_F \sum_{\substack{l_q=l-\mathrm{sgn}(eH),\\ l_q\geq 0,\; l_q+=2}}^{l_q=l+\mathrm{sgn}(eH)} \int \frac{\mathrm{d}^2 q_\parallel}{(2\pi)^4} \Bigg\{ \frac{B(q) + \sigma C(q) eH}{\mathcal{D}(q,-\sigma)} \\ &\qquad \times \int_{-\infty}^{\infty} \mathrm{d}q_2 \int_{-\infty}^{\infty} \mathrm{d}k_1 \; e^{-k_\perp^2/2|eH|} \left(2 - \frac{k_\perp^2}{k^2}\right) D(k^2)\Gamma(k^2) \Bigg\} \end{aligned} \quad (4.13)$$

where in the second term $\sigma = 1$ for $l_q = l + sgn(eH)$ and $\sigma = -1$ for $l_q = l - sgn(eH)$. This convention will be used for the other dressing functions, too. Similar we get

$$\begin{aligned} C(p) = \quad &- \quad \frac{2}{\chi(l)} g^2 C_F \int \frac{\mathrm{d}^2 q_\parallel}{(2\pi)^4} \Bigg\{ \sum_{\sigma=\pm} \frac{C(q) - B(q)\sigma/eH}{\mathcal{D}(q,\sigma)} \\ &\qquad \times \int_{-\infty}^{\infty} \mathrm{d}q_2 \int_{-\infty}^{\infty} \mathrm{d}k_1 \; e^{-k_\perp^2/2|eH|} \left(2 - \frac{k_\parallel^2}{k^2}\right) D(k^2)\Gamma(k^2) \Bigg\}_{l_q=l} \\ &+ \quad \frac{2}{\chi(l)} g^2 C_F \sum_{\substack{l_q=l-\mathrm{sgn}(eH),\\ l_q\geq 0,\; l_q+=2}}^{l_q=l+\mathrm{sgn}(eH)} \int \frac{\mathrm{d}^2 q_\parallel}{(2\pi)^4} \Bigg\{ \frac{C(q) + (\pm)B(q)/eH}{\mathcal{D}(q,-\sigma)} \\ &\qquad \times \int_{-\infty}^{\infty} \mathrm{d}q_2 \int_{-\infty}^{\infty} \mathrm{d}k_1 \; e^{-k_\perp^2/2|eH|} \left(2 - \frac{k_\perp^2}{k^2}\right) D(k^2)\Gamma(k^2) \Bigg\} \end{aligned} \quad (4.14)$$

and

$$
\begin{aligned}
A_\perp(p) = 1 \quad &+ \quad \frac{2}{\chi(l)} g^2 C_F \int \frac{\mathrm{d}^2 q_\parallel}{(2\pi)^4} \Bigg\{ \sum_{\sigma=\pm} \frac{A_\perp(q)}{\mathcal{D}(q,-\sigma)} \\
&\qquad \times \int_{-\infty}^{\infty} \mathrm{d}q_2 \int_{-\infty}^{\infty} \mathrm{d}k_1 \; e^{-k_\perp^2/2|eH|} \frac{1}{p_\perp^2} \left(2 - \frac{k_\parallel^2}{k^2} \right) p_\perp q_\perp D(k^2)\Gamma(k^2) \Bigg\}_{l_q=l} \\
&+ \quad \frac{2}{\chi(l)} g^2 C_F \sum_{\substack{l_q=l-\mathrm{sgn}(eH),\\ l_q\geq 0,\; l_q+=2}}^{l_q=l+\mathrm{sgn}(eH)} \int \frac{\mathrm{d}^2 q_\parallel}{(2\pi)^4} \Bigg\{ \frac{1}{p_\perp^2} \frac{A_\perp(q)}{\mathcal{D}(q,\sigma)} \\
&\qquad \times \int_{-\infty}^{\infty} \mathrm{d}q_2 \int_{-\infty}^{\infty} \mathrm{d}k_1 \; e^{-k_\perp^2/2|eH|} \left(2 \frac{p_\perp k_\perp q_\perp k_\perp}{k^2} - p_\perp q_\perp \frac{k_\perp^2}{k^2} \right) D(k^2)\Gamma(k^2) \Bigg\}.
\end{aligned}
\tag{4.15}
$$

Furthermore

$$
\begin{aligned}
A_\parallel(p) = 1 \quad &- \quad \frac{2}{\chi(l)} g^2 C_F \int \frac{\mathrm{d}^2 q_\parallel}{(2\pi)^4} \Bigg\{ \frac{1}{p_\parallel^2} \sum_{\sigma=\pm} \frac{A_\parallel(q) + eH\sigma D(q)}{\mathcal{D}(q,\sigma)} \int_{-\infty}^{\infty} \mathrm{d}q_2 \int_{-\infty}^{\infty} \mathrm{d}k_1 \; e^{-k_\perp^2/2|eH|} \\
&\qquad \times \left(\frac{k_\parallel^2}{k^2} p_\parallel q_\parallel \cos(\phi) - 2 \frac{(q_\parallel p_\parallel \cos(\phi) - p_\parallel^2)(q_\parallel^2 - q_\parallel p_\parallel \cos(\phi))}{k^2} \right) p_\perp q_\perp D(k^2)\Gamma(k^2) \Bigg\}_{l_q=l} \\
&+ \quad \frac{2}{\chi(l)} g^2 C_F \sum_{\substack{l_q=l-\mathrm{sgn}(eH),\\ l_q\geq 0,\; l_q+=2}}^{l_q=l+\mathrm{sgn}(eH)} \int \frac{\mathrm{d}^2 q_\parallel}{(2\pi)^4} \Bigg\{ \frac{A_\parallel(q) - (\pm) eH D(q)}{\mathcal{D}(q,-\sigma)} \\
&\qquad \times \int_{-\infty}^{\infty} \mathrm{d}q_2 \int_{-\infty}^{\infty} \mathrm{d}k_1 \; e^{-k_\perp^2/2|eH|} \frac{1}{p_\parallel^2} \left(2 - \frac{k_\perp^2}{k^2} \right) D(k^2)\Gamma(k^2) \Bigg\},
\end{aligned}
\tag{4.16}
$$

and

$$
\begin{aligned}
D(p) \quad &= \quad \frac{2}{\chi(l)} g^2 C_F \int \frac{\mathrm{d}^2 q_\parallel}{(2\pi)^4} \Bigg\{ \frac{1}{p_\parallel^2} \sum_{\sigma=\pm} \frac{D(q) + A_\parallel(q)\sigma/eH}{\mathcal{D}(q,\sigma)} \int_{-\infty}^{\infty} \mathrm{d}q_2 \int_{-\infty}^{\infty} \mathrm{d}k_1 \; e^{-k_\perp^2/2|eH|} \\
&\qquad \times \left(\frac{k_\parallel}{k^2} p_\parallel q_\parallel \cos(\phi) - 2 \frac{(q_\parallel p_\parallel \cos(\phi) - p_\parallel^2)(q_\parallel^2 - q_\parallel p_\parallel \cos(\phi))}{k^2} \right) p_\perp q_\perp D(k^2)\Gamma(k^2) \Bigg\}_{l_q=l} \\
&+ \quad \frac{2}{\chi(l)} g^2 C_F \sum_{\substack{l_q=l-\mathrm{sgn}(eH),\\ l_q\geq 0,\; l_q+=2}}^{l_q=l+\mathrm{sgn}(eH)} \int \frac{\mathrm{d}^2 q_\parallel}{(2\pi)^4} \Bigg\{ \frac{1}{p_\parallel^2} \frac{D(q - (\pm) A_\parallel(q)/eH}{\mathcal{D}(q,-\sigma)} \\
&\qquad \times \int_{-\infty}^{\infty} \mathrm{d}q_2 \int_{-\infty}^{\infty} \mathrm{d}k_1 \; e^{-k_\perp^2/2|eH|} \left(2 - \frac{k_\perp^2}{k^2} \right) D(k^2)\Gamma(k^2) \Bigg\}.
\end{aligned}
\tag{4.17}
$$

Fig. (14) and Fig. (15) display the latter dressing functions for various values of the magnetic fields. It is interesting to see that the additional spin dependent terms C and D seem to prevent a non trivial solution for the quark DSE. This can be infered from the exact form of the equations above. The spin-independent structures and their spin-dependent equivalents are not completely similar, since the former have non vanishing bare limits. For $B(p)$ this is the bare mass, whereas $A_\parallel = A_\perp = 1$ in the

absence of interactions. This leads to the observation that in the chiral limit (e.g. no "driving term" for $B(p)$) only the trivial zero solution to the quark DSE is found. In some sense a finite bare mass weakens the argument that those additional structures must not appear, since for a massive particle both spin directions, e.g. helicities are not clearly distinguished.

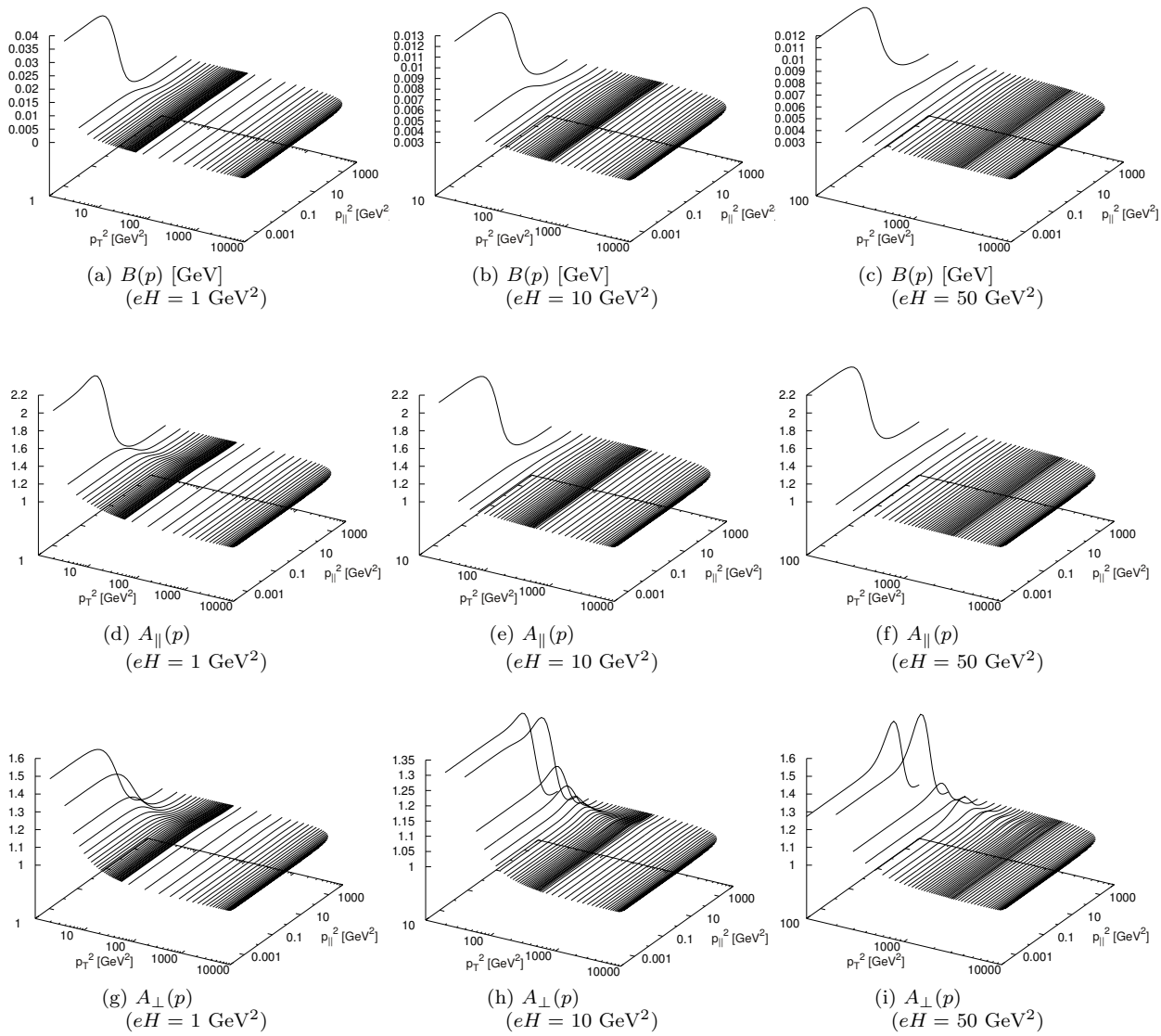

(a) $B(p)$ [GeV] ($eH = 1$ GeV^2)
(b) $B(p)$ [GeV] ($eH = 10$ GeV^2)
(c) $B(p)$ [GeV] ($eH = 50$ GeV^2)
(d) $A_{||}(p)$ ($eH = 1$ GeV^2)
(e) $A_{||}(p)$ ($eH = 10$ GeV^2)
(f) $A_{||}(p)$ ($eH = 50$ GeV^2)
(g) $A_{\perp}(p)$ ($eH = 1$ GeV^2)
(h) $A_{\perp}(p)$ ($eH = 10$ GeV^2)
(i) $A_{\perp}(p)$ ($eH = 50$ GeV^2)

Figure 14: quark dressing functions $A_{||}$, $A_{\perp}$ and B for $eH = 1$ GeV^2 (left row), $eH = 10$ GeV^2 (middle row) and $eH = 50$ GeV^2 (right row)

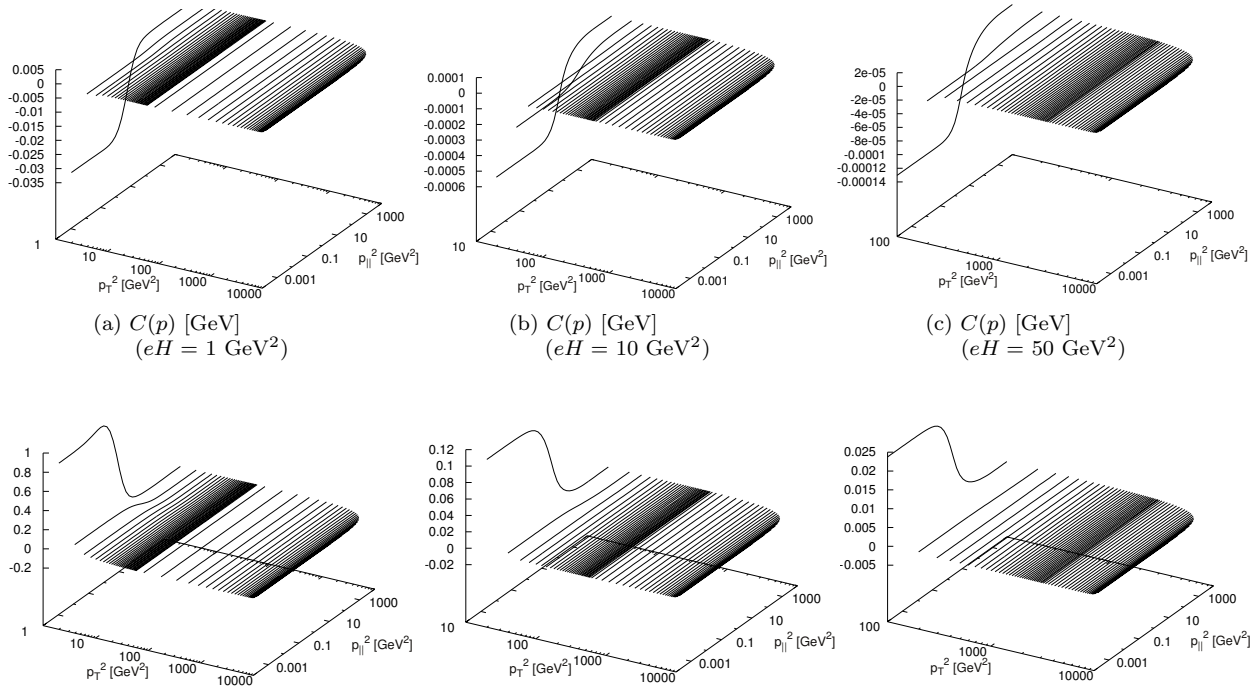

(a) $C(p)$ [GeV] ($eH = 1$ GeV^2)
(b) $C(p)$ [GeV] ($eH = 10$ GeV^2)
(c) $C(p)$ [GeV] ($eH = 50$ GeV^2)
(d) $D(p)$ ($eH = 1$ GeV^2)
(e) $D(p)$ ($eH = 10$ GeV^2)
(f) $D(p)$ ($eH = 50$ GeV^2)

Figure 15: quark dressing functions C and D for $eH = 1$ GeV^2 (left row), $eH = 10$ GeV^2 (middle row) and $eH = 50$ GeV^2 (right row)

4.2.2 Chiral Condensate

An argument supporting the vanishing of $C(p)$ and $D(p)$ can be found when looking at the order parameter that indicates chiral symmetry breaking. The chiral condensate is now found to depend on $C(p)$ in addition

$$-\langle\bar{q}q\rangle = N_c \frac{eH}{2\pi^2} \sum_{l_q=0} \int_0^\infty \mathrm{d}q_\| q_\| \sum_\sigma \frac{B(q) - \sigma(eH)C(q)}{\mathcal{D}_F(q,\sigma)} \tag{4.18}$$

where

$$\mathcal{D}_F(q,\sigma) = B^2(q) + A_\|^2(q)q_\|^2 + A_\perp^2(q)q_\perp^2 + (eH)^2 q_\|^2 D^2(q) + 2\sigma|eH||q_\||\left|B(q)D(q) - 2A_\|(q)C(q)\right| \tag{4.19}$$

It can be seen that the contribution to the dynamical mass generation is shared between these two tensor structures.
Fig. (17a) shows the chiral condensate that is obtained once the quark propagator, Eq.(3.52), with this "full" tensor structure is included. It is apparent that there is a cancellation between $B(p)$ and $C(p)$ already in the solution of the quark-DSE and the chiral condensate is thus modified drastically. In the case of zero bare mass the cancellation is perfect and therefore no chiral condensate is created. For finite bare masses one notes two things, however. First, when going to zero magnetic field, the same limit for the chiral condensate is obtained than was with the simpler tensor structure. This is evident since the spin-dependent structures get switched off when $eH \to 0$. Second the effect of magnetic catalysis is suppressed, as can be seen from the very small slope of the chiral condensate.

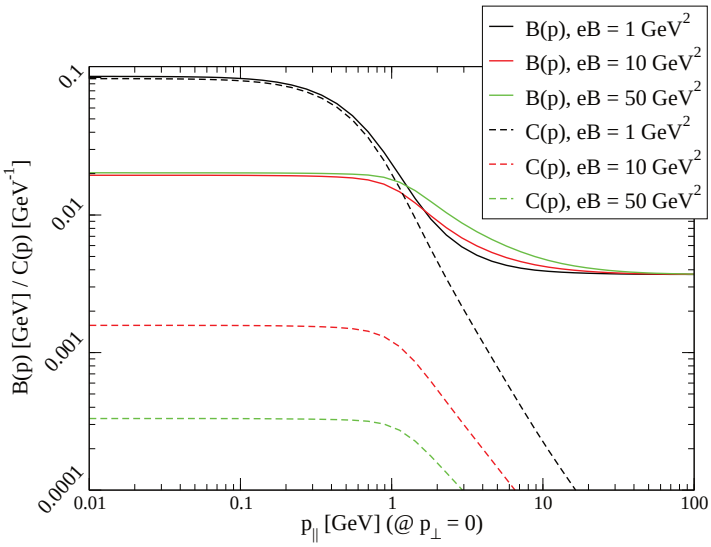

Figure 16: Scalar dressing function for the quark propagator Eq.(3.52) for different magnetic fields for a bare quark mass of m = 3.7 MeV

It is striking that the slope of the chiral condensate increases with growing bare mass. This is in contradiction to the behaviour of this order parameter in section Fig. (9). This increase in the slope might again be contributed to the assumption that a finite bare mass destroys the cancellation between $B(p)$ and $C(p)$ (related to the fact that helicity is not a well defined quantity for a massive particle).

4.2.3 Spin Structure

It was found in section 4.1.4 that the spin-structure of the QCD vacuum is dominated by the special role of the lowest Landau level when there are no spin dependent tensor structures in the quark propagator. This property is modified once tensor structures are included that include spin effects by themselves. For the full quark tensor structure the expectation value of the polarization operator $\sigma^{\mu\nu}$ has only the component σ^{12}

$$\langle\sigma^{12}\rangle = N_c \frac{eH}{2\pi^2} \sum_{l_q=0} \int_0^\infty \mathrm{d}q_\parallel q_\parallel \sum_\sigma \frac{\sigma B(q) - (eH)C(q)}{\mathcal{D}_F(q,\sigma)} \tag{4.20}$$

with $\mathcal{D}_F(q,\sigma)$ as defined in Eq.(4.19). Compared to the chiral condensate,Eq.(4.18), the roles of $B(q)$ and $C(q)$ are switched here. In addition there are now explicit contribution for higher landau levels that stem from $C(p)$.

$$\langle\sigma^{12}\rangle = N_c \frac{eH}{2\pi^2} \int_0^\infty \mathrm{d}q_\parallel q_\parallel \frac{\Delta \mathrm{sgn}(eH) B(q)}{\mathcal{D}_F(q,\sigma)} - N_c \frac{(eH)^2}{2\pi^2} \sum_{l_q=0} \int_0^\infty \mathrm{d}q_\parallel q_\parallel \sum_\sigma \frac{C(q)}{\mathcal{D}_F(q,\sigma)} \tag{4.21}$$

The results for $\langle\sigma^{12}\rangle$ are shown in Fig. (17b). The differences to the calculations with the simple tensor structure are apparent. Similar as for the chiral condensate in Fig. (17a), the effect of the magnetic field is much smaller. Further, the spin-tensor expectation value seems to be strongly bare mass dependent in contrast to the calculations for $A_\parallel(p)$, $A_\perp(p)$ and $B(p)$ only. These findings go along with the results of section 4.2.2.

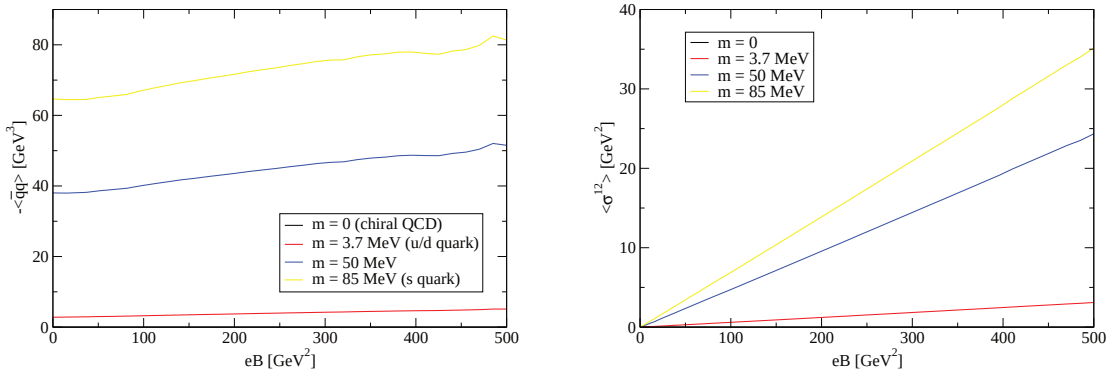

(a) $-\langle\bar{q}q\rangle$ (b) $\langle\sigma^{12}\rangle$

Figure 17: Chiral condensate and the expectation value of the spin polarization tensor, when explicit spin dependent structures appear in the quark propagator.

From what we see from the calculations involving spin-dependent tensor structures, it becomes clear that these indeed must not be included. They would cause the position of the quark propagator's poles to be dependent on the direction of the magnetic field. Although it looks as if the quark self energy would be spin independent, since there are always two spin directions corresponding to each Landau level, this is not true for the lowest level, for which only the spin direction along the magnetic field exists.
A certain definition of a magnetic field comes with the definition of a certain reference frame. Why should the behaviour of the quark-self energy be dependent on this specific choice? From now on, I will proceed using the quark propagator in its "simple" form

$$S(x,y) = \sum\!\!\!\!\!\!\int \frac{\mathrm{d}^4 q}{(2\pi)^4}\; E_q(x) \frac{1}{A(q)_{\parallel} i\gamma q_{\parallel} + A(q)_{\perp} i\gamma q_{\perp} + B(q)} \bar{E}_q(y) \tag{4.22}$$

This expression should capture all possible modifications of the quark propagator in a constant magnetic field along the z-axis.

4.3 Possible Simplifications

Having derived the exact form of the quark-gluon vertex in section 3 the question arises whether one can simplify the equations obtained within the Ritus formalism to simplify numerical procedures. In this section systematic studies will be conducted to investigate whether important qualitative features can be reproduced using simpler ansätze at least to a certain precision.
By looking at Eq.(3.31), there are in principle two ways of simplifying the equations. First, one could leave out the spin projectors at the vertex, thereby ignoring the anisotropy of the very same. With the knowledge obtained so far, one could still allow for couplings to longitudinal/transverse (wrt. to the magnetic field) gluons inducing either no changes of the Landau level or permitting the transition to a higher or lower landau level. The advantage of this ansatz would be that it simplifies the functional form of the vertex and reduces significantly the computation time (approximately half the computation time since only half the number of angular integrals need to be calculated). This might be helpfull in the unquenched case.
The second possible simplification is more drastic for it ignores major aspects of the Dyson-Schwinger equations in magnetic fields. The idea is to start from the DSE in vacuum, which is given in a plane wave eigensystem and modify the vacuum quark gluon vertex by the exponential factor $\exp\left(-k_\perp/2\left|eH\right|\right)$, thereby hoping to mimic the effect of the magnetic field. A Landau level quantization is used in this ansatz, too.
Fig. (18) displays the scalar part of the quark propagator $B(p)$ derived from these simplifications in comparison with the true result. Shown is the dependence along $p_\parallel$ for the lowest landau level. Same colors correspond to the same magnetic field strength. One can see that the approach ignoring the isotropy at the vertex (denoted as "no spin projectors") shows, at least qualitatively, for all field strengths a similar result than the exact treatment. The second, more drastic simplification (here denoted as "naive ansatz"), shows at least for small magnetic fields a similar shape but deviates drastically for larger fields.
Fig. (19) shows the unregularized chiral condensate obtained from these approximation schemes. As it can be seen, the second approach gives completely different results, whereas the first approach at least shows the qualitative correct shape compared to the exact calculation.

These findings show that the approximation made here are in no way compatible with the exact result. When investigating QCD in external magnetic fields, it is essential not only to perform the expansion in the fermionic Ritus eigenfunctions, but also to correctly include the coupling of the latter to neutral particles.
However, to test further calculations such as for example in the unquenched case, which is numerically more demanding, the approxiamtion scheme ignoring the vertex anisotropy could be used, for it at least shows the qualitative correct form.

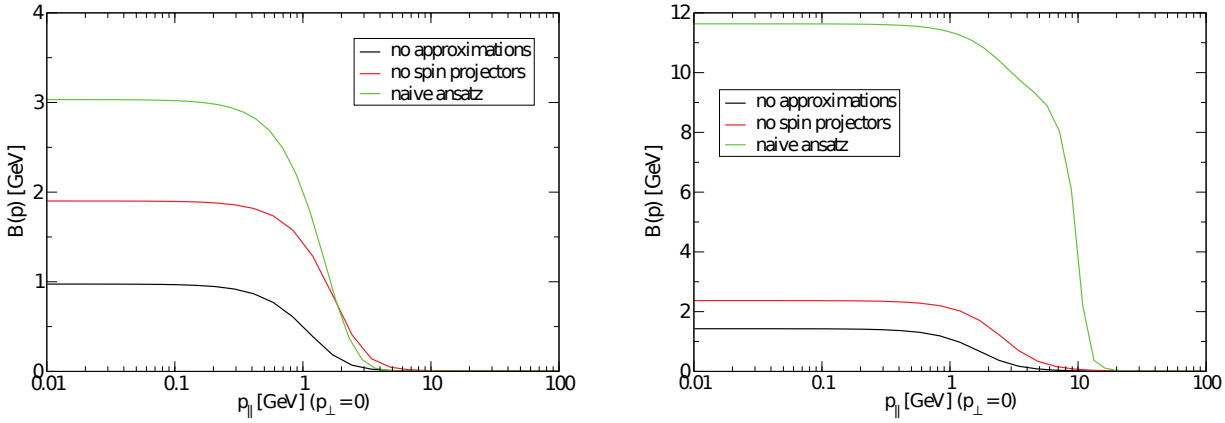

(a) eB = 1 GeV^2

(b) eB = 10 GeV^2

Figure 18: Comparison of the scalar part of the quark propagator for various simplifications for $m =$ 3.7 MeV at $\mu = 100$ GeV.

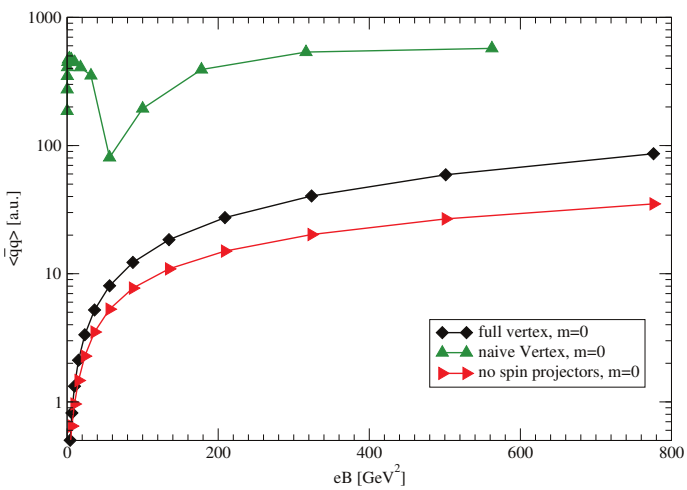

Figure 19: Comparison of the chiral condensate obtained from various simplification of the Ritus method for $m = 0$.

5 Unquenched QCD

In the previous chapters, we neglected the quark loop in the gluon self-energy, working in a quenched framework. Although gluon and ghost loops were included in the phenomenological dressing function $Z(k^2)$, used in Eq.(3.25), the feedback of the fermionic sector to the gauge sector introduces important effects that were neglected before.
It was shown in [56] that the modification of the gluon self-energy in a magnetic field inverts the magnetic catalysis once a certain field strength is reached. This is called inverse magnetic catalysis and it dominates the chiral condensate for large eH. These two competing effects will have an important influence on the thermodynamic properties of QCD. Therefore, the following section aims to establish the techniques necessary to formulate unquenched QCD in a magnetic field combining the Ritus method with the Dyson Schwinger approach.
Furthermore inverse magnetic catalysis renders the chiral condensate, as a function of eH, Lebesgue integrable, a condition necessary for the existence of its Fourier transform. this might give access to the dressed Wilson [21, 22] loop in our continuum DSE framework.

5.1 Polarization Tensor In External Fields

As was shown in the previous sections, magnetic fields introduce anisotropies into a quantum theory. The gluon couples to charged fermions, so that a systematic investigation of its polarization tensor structure is in order. Indeed, a magnetic field will modify $\Pi^{\mu\nu}$ in a non-trivial way. We will therefore establish an orthogonal basis for the gluon polarization tensor [57–59], well suited to accomodate for these.
There are four linear independent vectors which can be constructed from k^μ, $F^{\mu\nu}$ and ${}^*F^{\mu\nu}$

$$k^\mu, \qquad F^{\mu\nu}k_\nu, \qquad F^{\mu\nu}F_{\nu\alpha}k^\alpha, \qquad {}^*F^{\mu\nu}k_\nu. \tag{5.1}$$

Simliarly one can find four independent (pseudo-)scalar structures

$$\frac{1}{4}F^{\mu\nu}F_{\mu\nu}, \qquad \frac{1}{4}{}^*F^{\mu\nu}F_{\mu\nu}, \qquad k^2, \qquad (k_\nu F^{\nu\mu})^2, \tag{5.2}$$

which all contain an even number of $F^{\mu\nu}$ and ${}^*F^{\mu\nu}$. $\Pi^{\mu\nu}$ being symmetric (it belongs to a boson!) contains ten independent components. Using the Ward identity,

$$\Pi^{\mu\nu}k_\nu = 0, \tag{5.3}$$

this reduces to six components. Furthermore Furrys theorem [61] tells us that all components of $\Pi^{\mu\nu}$ with an odd number of $F_{\mu\nu}s$ vanish. Since all scalar components Eq.(5.2) are proportional to an even power of the latter, it follows that all possible coefficients are even in $F_{\mu\nu}$. Therefore, the basis tensors cannot be odd. This further reduces the number of components by two and we are left with four possible linear independent basis tensors.
Finding those is essentially an eigenvalue problem. $\Pi^{\mu\nu}$ has four orthogonal eigenvectors b_i^μ with corresponding eigenvalues

$$\kappa_i = \kappa_i\left(\frac{1}{4}F^{\mu\nu}F_{\mu\nu}, \frac{1}{4}{}^*F^{\mu\nu}F_{\mu\nu}, k^2, (k_\nu F^{\nu\mu})^2\right). \tag{5.4}$$

Having solved the eigenvalue problem, the polarization tensor can be written in its eigenbasis

$$\Pi^{\mu\nu}(k,k') = (2\pi)^4\delta^{(4)}(k'-k)\Pi^{\mu\nu}(k), \tag{5.5}$$

$$\Pi^{\mu\nu}(k) = \sum_{i=0}^{3}\kappa_i\frac{b_i^\mu b_i^\nu}{(b_i)^2}. \tag{5.6}$$

The first eigenvector is $b_0^\mu = k^\mu$ with eigenvalue 0, since $\Pi^{\mu\nu}k_\nu = 0$. The other eigenvectors are (see [57])

$$b_1^\mu = (F^{\mu\nu}F_{\nu\rho}k^\rho)k^2 - k^\mu(k_\nu F^{\nu\alpha}F_{\alpha\beta}k^\beta) \tag{5.7}$$
$$b_2^\mu = {}^*F^{\mu\nu}k_\nu \tag{5.8}$$
$$b_3^\mu = F^{\mu\nu}k_\nu \tag{5.9}$$

from which it is found that the projectors along those eigenvectors look like

$$\begin{aligned} \frac{b_2^\mu b_2^\nu}{(b_2)^2} &= \frac{\tilde{k}_\parallel^\mu \tilde{k}_\parallel^\nu}{\tilde{k}_\parallel^2} = \left(\delta_\parallel^{\mu\nu} - \frac{k_\parallel^\mu k_\parallel^\nu}{k_\parallel^2}\right) \equiv P_\parallel^{\mu\nu} \\ \frac{b_3^\mu b_3^\nu}{(b_3)^2} &= \frac{\tilde{k}_\perp^\mu \tilde{k}_\perp^\nu}{\tilde{k}_\perp^2} = \left(\delta_\perp^{\mu\nu} - \frac{k_\perp^\mu k_\perp^\nu}{k_\perp^2}\right) \equiv P_\perp^{\mu\nu} \end{aligned} \tag{5.10}$$

where we have defined the orthogonal momenta (being orthogonal to its corresponding partner, e.g. $\tilde{k}_\parallel \perp k_\parallel$ and similar for $\tilde{k}_\perp$)

$$\tilde{k}_\parallel^\alpha = \epsilon_\parallel^{\alpha\beta}k_\parallel^\beta \quad \alpha,\beta = 3,0, \tag{5.11}$$
$$\tilde{k}_\perp^\alpha = \epsilon_\perp^{\alpha\beta}k_\perp^\beta \quad \alpha,\beta = 1,2 \tag{5.12}$$

with $\epsilon_\perp^{12} = -\epsilon_\perp^{12} = 1$, $\epsilon_\perp^{11} = \epsilon_\perp^{22} = 0$ and correspondingly $\epsilon_\parallel^{30} = -\epsilon_\parallel^{03} = 1$, $\epsilon_\parallel^{33} = \epsilon_\parallel^{00} = 0$. Obviously $k_i^\mu \tilde{k}_j^\mu = 0$ $(i,j = \perp, \parallel)$ and further $k_i^2 = \tilde{k}_i^2$. For a constant magnetic field the last tensor structure is easily found

$$\frac{b_1^\mu b_1^\nu}{(b_1)^2} = \frac{(k_\perp^2 k_\parallel^\mu - k_\parallel^2 k_\perp^\mu)(k_\perp^2 k_\parallel^\nu - k_\parallel^2 k_\perp^\nu)}{k_\parallel^2 k_\perp^2 k^2} \equiv P_0^{\mu\nu}. \tag{5.13}$$

Note that because of the completeness of the basis, we can write

$$\delta^{\mu\nu} = P_0^{\mu\nu} + P_\parallel^{\mu\nu} + P_\perp^{\mu\nu} + P_L^{\mu\nu}, \tag{5.14}$$

where $P_L^{\mu\nu} = k^\mu k^\nu / k^2$. The structures $P_\parallel^{\mu\nu}$, $P_\perp^{\mu\nu}$ and $P_0^{\mu\nu}$ constitue a complete orthonormal basis for the transverse subspace $P^{\mu\nu}$. The transverse subspace is defined by

$$P^{\mu\nu} = \delta^{\mu\nu} - \frac{k^\mu k^\nu}{k^2} = P_0^{\mu\nu} + P_\parallel^{\mu\nu} + P_\perp^{\mu\nu} \tag{5.15}$$

and therefore $P_0^{\mu\nu}$ has an alternative expression to Eq.(5.13)

$$P_0^{\mu\nu} = \delta^{\mu\nu} - \frac{k^\mu k^\nu}{k^2} - \frac{\tilde{k}_\parallel^\mu \tilde{k}_\parallel^\nu}{\tilde{k}_\parallel^2} - \frac{\tilde{k}_\perp^\mu \tilde{k}_\perp^\nu}{\tilde{k}_\perp^2} = \frac{k_\parallel^\mu k_\parallel^\nu}{k_\parallel^2} + \frac{k_\perp^\mu k_\perp^\nu}{k_\perp^2} - \frac{k^\mu k^\nu}{k^2}, \tag{5.16}$$

which is easier to use in certain calculations. The basis properties of the projectors found here can be seen from

$$P_i^{\mu\alpha} P_j^{\alpha\nu} = \delta_{ij} P^{\mu\nu}, \tag{5.17}$$
$$P_i^{\mu\mu} = 1. \tag{5.18}$$

With Eqs. (5.10) - (5.18) the most general form of the gluon propagator in the presence of an external magnetic field along the z-axis is

$$D^{\mu\nu}(x,y) = \int \frac{\mathrm{d}^4 k}{(2\pi)^4} \left(\frac{1}{k^2 - \kappa_0} P_0^{\mu\nu}(k) + \frac{1}{k^2 - \kappa_\parallel} P_\parallel^{\mu\nu}(k) + \frac{1}{k^2 - \kappa_\perp} P_\perp^{\mu\nu}(k) \right) e^{ik(x-y)} \tag{5.19}$$

or

$$D^{\mu\nu}(k,k') = (2\pi)^4\delta^{(4)}(k'-k)\left(\frac{Z_0}{k^2}P_0^{\mu\nu}(k) + \frac{Z_\parallel}{k^2}P_\parallel^{\mu\nu}(k) + \frac{Z_\perp}{k^2}P_\perp^{\mu\nu}(k)\right). \tag{5.20}$$

The inverse propagator follows as

$$D^{-1\mu\nu}(k,k') = (2\pi)^4\delta^{(4)}(k'-k)k^2\left(Z_0^{-1}P_0^{\mu\nu}(k) + Z_\parallel^{-1}P_\parallel^{\mu\nu}(k) + Z_\perp^{-1}P_\perp^{\mu\nu}(k)\right) \tag{5.21}$$

where, with the eigenvalues κ_i from Eq.(5.4), we defined

$$Z_i \equiv \frac{1}{1-\kappa_i/k^2} \qquad i \in \{0,\parallel,\perp\} \tag{5.22}$$

The form of the gluon propagator illustrates the important effect, which was introduced as "vacuum birefringence" in [62], denoting the non degeneracy of the physical gluon modes. Stated otherwise, the refractive indices of different gluon polarizations deviate from each other.
The behaviour of the gluon originates from the presence of a medium of fermion-antifermion pairs, which is affected by the external field. Hence whereas the quark Dyson Schwinger equation describes the direct interaction of the (valence) quarks with the magnetic field, the gluon DSE gets modified by the interaction with the medium (sea quarks) that the gauge boson is propagating through.

5.2 The Gluon Dyson Schwinger Equation

The Dyson Schwinger equation for the gluon propagator is displayed in Fig. (4). The diagrams contributing to the quenched calculations in the preceeding sections included these diagrams, except the one involving the quark loop. Ignoring the feedback of the fermionic sector to the gauge sector, these diagrams where parameterized by the (isotropic) gluon dressing function $Z(k)$ which was obtained from the lattice (see discussion in appendix B).
In order to include this feedback, one needs to solve the complete Dyson-Schwinger equations for the gluon and the quark simultaneously. Unfortunately, the gauge sector diagrams of the gluon DSE are coupled to the ghost sector and to three- and four-gluon vertices which still are subject to ongoing investigations. Solving the full gluon DSE is therefore not yet possible.
According to [63] there is a way to approximately solve the unquenched gluon DSE without all these complications starting from the parameterization of the quenched gluon. In fact one could unquench the gluon DSE on top of the gauge-sector-only calculations. We include the quark sector by setting

$$D^{-1}_{\mu\nu}(k) = D^{-1}_{(0)\mu\nu}(k) + \Pi^{\mathrm{g}}_{\mu\nu}(k) + \Pi^{\mathrm{q}}_{\mu\nu}(k) \approx D^{-1\ \mathrm{eff}}_{\mu\nu}(k) + \Pi^{\mathrm{q}}_{\mu\nu}(k), \tag{5.23}$$

where the quenched contributions are factorized into the effective propagtor $D^{-1\ \mathrm{eff}}_{\mu\nu}(k)$, which is only

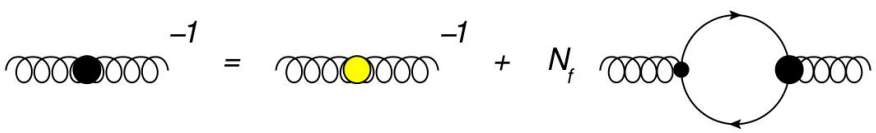

Figure 20: Pictographic representation of the simple ansatz of [63] used to unquench the gluon.

dressed by the gauge sector. It is denoted with the yellow dot in Fig. (20). This ansatz neglects any effects of the quark on diagrams contributing to $D^{-1\ \mathrm{eff}}_{\mu\nu}(k)$, e.g. in the ghosts as well as three- and four-gluon interactions. It was shown in [63] that this is actually a very good approximation in the vacuum case and at finite tempeartures. For the following calculations it is assumed that this holds resonably well in the presence of a magnetic field, although no systematic study was performed so far. Within this approximation the effective propagator in Eq.(5.23) is taken to be isotropic wrt. its

polarization, which is somewhat justified when realizing that there is no direct appearance of charged particles in this sector. The gluon polarization anisotropy may be dominated by the quark loop anyway.

In order to include the effect of the magnetic field onto the gluon sector, the Ritus method will be employed for the quark loop in the gauge boson self-energy. The DSE in position space within the ansatz from above reads

$$D^{-1}_{\mu\nu}(x,y) = D^{-1\ \mathrm{eff}}_{\mu\nu}(x,y) + \Pi^{\mathrm{q}}_{\mu\nu}(x,y), \tag{5.24}$$

where

$$\Pi^{\mathrm{q}}_{\mu\nu}(x,y) = -g^2 N_c\ \mathrm{tr}\left(\gamma_\mu S(x,y)\Gamma_\nu(y)S(y,x)\right) \tag{5.25}$$

From now on any index "q" or "eff" will be dropped. It should be clear from the context, which part of the gluon self-energy is meant. The gluon self-energy is diagonal in Fourier space

$$\Pi^{\mu\nu}(k,k') = \int \mathrm{d}^4x\ \mathrm{d}^4y\ e^{-i(kx-k'y)}\Pi^{\mu\nu}(x,y) = (2\pi)^4\delta^{(4)}(k-k')\Pi^{\mu\nu}(k). \tag{5.26}$$

This quantity is obtained by using the representation for the quark propagator $S(x,y)$ (see Eq.(3.23))

$$\begin{aligned}\Pi^{\mu\nu}(k,k') = -g^2 N_c \sum\!\!\!\!\!\!\int \frac{\mathrm{d}^4q}{(2\pi)^4}\frac{\mathrm{d}^4q'}{(2\pi)^4}\mathrm{tr}\Big(&\left[\int \mathrm{d}^4x\ \bar{E}_{q'}(x)\gamma^\mu E_q(x)e^{-ikx}\right] S(q)\\ &\times\left[\int \mathrm{d}^4y\ \bar{E}_q(y)\Gamma^\nu(y)E_{q'}(y)e^{ik'y}\right] S(q')\Big),\end{aligned} \tag{5.27}$$

where the same truncation is used for the quark-gluon vertex as in the quenched case. Here, $S(q)$ denotes the quark propagator in Ritus space. The calculations can be done in analogy to section 3.2. Again, the simplifications leading to Eq.(3.34) are employed, rendering also the gluon polarization tensor unreliable at small magnetic fields,

$$\begin{aligned}\Pi^{\mu\nu}(k,k') = -(2\pi)^4\delta^{(3)}(k-k')g^2N_c\sum_{l,l'}\int\frac{\mathrm{d}^2q_\parallel}{(2\pi)^4}\int_{-\infty}^{\infty}\mathrm{d}q_2\ e^{-\frac{k_\perp^2+k_\perp'^2}{4|eH|}}e^{i(k_1'-k_1)q_2/eH}e^{-i(k_1'-k_1)k_2'/2eH}\\ \times\sum_{\sigma_1,\sigma_2,\sigma_3,\sigma_4}\delta_{n_1(l',\sigma_1)n_2(l,\sigma_2)}\delta_{n_3(l',\sigma_3)n_4(l,\sigma_4)}\mathrm{tr}\left(\Delta(\sigma_1)\gamma^\mu\Delta(\sigma_2)S(q)\Delta(\sigma_3)\gamma^\nu\Delta(\sigma_4)S(q')\right)\Gamma(k).\end{aligned} \tag{5.28}$$

This expression is apparently diagonal in $k_\parallel$ and k_2. By using

$$\int_{-\infty}^{\infty}\mathrm{d}q_2\ e^{i(k_1'-k_1)q_2/eH} = 2\pi\delta(k_1'-k_1)eH \tag{5.29}$$

the anticipated diagonality can be made more obvious and we obtain

$$\begin{aligned}\Pi^{\mu\nu}(k,k') &= (2\pi)^4\delta^{(4)}(k'-k)\Pi^{\mu\nu}(k)\\ \Pi^{\mu\nu}(k) &= 2\pi g^2N_ceH\sum_{l,l'}\int\frac{\mathrm{d}^2q_\parallel}{(2\pi)^4}\Bigg\{e^{-k_\perp^2/2|eH|}\Gamma(k)\\ &\qquad\times\sum_{\{\sigma_i\}}\delta_{n_1n_2}\delta_{n_3n_4}\mathrm{tr}\left(\Delta(\sigma_1)\gamma^\mu\Delta(\sigma_2)S(q)\Delta(\sigma_3)\gamma^\nu\Delta(\sigma_4)S(q')\right)\Bigg\}\end{aligned} \tag{5.30}$$

The relationship between q and q' is given by

$$q_0' = q_0 - k_0 \qquad q_3' = q_3 - k_3 \tag{5.31}$$

$$q'_\perp = \sqrt{2|eH|l'} \quad q_\perp = \sqrt{2|eH|l}. \tag{5.32}$$

We define

$$\mathcal{D}(q,q') = [B^2(q) + A_\parallel^2(q)q_\parallel^2 + A_\perp^2(q)q_\perp^2][B^2(q') + A_\parallel^2(q')q_\parallel'^2 + A_\perp^2(q')q_\perp'^2]. \tag{5.33}$$

The trace in Eq.(5.31) can be performed easily, yielding

$$\mathrm{tr}\,(\Delta(\sigma_1)\gamma^\mu\Delta(\sigma_2)S(q)\Delta(\sigma_3)\gamma^\nu\Delta(\sigma_4)S(q')) = \frac{T_1^{\mu\nu} + T_2^{\mu\nu} + T_3^{\mu\nu}}{\mathcal{D}(q,q')}, \tag{5.34}$$

where

$$\begin{aligned}
T_1^{\mu\nu} &= 2B(q)B(q')\left(\delta_\parallel^{\mu\nu}\delta_{\sigma_1,\sigma_2}\delta_{\sigma_3,\sigma_4}\delta_{\sigma_1,\sigma_3} + \delta_\perp^{\mu\nu}\delta_{\sigma_1,-\sigma_2}\delta_{\sigma_3,-\sigma_4}\delta_{\sigma_1,-\sigma_3}\right) \\
T_2^{\mu\nu} &= 2A_\perp(q)A_\perp(q')\left(q_\perp q'_\perp\delta_\parallel^{\mu\nu}\delta_{\sigma_1,\sigma_2}\delta_{\sigma_3,\sigma_4}\delta_{\sigma_1,-\sigma_3} + [q_\perp q'_\perp\delta_\perp^{\mu\nu} - 2q_\perp^\mu q_\perp'^\nu]\delta_{\sigma_1,-\sigma_2}\delta_{\sigma_3,-\sigma_4}\delta_{\sigma_1,\sigma_3}\right) \\
T_3^{\mu\nu} &= 2A_\parallel(q)A_\parallel(q')\left([q_\parallel\cdot q'_\parallel\delta_\parallel^{\mu\nu} - 2q_\parallel^\nu q_\parallel'^\mu]\delta_{\sigma_1,\sigma_2}\delta_{\sigma_3,\sigma_4}\delta_{\sigma_1,\sigma_3} + q_\parallel\cdot q'_\parallel\delta_\perp^{\mu\nu}\delta_{\sigma_1,-\sigma_2}\delta_{\sigma_3,-\sigma_4}\delta_{\sigma_1,-\sigma_3}\right).
\end{aligned} \tag{5.35}$$

Inserting these three expressions in Eq.(5.31) shows properties that are familiar, as we saw them in the calculations for the quark self-energy before. When combining the Kronecker deltas, the "usual" Landau level transitions appear

$$\begin{aligned}
\delta_{n_1(l',\sigma_1)n_2(l,\sigma_2)}\delta_{n_3(l',\sigma_3)n_4(l,\sigma_4)}\delta_{\sigma_1,\sigma_2}\delta_{\sigma_3,\sigma_4}\delta_{\sigma_1,\pm\sigma_3} &\propto \delta_{l,l'} \\
\delta_{n_1(l',\sigma_1)n_2(l,\sigma_2)}\delta_{n_3(l',\sigma_3)n_4(l,\sigma_4)}\delta_{\sigma_1,-\sigma_2}\delta_{\sigma_3,-\sigma_4}\delta_{\sigma_1,\mp\sigma_3} &\propto \delta_{l+\sigma_1\mathrm{sgn}(eH),l'}
\end{aligned} \tag{5.36}$$

From this it can be seen that essentially two things can happen for the quark loop. First, it might be that the gluon splits into fermion and anti-fermion, both which are on the same Landau level. Those two are absorbed into the outgoing gluon.
Second, the anti-fermion could be in a Landau level higher or lower compared to the fermion, similar as before. Other cases are not compatible with the coupling to a spin one particle.

The gluon DSE reads, after using the previous results,

$$\begin{aligned}
k^2\left(Z_0^{-1}(k)P_0^{\mu\nu} + Z_\parallel^{-1}(k)P_\parallel^{\mu\nu} + Z_\perp^{-1}(k)P_\perp^{\mu\nu}\right) &= k^2 Z^{-1}(k)P^{\mu\nu} \\
-2\pi g^2 eHN_c e^{-k_\perp^2/2|eH|}\Gamma(k)\sum_{l,l'}\int\frac{\mathrm{d}^2q_\parallel}{(2\pi)^4}\sum_{\{\sigma_i\}}\delta_{n_1n_2}\delta_{n_3n_4}\frac{T_1^{\mu\nu} + T_2^{\mu\nu} + T_3^{\mu\nu}}{\mathcal{D}(q,q')}.
\end{aligned} \tag{5.37}$$

Solving this equation is now straightforward. After having constructed an orthogonal eigenbasis for the gluon polarization tensor, the contributions of the different tensor subspaces can be projected out, reducing the complete equation to three scalar equations.

5.3 Analytic Behaviour of the Gluon Self Energy

An analytic solution of the gluon DSE with dynamical quarks does not exist so far. Numerical studies however are plagued with difficulties when we try to find a solution for the gluon DSE. The usual numerical approaches come with the negligence of important symmetries. A momentum cutoff, as it is employed in this work, violates gauge invariance explicitly. Gauge invariant regularization procedures such as dimensional regularization are difficult to implement numerically.

Furthermore we know that the necessity of regularization and renormalization stems from the structure of the vacuum of the quantum theory. Therefore one has to understand the influence of such effects on the quantum system in a non trivial background such as a magnetic field. It is important to grasp the mechanism of the effective dimensional reduction in the presence of the latter.

This section aims to obtain as much information as possible from the gluon DSE by analytic calculation. A simple calculation with bare quarks in the lowest Landau level approximation is presented below. An analytic approach to the gluon self energy including all Landau levels is very difficult, because of the anisotropy of the $\|$- and $\perp$- directions.

The gluon self energy in the lowest Landau level approximation, with bare quarks, is given by

$$\Pi^{\mu\nu}(k) = -\frac{\beta}{2}\int \frac{\mathrm{d}^2 q_\|}{(2\pi)^4}\mathrm{tr}\left(\gamma_\|^\mu \frac{m - i\gamma q_\|}{q_\|^2 + m^2}\gamma_\|^\nu \frac{m - i\gamma q'_\|}{q'^2_\| + m^2}\Delta(\mathrm{sgn}(eH)\right), \tag{5.38}$$

where $\beta = \beta(k, eH) \equiv 4\pi g^2 N_c eH\Gamma(k^2)e^{-k_\perp^2/2|eH|}$ and as before $q'_\| = q_\| - k_\|$. Performing the trace yields

$$\Pi^{\mu\nu}(k) = -\beta\int \frac{\mathrm{d}^2 q_\|}{(2\pi)^4}\frac{(m + q_\| \cdot q'_\|)\delta^{\mu\nu} - 2q_\|^\mu q'^\nu_\|}{(m^2 + q_\|^2)(m^2 + q'^2_\|)} \tag{5.39}$$

Eq.(5.39) can be evaluated with standard methods. Using the Feynman parameter trick and substituting $\tilde{q}_\| = q_\| - xk_\|$ gives

$$\Pi^{\mu\nu}(k) = -\beta\int_0^1 \mathrm{d}x\left([m^2 + x(x-1)k_\|^2]\delta^{\mu\nu} - 2x(x-1)k_\|^\mu k_\|^\nu\right)\int \frac{\mathrm{d}^2\tilde{q}_\|}{(2\pi)^4}\frac{1}{(\tilde{q}^2 + D)^2} \tag{5.40}$$

Here we have defined $D \equiv m^2 + x(1-x)k_\|^2$. The integral over $\mathrm{d}^2\tilde{q}_\|$ is convergent and gives

$$\int \mathrm{d}^2\tilde{q}_\| \frac{1}{(\tilde{q}^2 + D)^2} = \frac{\pi}{D} \tag{5.41}$$

Performing the integration over x we obtain

$$\Pi^{\mu\nu}(k) = g^2 N_c \frac{eH}{(2\pi)^2}\Gamma(k^2)e^{-k_\perp^2/2|eH|}\left(1 - \frac{1}{2z\sqrt{1+1/z}}\log\frac{\sqrt{1+1/z}+1}{\sqrt{1+1/z}-1}\right)P_\|^{\mu\nu}(k) \tag{5.42}$$

with $z = k_\|^2/4m^2$ as it is also found in [41] for QED. Fig. (21) shows the gluon self energy in this approximation as a function of $k_\perp$ and $k_\|$. The quark mass was taken $m = 3.7$ MeV.

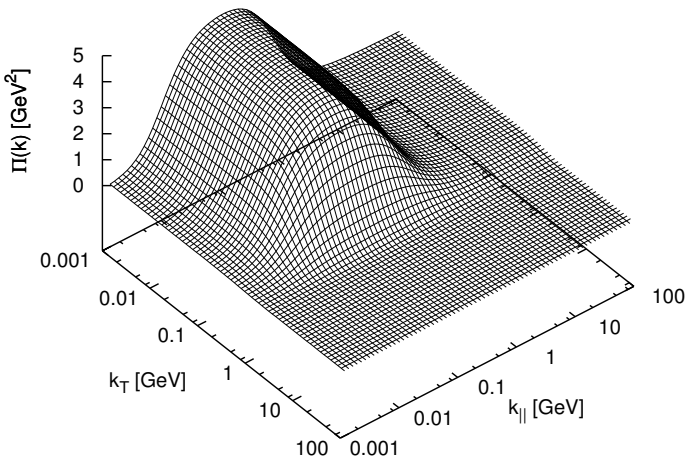

Figure 21: Gluon self energy in the lowest Landau level approximation with bare quarks ($m = 3.7$ MeV).

5.4 Solution of the Coupled Gluon and Quark DSE

The gluon Dyson-Schwinger equation with dynamical quarks, Eq.(5.37), can be decomposed into its contributions from the polarization subspaces denoted by $P_\perp^{\mu\nu}$, $P_\parallel^{\mu\nu}$ and $P_0^{\mu\nu}$. In the following $Z(k)$ stands for the dressing function of the quenched isotropic gluon propagator, e.g. the contribution of the effective propagator in Eq.(5.24). Thus the equations for the dressing functions for the full gluon propagator are in a compact notation

$$Z_\parallel^{-1}(k) = Z_\parallel^{-1}(k) - \beta \sum_l \int \frac{\mathrm{d}^2 q_\parallel}{(2\pi)^4} \quad \kappa(l) \frac{M_\parallel(q,q')}{\mathcal{D}(q,q')}\Big|_{l'=l}, \tag{5.43}$$

$$Z_\perp^{-1}(k) = Z_\perp^{-1}(k) - \beta \sum_l \int \frac{\mathrm{d}^2 q_\parallel}{(2\pi)^4} \sum_{l'=l-\mathrm{sgn}(eH),l'\geq 0}^{l+\mathrm{sgn}(eH)} \frac{N_\perp(q,q')}{\mathcal{D}(q,q')}, \tag{5.44}$$

$$Z_0^{-1}(k) = Z_\perp^{-1}(k) - \beta \sum_l \int \frac{\mathrm{d}^2 q_\parallel}{(2\pi)^4} \left\{ \kappa(l) \frac{M_0(q,q')}{\mathcal{D}(q,q')}\Big|_{l'=l} + \sum_{l'=l-\mathrm{sgn}(eH),l'\geq 0}^{l+\mathrm{sgn}(eH)} \frac{N_0(q,q')}{\mathcal{D}(q,q')} \right\}. \tag{5.45}$$

Here β is as defined in Eq.(5.38) and $\mathcal{D}(q,q')$ as in Eq.(5.33). The factor $\kappa(l)$ accounts for the spin degeneracy of the Landau levels, which is one for the lowest level but two otherwise. We have defined

$$M_\parallel(q,q') = B(q)B(q') + A_\perp(q)A_\perp(q')q_\perp {q'}_\perp + A_\parallel(q)A_\parallel(q')\left(q_\parallel \cdot {q'}_\parallel - 2q_\parallel^2 \sin^2(\phi)\right), \tag{5.46}$$

$$N_\perp(q,q') = B(q)B(q') + A_\perp(q)A_\perp(q')q_\perp {q'}_\perp \left(1 - 2\frac{k_2^2}{k_\perp^2}\right) + A_\parallel(q)A_\parallel(q')q_\parallel \cdot {q'}_\parallel, \tag{5.47}$$

$$\begin{aligned} M_0(q,q') &= B(q)B(q')\frac{k_\perp^2}{k^2} + A_\perp(q)A_\perp(q')q_\perp {q'}_\perp \frac{k_\perp^2}{k^2} \\ &\quad + A_\parallel(q)A_\parallel(q')\left(q_\parallel \cdot {q'}_\parallel \frac{k_\perp^2}{k^2} - 2\frac{q_\parallel \cdot k_\parallel {q'}_\parallel \cdot k_\parallel}{k^2}\frac{k_\perp^2}{k_\parallel^2}\right), \end{aligned} \tag{5.48}$$

$$\begin{aligned} N_0(q,q') &= B(q)B(q')\frac{k_\parallel^2}{k^2} + A_\perp(q)A_\perp(q')q_\perp {q'}_\perp \left(\frac{k_\parallel^2}{k^2} - 2\frac{k_1^2}{k^2}\frac{k_\parallel^2}{k_\perp^2}\right) \\ &\quad + A_\parallel(q)A_\parallel(q')q_\parallel \cdot {q'}_\parallel \frac{k_\parallel^2}{k^2}. \end{aligned} \tag{5.49}$$

Here $Z_\parallel(k)$ only gets contributions when $l' = l$ and similar for $Z_\perp(k)$, where $l' = l \pm 1$. The third dressing functions receives contributions from both cases.

Regularization is a complicated issue, when solving the above equations numerically. As can be seen from section 5.3 and from dimensional considerations, the UV- and IR-behaviour of the quark contribution is twofold.

First, the dominating lowest Landau level contribution is effectivly 1+1 dimensional. This means that this contribution is UV finite, but infrared divergent, different as one is used to from vacuum calculations. Since high momentum modesin the quark loop are suppressed, the exact value of the UV cutoff Λ_{UV} does not matter (as long as $\Lambda_{\mathrm{UV}}^2 >> eH$). Furthermore there will be no terms $\propto \Lambda^n$, where n is some power, which normally arise in four dimensional calculations with a momentum cutoff. These terms are artifical and are caused by the explicit violation of gauge invariance. In 1+1 dimensions they do not appear at all. On the other hand infrared divergences must be regulated properly.

Second, including the higher Landau levels renders the quark loop effectivly 2+1 dimensional, which still guarantees UV-finiteness, but changes the infrared behaviour. The infrared behaviour will therefore be a mixture between the dominating lowest Landau level and the higher contributions. This suggest that these terms need to be regularized separatly. Section 5.4.1 illustrates the regularization procedure in the lowest Landau level approximation.

The gluon polarization tensor decomposition affects the structure of the quark self energy, too. Similar the quark DSE yields with the gluon propgator, Eq.(5.19),

$$
\begin{aligned}
B(p) \quad = \quad & m \; + \; g^2 C_F \int \frac{\mathrm{d}^2 q_\parallel}{(2\pi)^4} \int\limits_{-\infty}^{\infty} \mathrm{d}q_2 \int\limits_{-\infty}^{\infty} \mathrm{d}k_1 \frac{B(q)}{B^2(q) + A_\parallel^2(q) q_\parallel^2 + A_\perp^2(q) q_\perp^2} \\
& \times e^{-k_\perp^2/2|eH|} \Gamma(k^2) \left(\frac{Z_\parallel(k)}{k^2} + \frac{k_\perp^2}{k^2} \frac{Z_0(k)}{k^2} \right) \\
& + \; \frac{2}{\chi(l)} g^2 C_F \sum_{\substack{l_q = l - \mathrm{sgn}(eH), \\ l_q \geq 0,\; l_q + = 2}}^{l + \mathrm{sgn}(eH)} \int \frac{\mathrm{d}^2 q_\parallel}{(2\pi)^4} \int\limits_{-\infty}^{\infty} \mathrm{d}q_2 \int\limits_{-\infty}^{\infty} \mathrm{d}k_1 \frac{B(q)}{B^2(q) + A_\parallel^2(q) q_\parallel^2 + A_\perp^2(q) q_\perp^2} \\
& \times e^{-k_\perp^2/2|eH|} \Gamma(k^2) \left(\frac{Z_\perp(k)}{k^2} + \frac{k_\parallel^2}{k^2} \frac{Z_0(k)}{k^2} \right), \qquad (5.50)
\end{aligned}
$$

$$
\begin{aligned}
A_\parallel(p) \quad = \quad & 1 - g^2 C_F \int \frac{\mathrm{d}^2 q_\parallel}{(2\pi)^4} \int\limits_{-\infty}^{\infty} \mathrm{d}q_2 \int\limits_{-\infty}^{\infty} \mathrm{d}k_1 \frac{A_\parallel(q)}{B^2(q) + A_\parallel^2(q) q_\parallel^2 + A_\perp^2(q) q_\perp^2} \frac{e^{-k_\perp^2/2|eH|}}{p_\parallel^2} \Gamma(k^2) \\
& \times \left(\frac{Z_\parallel(k)}{k^2} \left[2 \frac{(p_\parallel q_\parallel \sin(\phi))^2}{k_\parallel^2} - p_\parallel \cdot q_\parallel \right] + \frac{Z_0(k)}{k^2} \left[2 \frac{k_\perp^2}{k_\parallel^2} \frac{p_\parallel \cdot k_\parallel q_\parallel \cdot k_\parallel}{k^2} - p_\parallel \cdot q_\parallel \frac{k_\perp^2}{k^2} \right] \right) \\
& + \frac{2}{\chi(l)} g^2 C_F \sum_{\substack{l_q = l - \mathrm{sgn}(eH), \\ l_q \geq 0,\; l_q + = 2}}^{l + \mathrm{sgn}(eH)} \int \frac{\mathrm{d}^2 q_\parallel}{(2\pi)^4} \int\limits_{-\infty}^{\infty} \mathrm{d}q_2 \int\limits_{-\infty}^{\infty} \mathrm{d}k_1 \frac{A_\parallel(q)}{B^2(q) + A_\parallel^2(q) q_\parallel^2 + A_\perp^2(q) q_\perp^2} \\
& \times \frac{e^{-k_\perp^2/2|eH|}}{p_\parallel^2} \Gamma(k^2) \left(\frac{Z_\perp(k)}{k^2} p_\parallel \cdot q_\parallel + \frac{Z_0(k)}{k^2} p_\parallel \cdot q_\parallel \frac{k_\parallel^2}{k^2} \right), \quad (5.51)
\end{aligned}
$$

$$
\begin{aligned}
A_\perp(p) \quad = \quad & 1 + g^2 C_F \int \frac{\mathrm{d}^2 q_\parallel}{(2\pi)^4} \int\limits_{-\infty}^{\infty} \mathrm{d}q_2 \int\limits_{-\infty}^{\infty} \mathrm{d}k_1 \frac{A_\perp(q)}{B^2(q) + A_\parallel^2(q) q_\parallel^2 + A_\perp^2(q) q_\perp^2} \frac{e^{-k_\perp^2/2|eH|}}{p_\perp^2} \Gamma(k^2) \\
& \times \left(\frac{Z_\parallel(k)}{k^2} p_\perp q_\perp + \frac{Z_0(k)}{k^2} p_\perp q_\perp \frac{k_\perp^2}{k^2} \right) \\
& + \frac{2}{\chi(l)} g^2 C_F \sum_{\substack{l_q = l - \mathrm{sgn}(eH), \\ l_q \geq 0,\; l_q + = 2}}^{l + \mathrm{sgn}(eH)} \int \frac{\mathrm{d}^2 q_\parallel}{(2\pi)^4} \int\limits_{-\infty}^{\infty} \mathrm{d}q_2 \int\limits_{-\infty}^{\infty} \mathrm{d}k_1 \frac{A_\perp(q)}{B^2(q) + A_\parallel^2(q) q_\parallel^2 + A_\perp^2(q) q_\perp^2} \\
& \times \frac{e^{-k_\perp^2/2|eH|}}{p_\perp^2} \Gamma(k^2) \left(\frac{Z_\perp(k)}{k^2} p_\perp q_\perp \left(1 - 2 \frac{k_2^2}{k_\perp^2} \right) + \frac{Z_0(k)}{k^2} p_\perp q_\perp \left(\frac{k_\parallel^2}{k^2} - 2 \frac{k_\parallel^2 k_1^2}{k_\perp^2 k^2} \right) \right). \quad (5.52)
\end{aligned}
$$

Eqs. (5.43)-(5.45) and (5.50)-(5.52) are coupled and need to be solved simultanously. The dressing functions $A_\parallel$, $A_\perp$ and B are functions of the scalar variables $p_\parallel^2$ and $p_\perp^2$, whereas the gluon dressing functions depend on $k_\parallel^2$, k_1 and k_2.
As was already seen in section 4.1.2 the quark self energy is UV-finite and the infrared behaviour is regulated by the dynamical quark mass. Therefore a cutoff regularization introduces no further complications.

5.4.1 Gluon Propagator With Bare Quarks in the Lowest Landau Level Approximation

In order to investigate the influence of a magnetic field onto the gluon propagator, we will calculate the gluon self energy with bare quarks in the lowest Landau level approximation. These calculations can be compared to the analytic solution, Eq.(5.42), after proper regularization of the divergences. In the lowest Landau level approximation the quark loop diverges as $1/\Lambda_{\rm IR}$, where $\Lambda_{\rm IR}$ is the (unphysical) infrared cutoff. The requirement of $\Pi^{\mu\nu}_{\rm LLL}(0) = 0$, as seen from Eq.(5.42), suggests the following regularization,

$$\Pi^{\mu\nu}_{\rm LLL}(k) \to \Pi^{\mu\nu}_{\rm LLL}(k) - \Pi^{\mu\nu}_{\rm LLL}(0), \tag{5.53}$$

since for zero external momentum the divergent part should persist only. From Eq.(5.42) it can be seen that in the present approach only $Z_\parallel(k)$ receives contributions from the quark loop, which means that $Z_\perp(k)$ and $Z_0(k)$ will remain as they were in the quenched approximation.
Fig. (22) displays a comparsion between the analytic solution of $Z_\parallel(k)$ and Eqs. (5.43)-(5.45) with $B(p) = m = 3.7$ MeV and $A_\parallel(k) = A_\perp(k) = 1$ on the lowest Landau level for $eH = 1$ GeV^2. The agreement is striking.

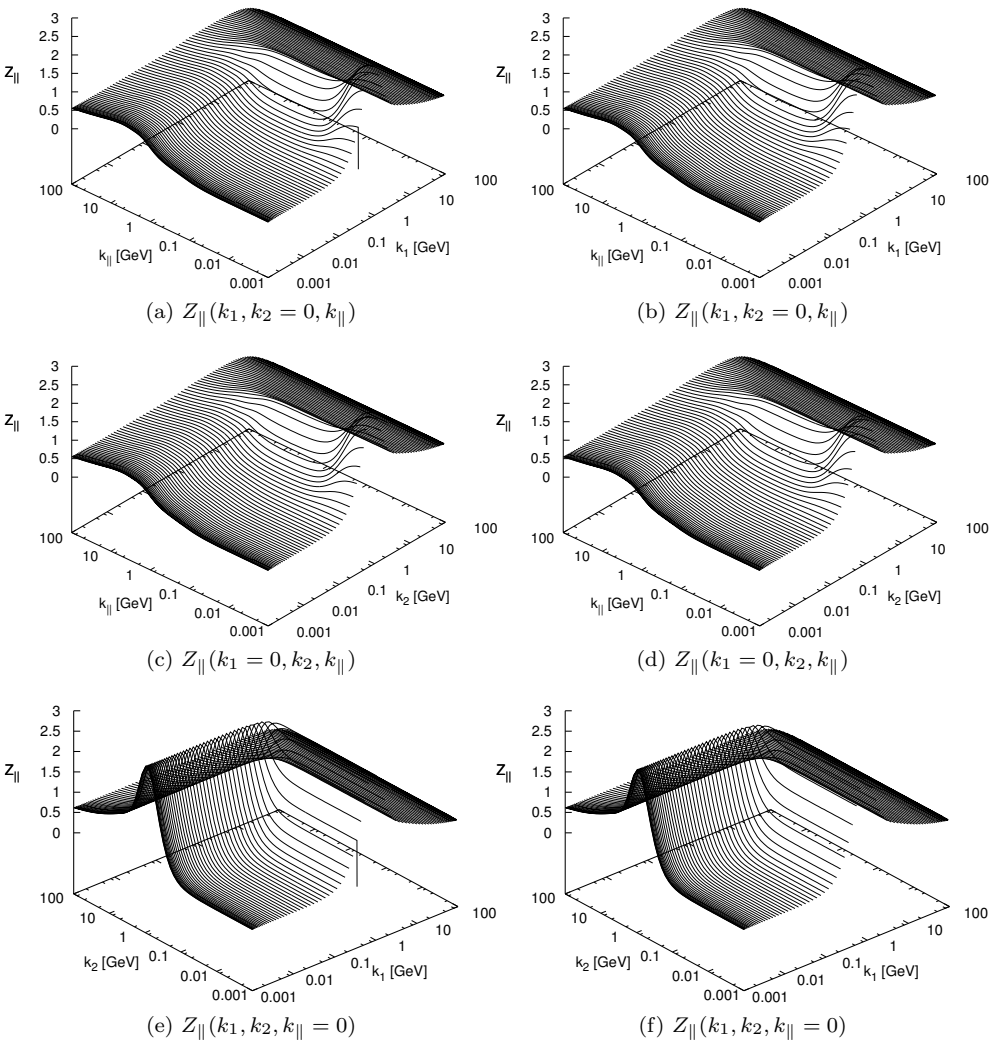

(a) $Z_\parallel(k_1, k_2 = 0, k_\parallel)$ (b) $Z_\parallel(k_1, k_2 = 0, k_\parallel)$

(c) $Z_\parallel(k_1 = 0, k_2, k_\parallel)$ (d) $Z_\parallel(k_1 = 0, k_2, k_\parallel)$

(e) $Z_\parallel(k_1, k_2, k_\parallel = 0)$ (f) $Z_\parallel(k_1, k_2, k_\parallel = 0)$

Figure 22: Gluon dressing function $Z_\parallel$ with bare quarks in the lowest Landau level approximation. Left: numerical (infrared regularized) solution. Right: analytic solution

Fig. (23) shows the same dressing function compared to the quenched approximation for $k_1 = k_2 = 0$, $eH = 0.1$ GeV^2 and $eH = 1$ GeV^2. The effect of the magnetic field is a reduction of the infrared by the external field towards the infrared. Already for $eH = 0.1$ GeV^2 the dressing function changes significantly. It can be seen that the unquenched curves converge to the quenched solution for large gluon momenta. Here the range up to $k_\parallel = 100$ GeV is shown only. In order to see this convergence for large magnetic fields, one needs to go to higher momenta.

Although the gluon self energy requires no UV-regularization, still renormalization is necessary for consistency. We can set the gluon dressing function to a certain value at a specific scale μ, corresponding to the renormalization procedure that was used for the Yang-Mills part of the gluon, $D^{-1\ \mathrm{eff}}_{\mu\nu}(k)$ from Eq.(5.24). The present calculations are for illustrative puropses only, no renormalization/rescaling was performed therefore.

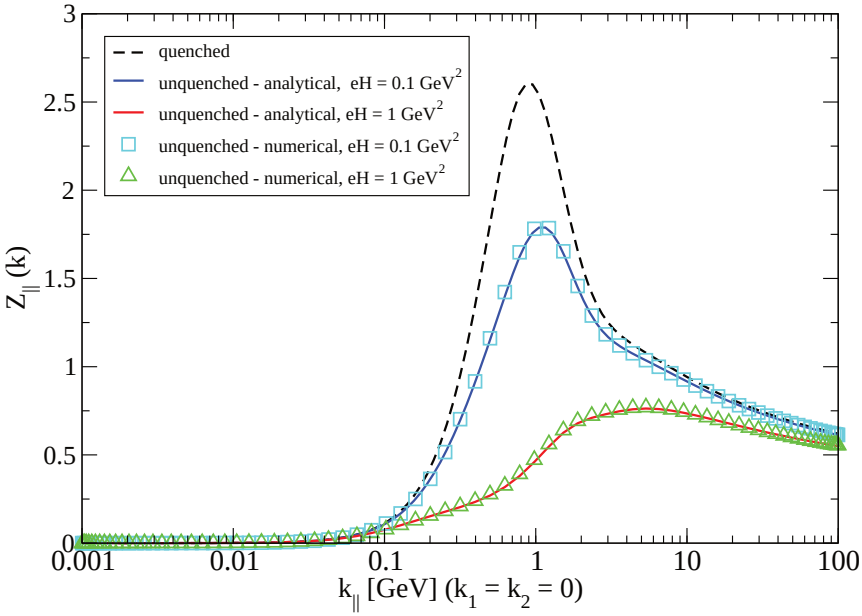

Figure 23: Gluon dressing function $Z_\parallel(k)$ for $k_1 = k_2 = 0$ with bare quarks ($m = 3.7$ MeV) in the lowest Landau level approximation.

5.4.2 Gluon Propagator With Bare Quarks With All Landau Levels

As anticpated before an infrared regularization procedure must be chosen with care in order to acknowledge the specific role of the lowest Landau level compared to the higher levels. In this section we are calculating the gluon polarization with bare quarks including *all* Landau levels.

In order to remove infrared divergences, which are $\propto \log \Lambda_{\mathrm{IR}}$ in 2+1 and $\propto 1/\Lambda_{\mathrm{IR}}$ in 1+1 dimension, we split the quark loop contribution of the gluon self energy into two terms,

$$\Pi^{\mu\nu}(k) = \Pi^{\mu\nu}_{l=0}(k) + \Pi^{\mu\nu}_{l>0}(k), \tag{5.54}$$

where $\Pi^{\mu\nu}_{l=0}$ denotes the contribution from the lowest Landau level and $\Pi^{\mu\nu}_{l>0}$ the higher levels. In analogy to Eq.(5.53) we regularize the IR divergences via

$$\begin{aligned} \Pi^{\mu\nu}_{l=0}(k) &\rightarrow \Pi^{\mu\nu}_{l=0}(k) - \Pi^{\mu\nu}_{l=0}(0) \\ \Pi^{\mu\nu}_{l>0}(k) &\rightarrow \Pi^{\mu\nu}_{l>0}(k) - \Pi^{\mu\nu}_{l>0}(0) \end{aligned} \tag{5.55}$$

One should note that, when using bare quarks, there is actually no lowest Landau level dominance, since $m = 3.7$ MeV for each level. The lowest Landau level dominance is a dynamical effect that can only be seen when using dressed quarks. Because of that, we expect that the results found here for bare quarks with all Landau levels overestimate the effect of the magnetic field. With dynamical quarks one would expect a result that does not deviate much from the lowest Landau level approximation, as seen in the unquenched case. Furthermore dressed quarks with a large dynamical mass of the order of several hundreds of MeV will alter the properties of the gluon polarization significantly, for they supress the self energy in the infrared. This section is meant to illustrate the infrared subtraction procedure in 2+1 dimensions only, therefore we will not be too concerned about the quantitative results found here.

As can be seen from Fig. (24), the effect of the additional higher Landau levels is that the gluon dressing function $Z_\parallel$ is stronger suppressed towards large $k_\parallel$, compared to the lowest Landau level approximation. This is caused by the enhancement of the gluon self energy. As described above, this is artificial to a certain extent, since higher Landau levels should have a small influence with dynamical quarks. Nevertheless the results found here are promising, as they confirm the validity of the regularization procedure described by Eq.(5.55). Fig. (25) shows a comparison between the gluon dressing function in the quenched approximation compared to the calculation including bare quarks ($m = 3.7$ MeV) in the lowest Landau level approximation (blue) and including all Landau levels (orange).

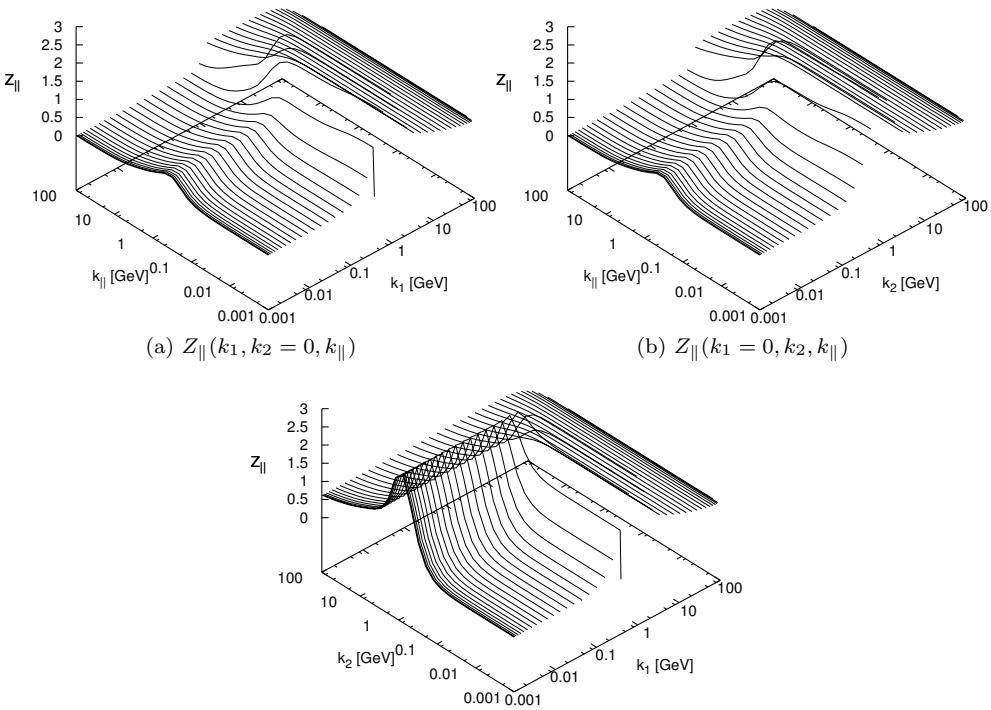

(a) $Z_\parallel(k_1, k_2 = 0, k_\parallel)$ (b) $Z_\parallel(k_1 = 0, k_2, k_\parallel)$

(c) $Z_\parallel(k_1, k_2 = 0, k_\parallel = 0)$

Figure 24: Gluon dressing function $Z_\parallel$ with bare quarks, including all Landau levels, for $eH = 0.1$ GeV^2.

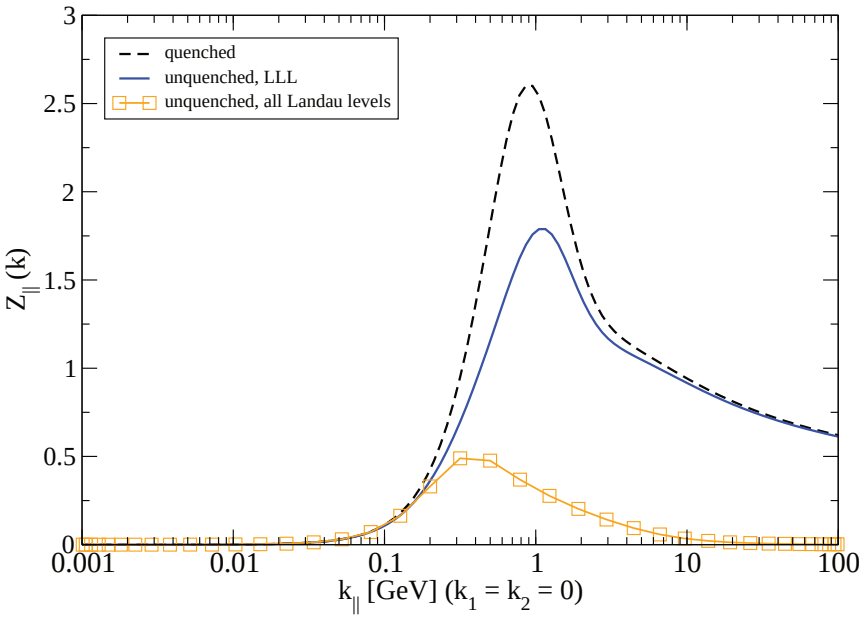

Figure 25: Gluon dressing function $Z_{\|}(k)$ for $k_1 = k_2 = 0$ with bare quarks ($m = 3.7$ MeV) with all Landau levels, compared to the lowest Landau level calculation and the quenched gluon approximation ($eH = 0.1$ GeV^2).

It is now straightforward to extend the calculations done here to the case of dynamical quarks. Unfortunately the fully coupled calculation is numerically very time consuming. Therefore the corresponding calculations could not be included here. Nevertheless one can anticipate the effects already from the present calculations. Since the magnetic field scales down the gluon dressing functions, the quark self energy, depending on the latter, might be reduced, too. Future calculations will have to show whether this is the dominant effect on the quark propagator at large magnetic fields.
However, the tracks, we need to follow, were outlined here, everything else should only be a matter of computational ressources.

6 Conclusion and Outlook

The previous sections have shown that magnetic fields are an excellent tool for the investigation of strongly interacting theories. This work was meant to establish the necessary techniques to include (constant) external magnetic fields into the Dyson-Schwinger framework.

The structure of the Landau gauge quark propagator in the quenched approximation was investigated in Chapter 3 and the modifications of the quark self interactions in a magnetic field were determined in Chapter 4. It was confirmed that an external magnetic field enhances dynamical mass generation and the chiral condensate was calculated as an order parameter for magnetic catalysis. The results for the chiral condensate were found to be in qualitative agreement with several other investigations. A quantitative agreement was difficult, since calculations are rarely found in the literature for the range of magnetic fields explored here.
The behaviour of quarks in magnetic fields is altered by the effective dimensional reduction from four to 2+1 dimensions, respectively 1+1 dimensions on the lowest Landau level.
Furthermore the spin structure of the QCD vacuum in the presence of a magnetic field was studied. It was found that even in the absence of explictly spin dependent tensor structures in the quark propagator, the expectation value of the spin tensor polarization operator $< \bar{\Psi}\sigma^{\mu\nu}\Psi >$ is non-zero for finite eH. The reason for that was found to be the special role of the lowest Landau level, which is not degenerate with respect to both spin directions along the magnetic field. From these findings the value of the magnetic susceptability of the QCD vacuum was determined and found to be in the range of several other calculations.
Based on symmetry considerations, it was shown that the dressed quark propagator is not allowed to have any spin dependent tensor structures. Therefore the propagator structure used here, is the most general one. Additionally various approximation schemes were investigated to test whether a simpler numerical treatment of magnetic fields is possible. None of these schemes was compatible with the proper results. It is essential to follow the tracks outlined here, when employing the Ritus ansatz, in order to capture the essential features of magnetic catalysis.

In Chapter 5 effects of external magnetic fields on the gluon propagator were discussed. An eigenbasis for the polarization structure was found from general considerations. With these findings an approximation was used to unquench the quark DSE. The coupled gluon and quark Dyson Schwinger equations in a magnetic background were determined.
It was discovered that the UV- and IR-behaviour of the quark loop contribution to the gluon self energy changes drastically compared to the vacuum case. Due to an effective dimensional regularization UV-divergences are removed. However, infrared divergences appear, which are different for the 1+1 dimensional lowest Landau level and all the subsequent (2+1 dimensional) Landau levels. A regularization procedure was established to handle these divergences.
An analytic solution to the gluon self energy with bare quarks in the lowest Landau level approximation was found and compared to infrared regularized numerical results. It was shown that these results were consistent.
In order to illustrate the infrared regularization for higher Landau levels, the gluon self energy was derived using bare quarks including all Landau levels. Although the results of these calculations are unphysical in the absence of dynamical quarks, it was shown that IR-regularization is reliable even when the problem involves different kind of divergences, depending on the dimensionality of the lowest Landau level and subsequent higher levels.

This thesis was meant to establish how magnetic fields can be included into the Dyson Schwinger framework in a systematic and consistent way, using the Ritus method. It was shown how quantum system can be expanded in Ritus eigenfunctions and "Feynman rules" were given, that one can use to include magnetic fields in any Feynman diagram involving fermions and gauge bosons. The emphasis was placed on the fundamental properties rather than quantitative exactness, which means that there

remain two points that are interesting to pursue in the future. First, in order to render the present ansatz numerically treatable, an approximation to the quark-gluon vertex was used. Strictly speaking the approximation is only valid once the magnetic field is rather large. Although it was shown that the approximation is very reliable and consistent, it might be helpful to further investigate its validity and to find ways to avoid its use. Second, the truncation of the quark-gluon vertex used here was adapted from the vacuum. Therefore it is certainly important to test this truncation in a systematic way in future calculations. Furthermore a lattice parameterization of this quantity in a magnetic background would certainly give deeper insights.

Overall this thesis shows that the effects of a magnetic field can be included in the Dyson Schwinger equations. The results found here compare nicely to other works. The present ansatz is worth to be continued in order to further investigate the influence of a magnetic field onto a strongly coupled QCD at finite temperature and density.

Acknowledgements

I am deeply thankful for the enormous support and encouragement of my supervisor Christian Fischer during my masters thesis and his inspiration contributing to my road of life. Furthermore I am grateful for all the great help and advice of my fellow co-workers and friends Jacqueline Bonnet, Jan Lüecker and Walter Heupel, just to name a few.
Thanks also to my family for their support. Last and most importantly I would like to thank my girl-friend Svende. Danke, dass du so ein toller Mensch bist. Ich weiß gar nicht, was ich ohne dich machen soll!

I acknowledge the financial and, more importantly, the non-material support by the *Studienstiftung des Deutschen Volkes*.

References

[1] D.J. Gross, F. Wilczek, Phys. Rev. Lett. 30 (1973) 1343

[2] C.D. Roberts, A.G. Williams, Prog. Part. Nucl. Phys. 33 (1994) 477

[3] C.D. Roberts, S.M. Schmidt, Prog. Part. Nucl. Phys. 45 (2000) 1

[4] R. Alkofer, L. von Smekal, Phys. Rept. 353 (2001) 281

[5] C. Wetterich, Phys. Lett. B 301 (1993) 90

[6] J. Berges, N. Tetradis, C. Wetterich Phys. Rept. 363 (2002) 223
and H. Gies, arXiv:hep-th/0611146 (2006)

[7] E.D. Bloom et al., Phys. Rev. Lett. 23 (1969) 930
and M. Breidenbach et al. Phys. Rev. Lett. 23 (1969) 935

[8] K. Fukushima, D.E. Kharzeev, H.J. Warringa, Phys. Rev. D 89 (2008) 074033

[9] V.P. Gusynin, V.A. Miransky, I.A. Shovkovy, Nucl. Phys. B 462 (1996) 249

[10] M. E. Peskin, D. V. Schroeder, *An Introduction to Quantum Field Theory*, Addison-Wesley (1995)

[11] M. Srednicki, *Quantum Field Theory*, Cambridge University Press (2007)

[12] E.S. Swanson, AIP Conf. Proc. 75 (2010) 1296

[13] A. Hauck, L. v. Smekal, and R. Alkofer, in *Quark Confinement and the Hadron Spectrum II*, edited by N. Brambilla and M. Prosperi, p. 258, World Scientific, 1997, preprint, ANL-PHY-8386-TH-96, UNITU-THEP-5/1996.

[14] C. Becchi, A.Rouet, R.Stora, Phys. Lett. B 52 (1974) 344
and C. Becchi, A.Rouet, R.Stora, Commun. Math. Phys. 42 (1975) 127

[15] I.V. Tyutin, Lebedev Phys. Inst. Preprint 39 (1975), arXiv:0812.0580

[16] V.N. Gribov, Nucl. Phys. B 139 (1978) 1

[17] N. Nakanishi, I. Ojima, *Covariant Operator Formalism of Gauge Theories and Quantum Gravity*, World Scientific (1990)

[18] S. Coleman, *Aspects of Symmetry*, Cambridge University Press (1988)

[19] K. Wilson, Phys. Rev. D 10 (1974) 2445 and H. Rothe *Lattice Gauge Theories: An Introduction*, World Scientific 2012 and C. Gattringer, C.B. Lang *Quantum Chromodynamics on the Lattice*, Springer 2010

[20] R. Alkofer, L. von Smekal, arXiv:hep-ph/0007355(2000)

[21] F. Bruckmann, G. Endrodi, Phys. Rev. D 84 (2011) 074506

[22] G.S. Bali, F. Bruckmann, G. Enrödi, Z.Fodor, S.D. Katz, S. Krieg, A. Schäfer, K.K. Szabo, JHEP 2 (2012) 44

[23] J. Bonnet, *Phase transitions in strongly interacting field theories: QED_3 vs. QCD*, PhD thesis, July 2013

[24] C.S. Fischer, J. Luecker, J.A. Mueller, Phys Lett. B 702 (2011) 438

[25] E. Bilgici, F. Bruckmann, C. Gattringer, C. Hagen, Phys. Rev. D 80 (2009) 094007, arXiv:0801.4051v2

[26] F. Synatschke, A. Wipf and K. Langfeld, Phys. Rev. D 77 (2008) 114018 arXiv:0803.0271

[27] C.S. Fischer, Topical Review *Infrared Properties of QCD from Dyson-Schwinger equations* arXiv:hep-ph/0605173v2

[28] J. Greensite, *An Introduction to the Confinment Problem*, Springer (2011)

[29] T. Kugo and I. Ojima, Prog. Theor. Phys. Suppl. 66 (1979) 1

[30] N. Gribov, Nucl. Phys. B 139 (1978) 1

[31] Zwanziger, Nucl. Phys. B 364 (1991) 127;
Nucl. Phys. B 399 (1993) 477; Nucl. Phys. B 412 (1994) 657

[32] I.A. Shovkovy, Lect. Notes Phys. 871 (2013) 13

[33] D.E. Kharzeev, L.D.McLerran, H.J. Warringa, Nucl. Phys. A 803 (2008) 227

[34] T. Vachaspati, Phys. Lett. B 265 (1991) 258

[35] V. Gusynin, V. Miransky, V. Shovkovy, Phys. Rev. Lett. 73 (1994) 3499

[36] F. Bruckmann, G. Enrodi, T.G.Kovacs, arXiv:1303.3972 (2013)

[37] V.I. Ritus, Ann. Phys. 69 (1972), 555

[38] Contributions of V.I. Ritus in *Issues in Intense-Field Quantum Electrodynamics*, ed. V.L. Ginzburg (Nova Science, Commack, 1987)

[39] D.M. Volkov, Z. Phys. 94 (1935), 250

[40] A.I. Nikishov and V.I. Ritus, Z. Eksp. Teor. Fiz 46 (1964), 776, 1768, Sov. Phys. JETP 19 (196),529, 1191

[41] C.N. Leung, S.-Y. Wang, Nucl. Phys. B 747 (2006), 266 and Ann. Phys. 322 (2007) 701

[42] C.N. Leung, Y.J. Ng, A.W. Ackley, Phys. Rev. D 54 (1996) 4181

[43] D.-S. Lee, C.N. Leung, Y.J. Ng, Phys. Rev D 55 (1997) 6504

[44] D.-S. Lee, C.N. Leung, Y.J. Ng, arXiv:hep-th/9701172v1 (1997)

[45] E.J. Ferrer, V. de la Incera, Phys. Rev. D 58 (1998) 065008

[46] G. Murguia, A. Raya, A. Sanchez, E. Reyes, Am. J. Phys. 78 (2010) 7

[47] N.D. Mermin, H. Wagner, Phys. Rev. Lett. 17 (1966) 1133
and S. Coleman, Commun. Math. Phys. 31 (1973) 259

[48] E. Rojas, A. Ayala, A. Bashir, A. Raya, Phys. Rev. D 77 (2008) 093004

[49] C.S. Fischer, A. Maas, J.A. Mueller, Eur. Phys. J. C 68 (2010) 165

[50] E.J. Ferrer, V. de la Incera, Nucl. Phys. B 824 (2010) 217

[51] M. Frasca, M. Ruggieri, Phys. Rev. D 83 (2011) 094024

[52] R. Gatto, M. Ruggieri, arXiv:1207.3190 (2012)

[53] V.M. Belyaev, K.I. Kogan, Yad. Fiz. 40 (1984) 1035

[54] B.L. Ioffe, A.V. Smilga, Nucl. Phys. B 232 (1984) 109

[55] A.V. Kurilin, Il Nuovo Cimento 112 A (1999) N. 9

[56] F. Bruckmann, G. Endrodi, T.G. Kovacs, JHEP 1304 (2013) 112

[57] A. Batalin, A.E. Shabad, Sov. Phys. JETP 33 (1971) 483

[58] A.E. Shabad, Ann. Phys. 90 (1975) 166

[59] W. Dittrich, H.Gies, *Probing the Quantum Vacuum, Perturbative Effective Action Approach in Quantum Electrodynamics and its Application*, Springer Tr. Mod. Phys. 166 (2000)

[60] E.J. Ferrer, V. de la Incera, Phys. Rev. D 58 (1998) 065008

[61] W. H. Furry, Phys. Rev. 51 (1939), 125

[62] K. Hattori, K. Itakura, arXiv:1209.2663 (2012)

[63] C.S. Fischer, J. Luecker Phys. Lett. B 718 (2013) 1036

A Euclidean Field Theory

Euclidean Field theory is under certain conditions an equivalent formulation of the true Minkowskian version of QFT. Using an euclidean metric clears some obstacles one encounters when trying to do calculations in Minkowski space time. Lorentz covariance is lost, but is turned into an $O(4)$ symmetry simplifying calculations.
In Minkowsky space with $(-,+,+,+)$ metric we write a four vector

$$p_M^\mu = (p_M^0, p_M^i) \tag{A.1}$$
$$p_{M\mu} = (-p_M^0, p_M^i) \qquad i = 1,2,3. \tag{A.2}$$

Going to euclidean space time is done by rotating the zero component into the imaginary plane

$$p_M^0 \to p_E^0 = ip_M^0 \tag{A.3}$$

This change implies that the dirac algebra based on dirac matrices in Minskowskian space time needs to be modified. Requiring invariance of the Dirac equation

$$(\not{p} + m)\Psi = 0, \tag{A.4}$$

it can be inferred that the equivalent continuation for the γ matrices is

$$\gamma_E^i = -i\gamma_M^i \qquad \gamma_E^0 = \gamma_M^0 \tag{A.5}$$

The form of the Dirac equation is then

$$(i\gamma \cdot p + m)\Psi, \tag{A.6}$$

where the index E for euclidean quantities is now omitted. The other euclidean rules follow easily

$$p_M^2 \to p_E^2 \tag{A.7}$$
$$\int \mathrm{d}^4 p_M \to i \int \mathrm{d}^4 p_E \tag{A.8}$$
$$\{\gamma_\mu, \gamma_\nu\} = 2\delta_{\mu\nu} \tag{A.9}$$

The volume element in spherical coordinates can now be written

$$\int \mathrm{d}^4 p_E = \int_0^\infty \mathrm{d}p_E \; p_E^3 \int_0^{2\pi} \mathrm{d}\phi \int_0^\pi \mathrm{d}\beta \sin\beta \int_0^\pi \mathrm{d}\theta \sin^2\theta. \tag{A.10}$$

Adding to the numerical simplifications, Euclidean space times also gives the here employed renormalization procedure a thorough foundation. In fact a momentum cutoff $p^2 < \Lambda^2$, which is nothing but a four dimensional ball around the origin, does not cut off arbitrary high momenta in the Minkowskian case. For the $O(4)$ symmetric Euclidean case however it does.

B Comments on the Truncation Scheme

A systematic investigation of truncation schemes in the presence of external fields still needs to be done. The truncation is mainly based on results found in [49] with some minor modifications. Here for the quark-gluon vertex $\Gamma^\nu \to \gamma^\nu \Gamma(k^2)$ with

$$\Gamma(k^2) = \frac{d_1}{d_2 + q^2} + \frac{q^2}{\Lambda^2 + q^2} \left(\frac{\beta_0 \alpha(\mu) \log q^2/\Lambda^2 + 1}{4\pi} \right)^{2\delta} \tag{B.1}$$

was used, where k is the gluon momentum. The paramters used are

$$d_1 = 7.9 \text{ GeV}^2 \quad d_2 = 0.5 \text{ GeV}^2 \tag{B.2}$$

$$\delta = -18/88 \quad \Lambda = 1.4 \text{ GeV} \tag{B.3}$$

This ansatz is simliar than in [49], however the Ball-Chiu form found in the latter was modified slightly. The appearence of the quark dressing functions in the vertex and therefore the Ward identity was neglected. The quantitative difference was compensated by the use of $d_1 = 7.9$ GeV^2 instead of $d_1 = 4.6$ GeV^2 as in the reference.
These simplifications come with some very nice properties. Since the vertex is not explicitely dependent on the quark propagator, its form in Ritus functions can be found more easily. The vertex above is given in terms of the gluon momentum only, which in the Ritus case is still a "physical" momentum (in contrast to the Ritus eigenvalues). Having a vertex, that explicitely depends on properties of the quark, means a phenomenological ansatz of its shape must be in terms of the Ritus eigenvalues. So far there exists no such study.
Some thoughs on the Ward identity in magnetic fields can be found in [60]. Certainly for a complete, quantitatively more accurate study, a quark gluon vertex has to be constructed with a little more care. Nevertheless the present ansatz is perhaps not too bad, for quite consistent results were found. This thesis might be used as a base to construct more accurate truncations.
Furthermore the quenched gluon propagator at zero temperature was taken as

$$Z(k^2) = \frac{q^2\Lambda^2}{(q^2+\Lambda^2)^2}\left[\left(\frac{c}{q^2+a\Lambda^2}\right)^b + \frac{q^2}{\Lambda^2}\left(\frac{\beta_0\alpha(\mu)\log q^2/\Lambda^2+1}{4\pi}\right)^\gamma\right] \tag{B.4}$$

with the parameters

$$a = 0.60 \qquad b = 1.36 \qquad \Lambda = 1.4 \text{ GeV} \tag{B.5}$$

$$c = 11.5 \text{ GeV}^2 \quad \beta_0 = 11N_c/3 \quad \gamma = -13/22 \tag{B.6}$$

where $\alpha(\mu) = 0.3$. This form of the quenched gluon propagator is probably very reliable also in the presence of a magnetic field. The diagrams that need to be resummed in order to get the quenched gluon do not contain any electrically charged particles explicitly. Therefore there is no difference between the quenched gluon in the vacuum and the finite eH case.
Once however the gluon becomes unquenched, things might look different. In the previous sections the Dyson-Schwinger equations were unquenched by including the quark loop in the gluon polarization, but continuing with Eq.(B.4) for the Yang-Mills part of the gauge boson self energy. The Yang-Mills sector will couple to the fermionic sector via higher n-point functions of course. This back coupling is neglected in such an ansatz. However the largest influence on the gluon polarization will come explicitely from the quark loop, which we include here. Perhaps the truncation in the unquenched case is not worse as at zero magnetic field.
Together the behaviour of gluon and vertex resemble asymptotic freedom in the high energy limit, thus giving the correct results when QCD becomes perturbative.

C Scalar Particles in Magnetic Fields

Fermions are not the only interesting particles to investigate in the presence of a magnetic field. There is no electrically charged scalar particle in the present form of standard model. Nevertheless composite particles such as pions play an important role in the dynamics of hadronic objects. It is therefore useful to extend the Ritus method to this sector.
Solving for the eigenfunctions of a scalar particles means finding the eigenfunctions of the Klein-Gordon equation in the presence of a constant vector potential. As can be seen from section 3.1

most of the work was actually done already. What we actually did in this section was to solve the Klein-Gordon equation for the spin up and down components of the fermion separately. As seen from Dirac's famous derivation, the square of the Dirac operator is nothing else but the Klein-Gordon operator. Hence we found the eigenfunctions already! The eigenfunctions of a scalar particle inside a magnetic field are

$$\begin{aligned} E_p(x) &= N(n) e^{i(p_0 x_0 - p_2 x_2 - p_3 x_3)} D_n(\rho) \\ \rho &= \sqrt{2|eH|}\left(x_1 - \frac{p_2}{eH}\right) \\ N(n) &= \frac{(4\pi\,|eH|)^{\frac{1}{4}}}{\sqrt{n!}}, \end{aligned} \tag{C.1}$$

where $n = k - \frac{1}{2}$ ($k \in \mathbb{N}_0$) and thus a similar Landau quantization follows with the eigenvalues (p_0, p_2, p_3, l), where similar as in the case of fermions l denotes the Landau level. The difference here is that there is no degeneracy with respect to spin, there is only one contribution to each Landau level. Stated otherwise: For scalar particles there is only orbital angular momentum.
Nevertheless completeness and orthonormality can be found easily

$$\int \mathrm{d}^4 x \quad \bar{E}_p(x) E_{p'}(x) = (2\pi)^4 \delta^{(4)}(p - p') \tag{C.2}$$

$$\sum\!\!\!\!\!\!\int \frac{\mathrm{d}^4 p}{(2\pi)^4} E_p(x) \bar{E}_p(y) = (2\pi)^4 \delta^{(4)}(x - y), \tag{C.3}$$

where as before

$$\sum\!\!\!\!\!\!\int \frac{\mathrm{d}^4 p}{(2\pi)^4} = \sum_{l=0}^{\infty} \int \frac{\mathrm{d}^2 p_{\parallel}}{(2\pi)^4} \int_{-\infty}^{\infty} \mathrm{d}p_2. \tag{C.4}$$

These findings are helpful when considering for example a ϕ^4 theory in the presence of a Abelian background field. However there are some obstructions we need to consider carefully, when investigating the only scalar particles realized in the standard model, mesons.
Mesons, such as for example pions, are composite particles, build up out of spin 1/2 fermions. Modifications due to the magnetic field will be on two scales. First, the particle reacts coherently as a charge one particle. Second, the building blocks, namely the quarks with fractional charges react to the magnetic field, too. In the case of electromagnetic probes such as high energetic photons the current scale is given by the compton wavelength of the photon. Form factors and structure functions parameterize both our restricted knowledge of the structure of hadronic objects as well as of the transition between those scales.
An external magentic field (of whatever form) might be an interesting subject to pursue further. Certainly strong electromagnetic waves with certain wavelengths (and therefore scales), as they are found for example in lasers, are a powerful experimental tool.

Ich erkläre hiermit an Eides statt, dass ich die vorliegende Arbeit selbstständig und ohne Benutzung anderer als der angegebenen Hilfsmittel angefertigt und wissenschaftlich erarbeitet habe; die aus fremden Quellen direkt oder indirekt übernommenen Gedanken sind als solche kenntlich gemacht. Bei den von mir durchgeführten Untersuchungen habe ich die Grundsätze guter wissenschaftlicher Praxis, wie sie in der "Satzung der Justus-Liebig-Universität Gießen zur Sicherung guter wissenschaftlicher Praxis" niedergelegt sind, eingehalten.
Die Arbeit wurde bisher in keiner Form einer anderen Prüfungskommission vorgelegt oder veröffentlicht.

Gießen, den 28. September 2013

Niklas Müller